

THE IMAGE PARAMETER METHOD FOR THE  
DESIGN OF THE FREQUENCY-UNSYMMETRICAL  
BAND-PASS LADDER FILTERS USING SPECIAL  
TYPES OF ELEMENTARY SECTIONS

Thesis for the Degree of Ph. D.  
MICHIGAN STATE UNIVERSITY  
Kudrat Soemintapoera  
1965

C.2



This is to certify that the

thesis entitled

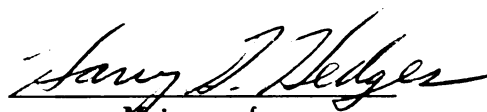
The Image Parameter Method For The  
Design of Frequency-unsymmetrical Band-  
pass Ladder Filters Using Special Types of  
Elementary Sections

presented by

Kudrat Soemintapoera

has been accepted towards fulfillment  
of the requirements for

Ph.D. degree in Elec. Engr.

  
Major professor

Date August 4, 1965

**ROOM USE ONLY**

## ABSTRACT

### THE IMAGE PARAMETER METHOD FOR THE DESIGN OF THE FREQUENCY-UNSYMMETRICAL BAND-PASS LADDER FILTERS USING SPECIAL TYPES OF ELEMENTARY SECTIONS

by Kudrat Soemintapoera

The design of electrical filters can be accomplished by either of two methods, viz., (1) the insertion parameter method which was developed by Cauer [CA 1] and Darlington [DA 1] or (2) the image parameter method which finds its origin in the early works of Campbell [CAM 1] and Zobel [ZO 1].

In insertion parameter theory, after special types of insertion loss requirements are selected (flat loss in both the pass and stop bands) exact formulas for the characteristic functions of the filter exist. However, in the general case, the insertion loss requirement in the block band is arbitrary and an approximation for the characteristic function is necessary. Only recently some work toward this general case has been conducted [FU 2]. The second part of filter design by the insertion parameter method is the determination of the network element values. This necessitates the solution of high-order equations and the method of zero shifting. It is known that in these calculations an abnormal number of digits must be consid-

ered, otherwise the calculated element values are far from accurate or unrealizable. On the other hand, filter design based on the image parameter method does not necessitate tedious calculations and the element values are explicitly given by very simple formulas. Discussions of the advantages and disadvantages of image parameter method over that of insertion parameter method can be found elsewhere [T0 1].

In this thesis some of the work done by Tokad [T0 1] for the low-pass filters are extended to the frequency unsymmetric band-pass filters. The contributions of this thesis are

1. Complete characterizations of the elementary basic sections are developed and the formulas for the element values of these sections are developed.
2. A systematic design technique is described for the frequency unsymmetric band-pass filters.
3. A general approach to the evaluation of terminating sections is given which utilizes a network transformation.
4. The image impedance function of a higher-order terminating section is studied and the results which are important to the designer

are shown.

In addition, discussions necessary for completeness in development of the primary subject material are given so as to make the thesis self contained.

8411  
1-20-66

THE IMAGE PARAMETER METHOD FOR THE DESIGN  
OF THE FREQUENCY-UNSYMMETRICAL BAND-PASS LADDER FILTERS  
USING SPECIAL TYPES OF ELEMENTARY SECTIONS

by

Kudrat Soemintapoera

A THESIS

Submitted to  
Michigan State University  
in partial fulfillment of the requirements  
for the degree of

DOCTOR OF PHILOSOPHY

Department of Electrical Engineering

1965

## ACKNOWLEDGEMENT

The author is indebted to his thesis advisor, Dr. Yilmaz Tokad, for his guidance and constant encouragement in the preparation of this thesis.

The author wishes to thank his major professor, Dr. Harry G. Hedges, for his guidance, his encouragement and his patient advices during the difficult phases of the author's study.

Thanks also are due to Dr. Joseph A Strelzoff and Dr. Edward Nordhaus for their encouragements.



## TABLE OF CONTENTS

CHAPTER I. INTRODUCTION . . . . .	1
CHAPTER II. SPECIAL TYPES OF ELEMENTARY SECTIONS FOR THE FREQUENCY UNSYMMETRIC BAND- PASS FILTERS. . . . .	4
2.1 Introduction . . . . .	4
2.2 The elementary sections . . . . .	8
2.3 General discussions of the elementary sections . . . . .	11
2.4 Analysis of the elementary sections . . . . .	15
2.5 H-functions and some basic sections of band-pass filters . . . . .	24
2.6 Equivalence of the elementary sections . . . . .	26
2.7 Further equivalence characteristics . . . . .	32
2.8 Pole distributions and structure configurations . . . . .	34
2.9 The impedances . . . . .	36
CHAPTER III. THE FREQUENCY TRANSFORMATION AND THE TEMPLATE METHOD . . . . .	51
3.1 Introduction . . . . .	51
3.2 Template for the low-pass filter . . . . .	51
3.3 Template for the band-pass filter . . . . .	55
3.4 Impedance with normalized frequency . . . . .	66
CHAPTER IV. TERMINATING SECTIONS . . . . .	69
4.1 Introduction . . . . .	69
4.2 The disassociate filter . . . . .	70
4.3 The image parameter ladder terminating sections . . . . .	74

CHAPTER V. FILTER DESIGN I - DERIVATION OF FORMULAS . . . . .	82
5.1 Introduction . . . . .	82
5.2 The characterizing function of the image parameter filters . . . . .	85
5.3 The chain matrix . . . . .	89
5.4 Current and voltage transmission factors (M and N) . . . . .	90
5.5 Entries of chain matrix in terms of the image parameters . . . . .	90
5.6 Insertion loss parameters . . . . .	92
5.7 The effective (operating) loss . . . . .	95
5.8 Derivation of insertion loss parameters in terms of image parameters . . . . .	101
5.9 Formulas for the operating loss design technique . . . . .	108
CHAPTER VI. FILTER DESIGN II - APPROXIMATION AND DESIGN PROCEDURE . . . . .	110
6.1 Introduction . . . . .	110
6.2 Approximation for the attenuation function of dissymmetrical filters . . . . .	112
6.3 The design procedure . . . . .	116
6.4 Some more study of the high order image impedance $Z_{T_m}$ and $Z_{\pi_m}$ . . . . .	121
CHAPTER VII. CONCLUSIONS AND FURTHER PROBLEMS . . . . .	127
BIBLIOGRAPHY. . . . .	129
APPENDIX. EVALUATION OF ATTENUATION FUNCTION BY DIGITAL COMPUTER . . . . .	134

## Chapter I

### INTRODUCTION

Although techniques for electrical filter design are well established, there is still improvement that can be accomplished in both the image parameter and the insertion parameter methods. In the insertion method, once the characteristic function is obtained, an exact realization is available. However if the loss requirement is not taken as one of a special kind (as is usually done) the calculation of the characteristic function requires some approximations. Such approximations are discussed in the literature [FR 1], [FU 2]. Even these approximations can effectively be done by reducing the problem to the use of the image transfer function as in the case of a reference filter [DA 1] or the method described by Fischer [FIS 1]. This, of course, indicates one phase of usefulness of the image parameter method. In general, it can be said that the image parameter method of filter design is well established. In many cases the filter so designed is sufficient for the particular purpose which lead to the design of the filter. However, certain considerations in terms of improving this design method may yield a more economical filter, i.e., a filter with fewer elements. Such

considerations can be found elsewhere [BE 2], [TO 1], [FIS 1,2]. Even though the design becomes more involved, still the simplicity in the calculation of the filter element values remains unaltered. However in the insertion loss parameter method calculation of the element values is a major problem. Therefore, the image parameter method, due to some of the simplicities in the design, is still widely in use.

In this thesis some of the improvements suggested for the image parameter method [TO 1], which cannot be used directly for frequency unsymmetric band-pass filters are considered. A complete study of elementary sections for this type of band pass filters is given. A technique for realizing frequency unsymmetric band pass filters based on the image parameter method is described. Further, the properties of certain terminating sections are investigated. A general development of the derivation of terminating sections is described. In this derivation there is no limitation on the complexity of the terminating sections as there is in methods previously given by the other authors [BO 1], [RE 1], [TO 1].

The method of design described in this thesis also contains the design of crystal ladder filters [SK 1]. In fact since the branches of the elementary sections are identical with the electrical circuit representation of a quartz crystal, a quartz crystal symbol is used in the

branches of these sections. However, crystal filters require additional conditions on their element values, therefore the method described in this thesis may not always lead to a filter whose branches may be replaced by crystals. This problem is not discussed in this thesis.

## Chapter II

### SPECIAL TYPES OF ELEMENTARY SECTIONS FOR THE FREQUENCY UNSYMMETRIC BAND-PASS FILTERS

#### 2.1 . Introduction.

The image attenuation function of band-pass filters which can be obtained by a real\* frequency transformation from a low-pass filter attenuation function, has a geometric symmetry property. Filters of this kind are generally called frequency symmetric band-pass filters. The frequency transformation, which is real, reduces the design of such band-pass filters to the design of low-pass filters. The low-pass filter can be realized through the existing several well known techniques and the inverse transformation yields the band-pass filter.

There are band-pass filters whose attenuation functions cannot be obtained through a real frequency transformation from the attenuation function of a low-pass filter. These band-pass filters exhibit non-symmetrical attenuation characteristics and therefore they

---

\* By the word "real" it is meant that the transformation function is a positive real function.

are, in general, referred to as frequency unsymmetrical band-pass filters. However, for some special cases, as Laurent [LA 1] has shown, it is possible to obtain such characteristics from the low-pass attenuation characteristics by means of a frequency transformation followed by a non-constant factor multiplication. This method yields a band-pass filter section which should be used, as it is, without any reference as to how it is derived.

In the design of the image parameter filters, the filters are considered as being composed of cascaded elementary sections. For this purpose there must be image impedance matching at the terminal pairs of the cascaded sections. The elementary sections used in image parameter filters are, in general,  $m$ -derived type sections. Laurent [LA 1] has described several elementary band-pass filter sections. One of the elementary sections (called a zig-zag filter section) is the one that is considered here in detail.

In this thesis, this elementary section (zig-zag filter) forms the basis for designing frequency unsymmetric band-pass filters. The zig-zag filter is a band-pass ladder network in which the attenuation poles are created, alternatively in the upper and the lower stop bands, by either (1) only series arms or (2) only parallel arms or (3) both the series and the parallel arms, so that the attenuation poles in the upper stop band are

created by the series arms while those in the lower stop band by the parallel arms. The latter type of filter is used as the ultimate form of the filter designed by the method developed in this thesis. In general, this type of filter is frequency unsymmetric.

Economical considerations are also important in the design of filters. For such reasons it is desirable to have the least number of inductors and capacitors possible. For practical reasons, minimum number of inductors is preferred. For ladder networks, this is achieved if most of the ladder arms are reactance networks which have the appearance of the electrical representation of a quartz crystal.

Watanabe [WA 1] has extended the necessary and sufficient conditions given by Fujisawa [FU 1] to the design of frequency unsymmetric band-pass filters based on the insertion loss method. His method results in a band-pass filter with minimum capacitors and inductors without mutual inductance. This network has most of its ladder branches in the form which could be considered as the electrical equivalent circuit of a quartz crystal. Thus, in this case, the zig-zag configuration appears but partially. In a recent article, using an insertion loss design technique, Schoeffler [SC 1] has obtained ladder filters in which all ladder arms are replaceable by crystals and some capacitors. In this



approach a special form of characteristic function is produced so that when the synthesis is carried out by the zero shifting method, a zig-zag type filter is obtained, i.e., most of the arms of the filter are made of reactance networks which represent a crystal.

An extensive survey [BE 1, CA 1, TO 1, MO 1, FIS 1,2, NO 1, RO 1,2, SA 1, CO 1, BR 1, MA 1, SH 1] has shown that a complete design procedure of frequency unsymmetric band-pass filters based on the image parameter theory does not exist. The present work is an attempt to design a frequency unsymmetric band-pass filter based on the image parameter design technique. Special elementary sections, to be used as building blocks of this filter, will produce a zig-zag filter of the third type mentioned above. This type of filter has a minimum number of capacitors and inductors. In certain cases it is possible to replace some or all ladder arms by crystals. Therefore, this configuration can also be utilized in the design of ladder band-pass crystal filters [SC 1,2]. It has been mentioned above that the elementary sections used in the design procedure to be described are of special form. These sections cannot be derived from other simpler sections as in the case of those derived from prototype sections by Zobel's  $m$ -derivation. For this reason it is necessary to investigate these elementary sections separately and establish the necessary

information for the design procedure. The following sections of this chapter are devoted to the descriptions of these elementary sections.

## 2.2 . The elementary sections.

The salient feature of the zig-zag filters to be considered are that (1) the series arms will produce poles of the attenuation function only in the upper stop band and (2) the parallel arms will produce poles of the attenuation function only in the lower stop band. The arms of this ladder filter are formed from a reactance network which is similar in appearance to that of the electrical representation of a quartz crystal. On the other hand, there are also elementary sections in which these types of reactances appear only in one of the components which form the ladder arms. However, these sections do not form elementary sections for the zig-zag filter of the third type. All the three types of elementary sections will however be considered here. Since reactance network shown in Fig. 2.2.1 resembles closely the equivalent circuit of a crystal, it will sometimes be replaced by the crystal symbol. Figure 2.2.2 a, b and c, represent the three types of elementary sections, their attenuation curves and image impedance curves, respectively. It is evident from Fig. 2.2.2 that only the

first type or only the second type of section will not be able to produce the zig-zag filters. This follows since type E.S.1 has an attenuation pole only in the lower stop band, type E.S.2 has an attenuation pole only in the upper stop band, while the E.S.Z. type section has one attenuation pole in each of the stop bands. In this latter section, the upper stop band attenuation pole is created by the series arm and the lower stop band attenuation pole is created by the parallel arm. The element values and further properties of these sections will be given later. First it is necessary to give some general discussions on these elementary sections.

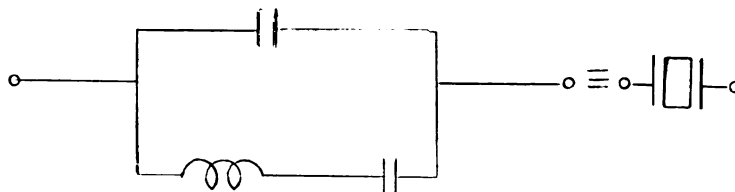
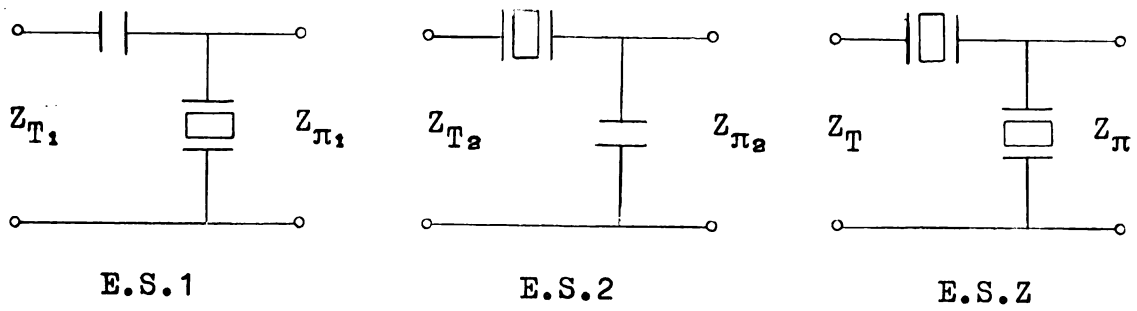
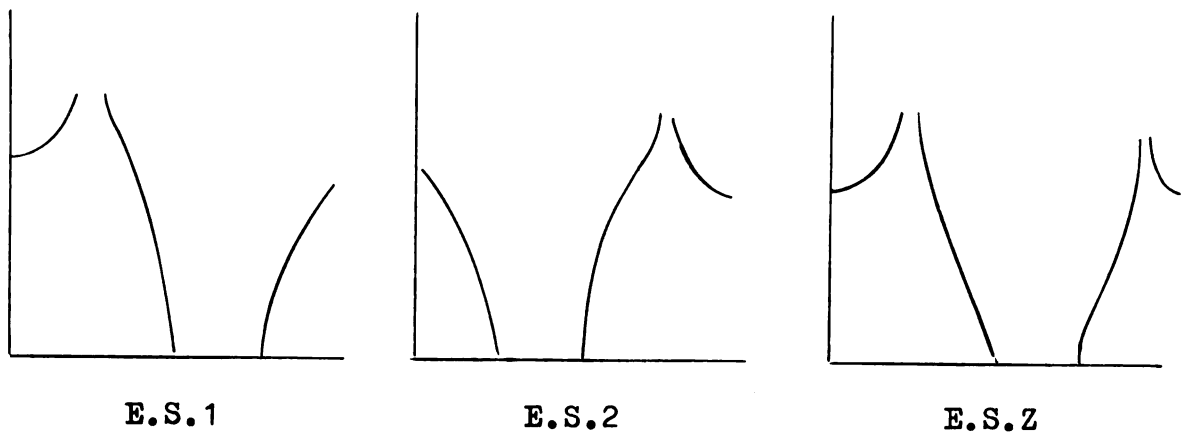


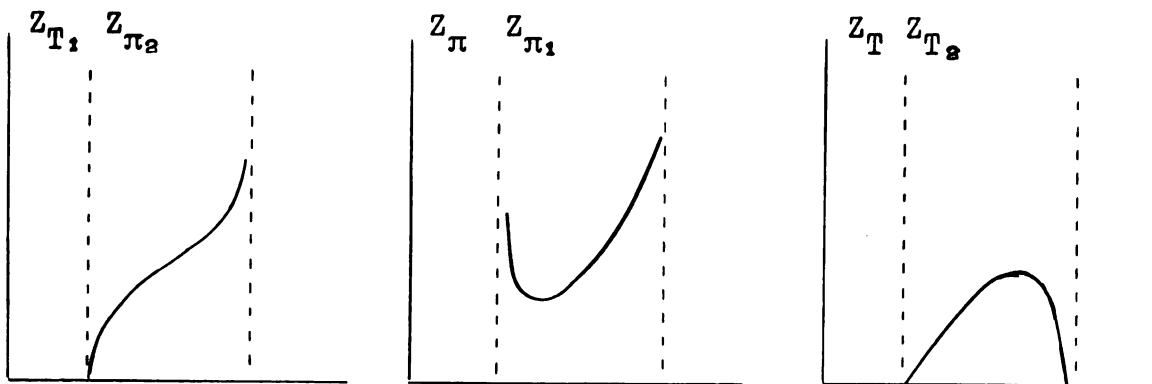
FIG. 2.2.1



(a) Elementary sections



(b) Attenuation Curves



(c) Image Impedance Curves

FIG. 2.2.2

### 2.3 . General discussions of the elementary sections.

In Fig. 2.3.1 the E.S.Z. section is shown in some detail. As is shown later, once the cut-off frequencies, the poles of the attenuation function and the constant of one of the image impedances are given, the section E.S.Z is completely determined.

In the design of image parameter band-pass filters these sections are connected in cascade as shown in Fig. 2.3.2 for  $n = 3$ . There exists, of course, image impedance matching between the interconnected terminal pairs. Note that in Fig. 2.3.2, the series and parallel arms of the filter are indicated by the symbol of a quartz crystal for convenience. The resulting filter has the form shown in Fig. 2.3.3.

The other types of elementary sections, i.e., E.S.1 and E.S.2 are shown in figures 2.3.4-a and 2.3.4-b. Their attenuation poles are on the lower and upper stop bands, respectively. Thus, the attenuation poles of the filters constructed in cascading the E.S.1 sections only are concentrated all in the lower stop band and those of the filters constructed from E.S.2 only, are concentrated in the upper stop band. Once the cut-off frequencies, the attenuation poles and the constant of one of its image impedances are given, the E.S.1 and E.S.2 are completely determined.

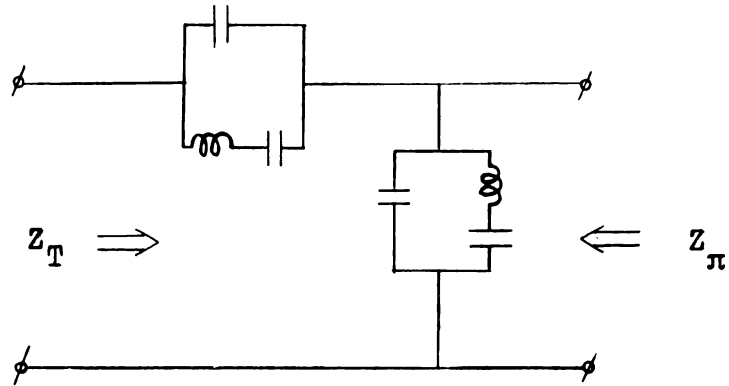


FIG. 2.3.1

$$Z_T = \frac{R_T}{s} \frac{\sqrt{(s^2 + \omega_1^2)(s^2 + \omega_2^2)}}{(s^2 + \omega_{01}^2)}$$

$$Z_\pi = \frac{R_\pi}{s} \frac{(s^2 + \omega_{01}^2)}{\sqrt{(s^2 + \omega_1^2)(s^2 + \omega_2^2)}}$$

- $\omega_{21}$  : upper stop band attenuation pole  
 $\omega_{01}$  : lower stop band attenuation pole  
 $\omega_0$  : confluence frequency (resonant frequency  
for the series arm and anti-resonant  
frequency for the parallel arm)  
 $\left. \begin{matrix} \omega_1 \\ \omega_2 \end{matrix} \right\}$  : the cut-off angular frequencies

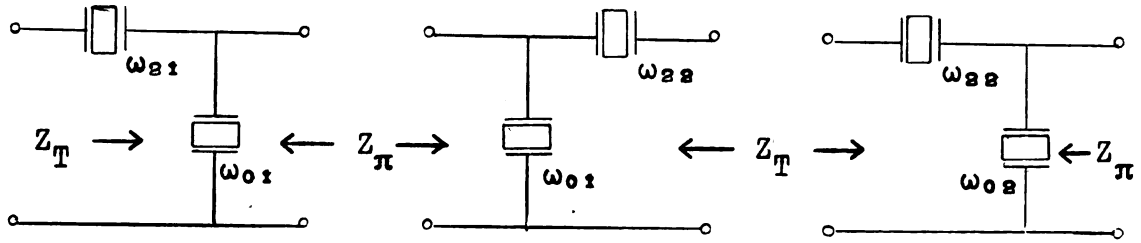


FIG. 2.3.2

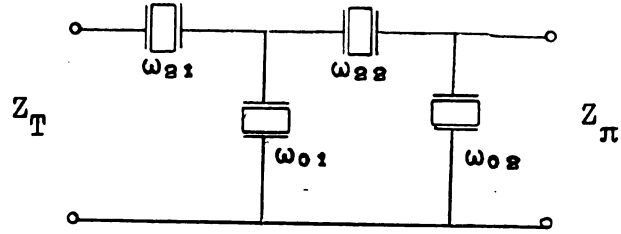


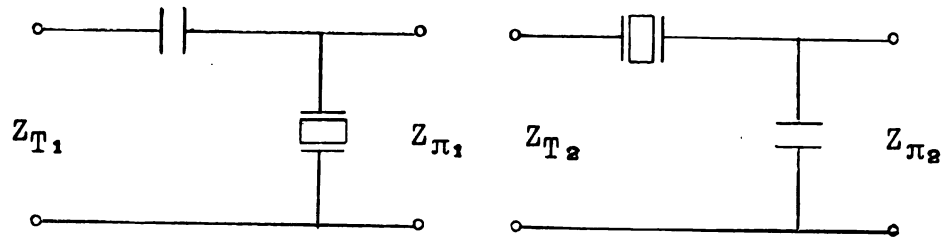
FIG. 2.3.3

$\omega_{01}$  : full pole

$\omega_{02}$  : half pole

$\omega_{22}$  : full pole

$\omega_{21}$  : half pole



(a)

FIG. 2.34

(b)

$$Z_{T_1} = \frac{R_{T_1}}{s} \sqrt{\frac{(s^2 + \omega_1^2)}{(s^2 + \omega_2^2)}}$$

$$Z_{\pi_1} = \frac{R_{\pi_1}}{s} \frac{(s^2 + \omega_{01}^2)}{\sqrt{(s^2 + \omega_1^2)(s^2 + \omega_2^2)}}$$

$$Z_{T_2} = \frac{R_{T_2}}{s} \frac{\sqrt{(s^2 + \omega_1^2)(s^2 + \omega_2^2)}}{(s^2 + \omega_{21}^2)}$$

$$Z_{\pi_2} = \frac{R_{\pi_2}}{s} \sqrt{\frac{(s^2 + \omega_1^2)}{(s^2 + \omega_2^2)}}$$

In forming a filter, these different types of elementary sections can be used provided the image impedance matching exists at the terminal pairs. One disadvantage of constructing filters this way is that, once the constant of one of the image impedances is given, the constants of all the image impedances of the elementary sections in the filter will automatically be fixed. This also means that the element values in these sections are fixed. Therefore, it might not be possible to replace the filter branches by the quartz crystals. In addition, since the impedance level at the other terminal pair is fixed, in general, there is a necessity to use an ideal transformer at this terminal pair.

A study of the pole locations of these elementary sections shows that the section E.S.Z can be considered as the cascade connection of E.S.1 and E.S.2. Indeed, this equivalence exists with the addition of an ideal transformer at one of the terminal pairs of the cascaded sections. It is necessary to study this equivalence relation, because it will help in the determination of the element values of composite filter which is formed by cascade connected sections. Before starting a discussion on this equivalence relation, in the next section, some analytical detail of the different types of elementary sections is given. The information obtained from these details of the sections is utilized for the design



of the band-pass filter having these sections.

#### 2.4 . Analysis of the elementary sections.

Each of the sections is treated separately in the following subsections of this section.

##### 2.4.1. Type 1. elementary section (E.S.1)

The network structure of E.S.1 is given in Fig. 2.4.1.

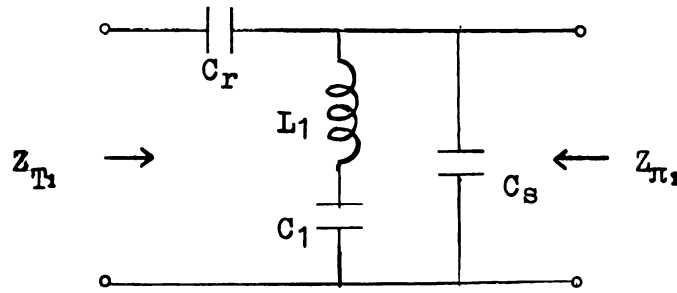


FIG. 2.4.1

The various functions of E.S.1 are given as follows.

$$Z_{T1} = \frac{1}{C_r} \sqrt{1 + \frac{C_r}{C_s}} \frac{1}{s} \sqrt{\frac{s^2 + \omega_1^2}{s^2 + \omega_2^2}} \quad (2.4.1)$$

$$Z_{\pi_1} = \frac{1}{C_s} \frac{1}{\sqrt{1 + \frac{C_r}{C_s}}} \frac{1}{s} \frac{(s^2 + \omega_{01}^2)}{\sqrt{(s^2 + \omega_1^2)(s^2 + \omega_2^2)}} \quad (2.4.2)$$

$$H = \frac{1}{\sqrt{1 + \frac{C_r}{C_s}}} \sqrt{\frac{(s^2 + \omega_2^2)}{(s^2 + \omega_1^2)}} \quad (2.4.3)$$

where

$\omega_1, \omega_2$  : cut-off angular frequencies

$$\begin{aligned}\omega_{01}^2 &= \frac{1}{L_1 C_1} \\ \omega_1^2 &= \frac{1}{L_1 C_1} + \frac{1}{1 + \frac{C_r}{C_s}} \frac{1}{L_1 C_s} \\ \omega_2^2 &= \frac{1}{L_1 C_1} + \frac{1}{L_1 C_s}\end{aligned}\tag{2.4.4}$$

The element values of this section can be expressed in terms of the parameters  $\omega_{01}, \omega_1, \omega_2$  and  $R_{T_1}$  as follows:

From equation (2.4.4):

$$\begin{aligned}\frac{C_1}{C_r} &= \frac{\omega_2^2 - \omega_{01}^2}{\omega_{01}^2} \\ \frac{C_r}{C_s} &= \frac{\omega_2^2 - \omega_1^2}{\omega_1^2 - \omega_{01}^2}\end{aligned}\tag{2.4.5}$$

Let  $C_r/C_s = K_1$  and let the constant of the image impedances be  $R_{T_1}$  and  $R_{\pi_1}$ , then:

$$\begin{aligned}K_1 &= \frac{\omega_2^2 - \omega_1^2}{\omega_1^2 - \omega_{01}^2} \\ R_{T_1} &= \frac{1}{C_r} \sqrt{1 + K_1}\end{aligned}$$

$$R_{\pi_1} = \frac{1}{C_s} \frac{1}{\sqrt{1 + K_1}}$$

Therefore:

$$\left. \begin{aligned} C_r &= \frac{1}{R_{T_1}} \sqrt{1 + K_1} \\ C_s &= \frac{1}{K_1 R_{T_1}} \sqrt{1 + K_1} \\ C_1 &= \frac{\omega_2^2 - \omega_{01}^2}{\omega_{01}^2} C_s \\ L_1 &= \frac{1}{\omega_{01}^2 C_1} \end{aligned} \right\} \quad (2.4.6)$$

$$R_{\pi_1} = \frac{K_1}{1 + K_1} R_{T_1} \quad (2.4.6-a)$$

Thus, when the critical frequencies and  $R_{T_1}$  (or  $R_{\pi_1}$ ) are known all the element values are determined from equation 2.4.6 and equation 2.4.6-a.

#### 2.4.2. Type 2. elementary section (E.S.2)

The network structure is shown in Fig. 2.4.2.

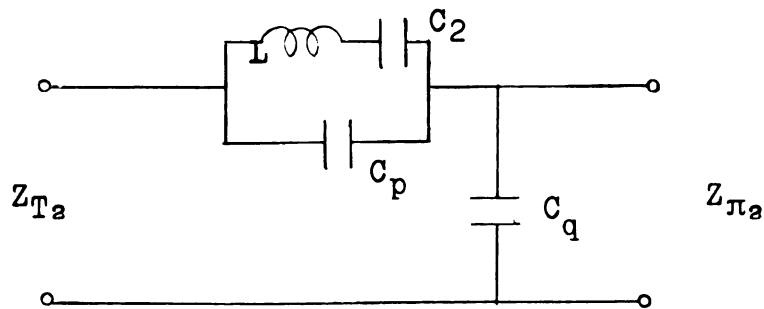


FIG. 2.4.2

The various functions of E.S.2 are given as follows:

$$Z_{T_2} = \frac{1}{C_p} \sqrt{1 + \frac{C_p}{C_q}} \frac{1}{s} \frac{\sqrt{(s^2 + \omega_1^2)(s^2 + \omega_2^2)}}{(s^2 + \omega_{21}^2)} \quad (2.4.7)$$

$$Z_{\pi_2} = \frac{1}{C_q} \frac{1}{\sqrt{1 + \frac{C_p}{C_q}}} \frac{1}{s} \sqrt{\frac{(s^2 + \omega_1^2)}{(s^2 + \omega_2^2)}} \quad (2.4.8)$$

$$H = \frac{1}{\sqrt{1 + \frac{C_p}{C_q}}} \sqrt{\frac{(s^2 + \omega_1^2)}{(s^2 + \omega_2^2)}} \quad (2.4.9)$$

where

$$\begin{aligned} \omega_1^2 &= \frac{1}{L_2 C_2} \\ \omega_2^2 &= \frac{1}{L_2 C_2} + \frac{1}{1 + \frac{C_q}{C_p}} \frac{1}{L_2 C_p} \\ \omega_{21}^2 &= \frac{1}{L_2 C_2} + \frac{1}{L_2 C_p} \end{aligned} \quad (2.4.10)$$

From equation 2.4.10 we have,

$$\begin{aligned} \frac{C_2}{C_p} &= \frac{\omega_{21}^2 - \omega_1^2}{\omega_1^2} \\ \frac{C_q}{C_p} &= \frac{\omega_{21}^2 - \omega_2^2}{\omega_2^2} \end{aligned} \quad (2.4.11)$$

Let  $C_p/C_q = K_2$ , then

$$K_2 = \frac{\omega_2^2 - \omega_1^2}{\omega_{21}^2 - \omega_2^2}.$$

Formulas for determining the element values are:

$$\left. \begin{aligned} R_{T_2} &= \frac{1}{C_p} \sqrt{1 + K_2} \\ C_p &= \frac{1}{R_{T_2}} \sqrt{1 + K_2} \\ C_q &= \frac{1}{K_2 R_{T_2}} \sqrt{1 + K_2} \\ C_2 &= \frac{\omega_{21}^2 - \omega_1^2}{\omega_1^2} C_p \\ L_2 &= \frac{1}{\omega_1^2 C_2} \end{aligned} \right\} \quad (2.4.12)$$

$$R_{\pi_2} = \frac{K_2}{1 + K_2} \quad (2.4.12-a)$$

Thus, as in the previous case, the element values and one of the impedance constants,  $R_{T_2}$  or  $R_{\pi_2}$ , are determined from Eqs. 2.4.12 and 2.4.12-a, if the critical frequencies and  $R_{T_2}$  (or  $R_{\pi_2}$ ) are given.

#### 2.4.3. Type 3. elementary section (E.S.Z)

The network structure is shown in Fig. 2.4.3.

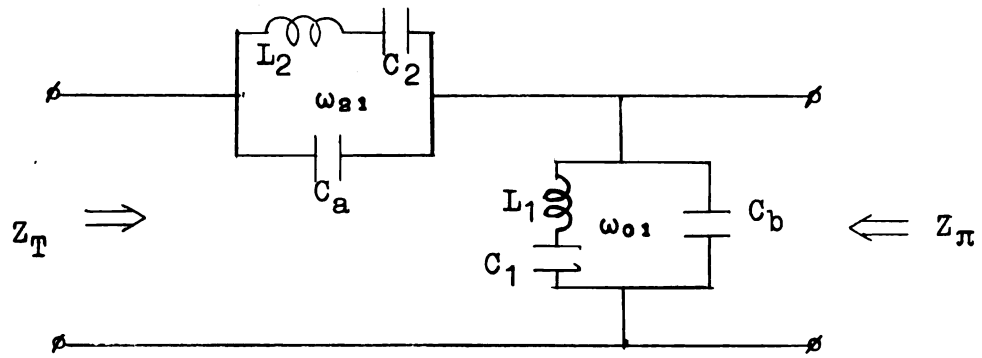


FIG. 2.4.3

The various functions for E.S.Z are given as follows:

The series and parallel arms reactances are:

$$\text{series arm: } x_1 = \frac{1}{C_{as}} \frac{s^2 + \omega_0^2}{s^2 + \omega_{21}^2}$$

$$\text{parallel arm: } x_2 = \frac{1}{C_{bs}} \frac{s^2 + \omega_{01}^2}{s^2 + \omega_0^2}$$

$\omega_0$ : confluent angular frequency ( $\omega_1 < \omega_0 < \omega_2$ )

The image parameters are:

$$Z_T = \frac{1}{C_a} \sqrt{1 + \frac{C_a}{C_b}} \cdot \frac{\sqrt{(s^2 + \omega_1^2)(s^2 + \omega_2^2)}}{s(s^2 + \omega_{21}^2)} \quad (2.4.13)$$

$$Z_\pi = \frac{1}{C_b} \frac{1}{\sqrt{1 + \frac{C_a}{C_b}}} \cdot \frac{(s^2 + \omega_{01}^2)}{s\sqrt{(s^2 + \omega_1^2)(s^2 + \omega_2^2)}} \quad (2.4.14)$$

$$H = \frac{1}{\sqrt{1 + \frac{C_a}{C_b}}} \frac{(s^2 + \omega_0^2)}{\sqrt{(s^2 + \omega_1^2)(s^2 + \omega_2^2)}} \quad (2.4.15)$$

where

$$\omega_0^2 = \frac{1}{L_2 C_2} \quad \text{or}$$

$$\omega_0^2 = \frac{1}{L_1 C_1} + \frac{1}{L_1 C_b} \quad (2.4.16)$$

$$\omega_{01}^2 = \frac{1}{L_1 C_1}$$

$$\omega_{21}^2 = \frac{1}{L_2 C_2} + \frac{1}{L_2 C_a}$$

At the cut-off angular frequencies  $\omega_1$  and  $\omega_2$ ,  $H$  becomes infinite, thus at these frequencies the denominator of  $H$  approaches zero. Since

$$H = \sqrt{\frac{x_1}{x_1 + x_2}} \frac{(s^2 + \omega_0^2)}{\sqrt{\frac{1}{C_a}(s^2 + \omega_0^2)^2 + \frac{1}{C_b}(s^2 + \omega_{01}^2)(s^2 + \omega_{21}^2)}},$$

then at  $s^2 = -\omega_1^2$ ,

$$\frac{C_a}{C_b} = - \frac{(-\omega_1^2 + \omega_0^2)^2}{(-\omega_1^2 + \omega_{01}^2)(-\omega_1^2 + \omega_{21}^2)} \quad (2.4.17-a)$$

and at  $s^2 = -\omega_2^2$ ,

$$\frac{C_a}{C_b} = - \frac{(-\omega_2^2 + \omega_0^2)^2}{(-\omega_2^2 + \omega_{01}^2)(-\omega_2^2 + \omega_{21}^2)} \quad (2.4.17-b)$$

Then from these two equations, 2.4.17-a and -b, we have

$$- \frac{(-\omega_1^2 + \omega_0^2)^2}{(-\omega_1^2 + \omega_{01}^2)(-\omega_1^2 + \omega_{21}^2)} = - \frac{(-\omega_2^2 + \omega_0^2)^2}{(-\omega_2^2 + \omega_{01}^2)(-\omega_2^2 + \omega_{21}^2)}$$

$$\frac{(-\omega_1^2 + \omega_0^2)}{(-\omega_2^2 + \omega_0^2)} = \pm \sqrt{\frac{(-\omega_1^2 + \omega_{01}^2)(-\omega_1^2 + \omega_{21}^2)}{(-\omega_2^2 + \omega_{01}^2)(-\omega_2^2 + \omega_{21}^2)}} .$$

Since only real frequencies are to be considered, in this expression the negative sign is used which gives (2.14.18)

$$\omega_0^2 = \frac{\omega_1^2 + \omega_2^2 \sqrt{\frac{(-\omega_1^2 + \omega_{01}^2)(-\omega_1^2 + \omega_{21}^2)}{(-\omega_2^2 + \omega_{01}^2)(-\omega_2^2 + \omega_{21}^2)}}}{1 + \sqrt{\frac{(-\omega_1^2 + \omega_{01}^2)(-\omega_1^2 + \omega_{21}^2)}{(-\omega_2^2 + \omega_{01}^2)(-\omega_2^2 + \omega_{21}^2)}}}$$

Substituting this expression into Eq. 2.4.17, we obtain: (2.4.19)

$$\frac{C_a}{C_b} = \frac{(\omega_2^2 - \omega_1^2)^2}{\left[ \sqrt{(\omega_2^2 - \omega_{01}^2)(\omega_{21}^2 - \omega_2^2)} + \sqrt{(\omega_1^2 - \omega_{01}^2)(\omega_{21}^2 - \omega_1^2)} \right]^2}$$

The numerical values of  $C_a$  and  $C_b$  are determined after the constant  $R_T$  or  $R_\pi$  of the impedances in Eq. 2.4.13 or Eq. 2.4.14 is given. Note that when one of the above constants is given the value of the other is fixed automatically. The values of the capacitors  $C_a$  and  $C_b$  are

$$C_a = \frac{1}{R_T} \sqrt{1 + K} \quad C_b = \frac{K}{R_T} \sqrt{1 + K}$$

where: (2.4.20)

$$R_T = \frac{1}{C_a} \sqrt{1 + K} \quad K = \frac{C_a}{C_b}$$



Other formulas necessary for the determination of the element values are developed in the following.

From Eq. 2.4.17:

$$K = \frac{(-\omega_1^2 + \omega_0^2)^2}{(\omega_1^2 - \omega_{01}^2)(\omega_{21}^2 - \omega_1^2)}$$

$$\omega_0^2 = \left[ \pm \sqrt{K(\omega_1^2 - \omega_{01}^2)(\omega_{21}^2 - \omega_1^2)} + \omega_1^2 \right]$$

where, since  $\omega_0 > \omega_1$ , the positive sign is to be used.

From Eq. 2.4.16

$$\omega_0^2 = \omega_{01}^2 \left( 1 + \frac{C_1}{C_b} \right)$$

and, then,

$$\frac{C_1}{C_b} = \frac{\omega_0^2 - \omega_{01}^2}{\omega_{01}^2} = \frac{\sqrt{K(\omega_1^2 - \omega_{01}^2)(\omega_{21}^2 - \omega_1^2)} + (\omega_1^2 - \omega_{01}^2)}{\omega_{01}^2}$$

Thus  $C_1$  is determined in terms of  $C_b$  and hence  $L_1$  is also found as

$$L_1 = \frac{1}{\omega_{01}^2 C_1}.$$

From the relation given in Eq. 2.4.16

$$\omega_{21}^2 = \omega_0^2 \left( 1 + \frac{C_2}{C_a} \right)$$

then

$$C_2 = \frac{1}{C_a} \left( \frac{\omega_{21}^2}{\omega_0^2} - 1 \right)$$

which determines also  $L_2$  by the relation

$$L_2 = \frac{1}{\omega_0^2 C_2} .$$

Further, we have the relation

$$R_{\pi} = \frac{1}{C_b} \frac{1}{\sqrt{1+K}} = \frac{K}{1+K} R_T . \quad (2.4.21)$$

In the above analysis, the factor  $K_1$ ,  $K_2$  or  $K$  appears for each different section. These factors are used later as the characterizing factor for these sections.

## 2.5 . H-functions and some basic sections of band-pass filters.

The H-functions of the sections E.S.1 and E.S.2 have similar frequency dependent parts as the H-functions of the sections shown in Figs. 2.5.1 and 2.5.2.

For E.S.1, the expression for the H-function is:

$$H = \frac{1}{\sqrt{1+K_1}} \sqrt{\frac{(s^2 + \omega_2^2)}{(s^2 + \omega_1^2)}} = \sqrt{\frac{(\omega_1^2 - \omega_{01}^2)}{(\omega_2^2 - \omega_{01}^2)}} \sqrt{\frac{(\omega^2 - \omega_2^2)}{(\omega^2 - \omega_1^2)}}$$

The H-function of the section in Fig. 2.5.1 is

$$H = \sqrt{\frac{\omega_1}{\omega_2}} \sqrt{\frac{(\omega^2 - \omega_2^2)}{(\omega^2 - \omega_1^2)}} . \quad (2.5.1)$$

Therefore, if one performs an  $m$ -derivation operation on this section (series  $m$ -derivation) a section which has similar structure and  $H$ -function to the E.S.1 will be obtained where for the  $m$ -parameter the expression used is

$$m^2 = \frac{\omega_2}{\omega_1} \frac{\omega_1^2 - \omega_{01}^2}{\omega_2^2 - \omega_{01}^2} \quad .$$

The section in Fig. 2.5.1 is called the basic section for the band-pass filters.

For the E.S.2 section, the  $H$ -function is

$$H = \frac{1}{\sqrt{1 + K_2}} \sqrt{\frac{(s^2 + \omega_1^2)}{(s^2 + \omega_2^2)}}$$

$$H = \sqrt{\frac{(\omega_{21}^2 - \omega_2^2)}{(\omega_{21}^2 - \omega_1^2)}} \sqrt{\frac{(\omega^2 - \omega_1^2)}{(\omega^2 - \omega_2^2)}} \quad .$$

Similarly, from the section shown in Fig. 2.5.2, after the application of Zobel  $m$ -derivation, a structure having the same circuit configuration and  $H$ -function as that of the section E.S.2 can be obtained. The  $H$ -function of E.S.2 is

$$H = \sqrt{\frac{(\omega^2 - \omega_1^2)}{(\omega^2 - \omega_2^2)}} \quad .$$

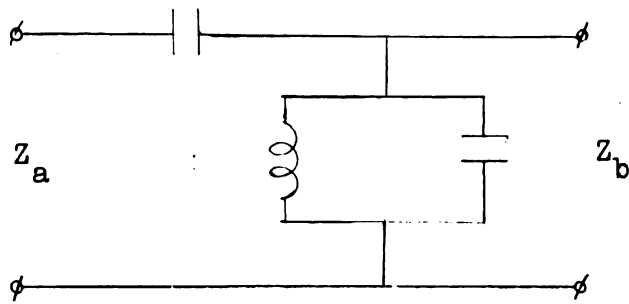


FIG. 2.5.1

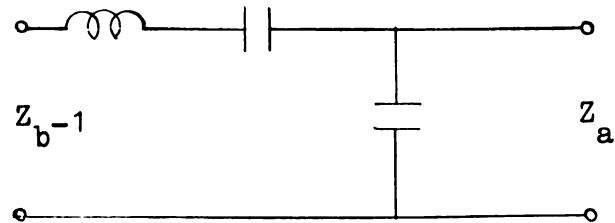


FIG. 2.5.2

## 2.6 . Equivalence of the elementary sections.

Comparing the image impedances of E.S.1, E.S.2 and E.S.Z we notice the following:

1.  $Z_{\pi_2}$  has the same expression as  $Z_{T_1}$ , except for the constant.
2.  $Z_{T_2}$  has the same expression as  $Z_T$ , except for the constant.

3.  $Z_{\pi_1}$  has the same expression as  $Z_{\pi}$ , except for the constant.

By adjusting the values of the constant in the image impedances (this can be done by adjusting the element values) an image impedance matching can be provided for the cascaded E.S.1 and E.S.2 sections at their interconnected terminal pairs. The resulting section will have the same image impedances as that of E.S.2 except for the constants (see Figs. 2.5.3 and 2.5.4). However this cascaded E.S.1 and E.S.2 section and E.S.2 have identical H-functions. Complete equivalence will be obtained if an ideal transformer is connected at the end of the cascaded network shown in Fig. 2.5.5.

From Eq. 2.4.12-a and Eq. 2.4.6-a, in Fig. 2.5.3 with  $R_{\pi_2} = R_{T_1}$ , we have

$$R_{\pi_1} = \frac{K_1}{1 + K_1} R_{T_1} = \frac{K_1}{1 + K_1} R_{\pi_2} = \frac{K_1}{1 + K_1} \frac{K_2}{1 + K_2} R_{T_2}.$$

For the network in Fig. 2.5.4, from Eq. 2.4.21 we have

$$R_{\pi} = \frac{K}{1 + K} R_T.$$

If the constant factors  $R_{\pi_1}$  and  $R_{\pi}$  are equal, then the constant factors on the other side of the networks, i.e.,  $R_{T_2}$  and  $R_T$ , will be identical when an ideal transformer is connected at the terminals of one of the

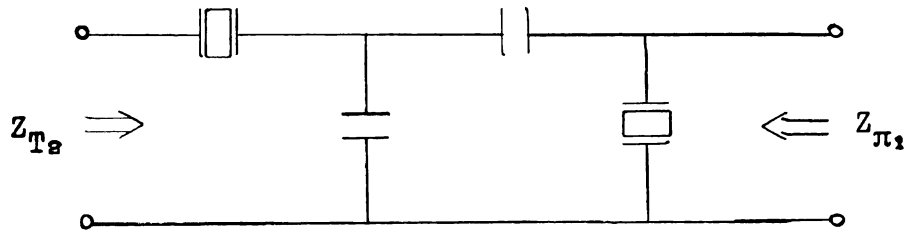


FIG. 2.5.3

A cascade of E.S.1 and E.S.2

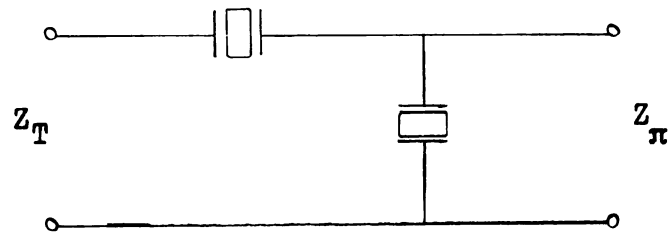


FIG. 2.5.4

E.S.2

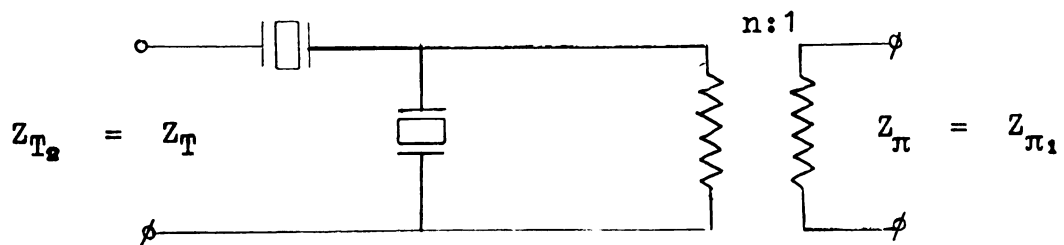


FIG. 2.5.5

Equivalent network

equivalent networks. Let this transformer be connected at the terminal pairs of E.S.2 as shown in Fig. 2.5.5. Then the transformer ratio is given by

$$n^2 = \frac{R_{T_1}}{R_{T_2}} + \left[ \sqrt{\frac{\omega_{21}^2 - \omega_2^2}{\omega_{21}^2 - \omega_1^2}} + \sqrt{\frac{\omega_1^2 - \omega_{01}^2}{\omega_2^2 - \omega_{01}^2}} \right]^2.$$

It remains to investigate whether the networks in Figs. 2.5.3 and 2.5.5 have equivalent H-functions. The H-function of the network in Fig. 2.5.3 is a composite H-function, i.e., it is related to the H-functions of both E.S.1 and E.S.2. Let the H-function of E.S.1 be  $H_1$  and that of E.S.2 be  $H_2$ . Then the H-function of the composite network in Fig. 2.5.3 is

$$H = \frac{H_1 + H_2}{1 + H_1 H_2}.$$

Since

$$H_1 = \frac{1}{\sqrt{1 + K_1}} \sqrt{\frac{s^2 + \omega_1^2}{s^2 + \omega_2^2}}$$

and

$$H_2 = \frac{1}{\sqrt{1 + K_2}} \sqrt{\frac{s^2 + \omega_2^2}{s^2 + \omega_1^2}}$$

then

$$H = \frac{\frac{(s^2 + \omega_1^2)}{\sqrt{1 + K_1}} + \frac{(s^2 + \omega_2^2)}{\sqrt{1 + K_2}}}{\left[ 1 + \frac{1}{\sqrt{(K_1 + 1)(K_2 + 1)}} \right] \left[ \sqrt{(s^2 + \omega_1^2)(s^2 + \omega_2^2)} \right]}$$

$$H = \frac{s^2 + \left[ \frac{\sqrt{1+K_2} \omega_1^2 + \sqrt{1+K_1} \omega_2^2}{\sqrt{1+K_1} + \sqrt{1+K_2}} \right]}{\left[ \frac{1 + \sqrt{(1+K_1)(1+K_2)}}{\sqrt{1+K_1} + \sqrt{1+K_2}} \right] \left[ \sqrt{(s^2 + \omega_1^2)(s^2 + \omega_2^2)} \right]}.$$

From this final expression and Eq. 2.4.15 we have

$$\begin{aligned} & \frac{\omega_1^2 \sqrt{1+K_1} + \omega_2^2 \sqrt{1+K_2}}{\sqrt{1+K_1} + \sqrt{1+K_2}} \\ &= \frac{\omega_1^2 + \omega_2^2 \sqrt{\frac{(\omega_1^2 - \omega_{01}^2)(\omega_{21}^2 - \omega_1^2)}{(\omega_2^2 - \omega_{01}^2)(\omega_{21}^2 - \omega_2^2)}}}{1 + \sqrt{\frac{(\omega_1^2 - \omega_{01}^2)(\omega_{21}^2 - \omega_1^2)}{(\omega_2^2 - \omega_{01}^2)(\omega_{21}^2 - \omega_2^2)}}} = \omega_0^2. \end{aligned}$$

On the other hand, since

$$\begin{aligned} & 1 - \left[ \frac{1 + \sqrt{(1+K_1)(1+K_2)}}{\sqrt{1+K_1} + \sqrt{1+K_2}} \right] \\ &= \frac{K_1 K_2}{\left[ \sqrt{1+K_1} + \sqrt{1+K_2} \right]} \\ &= \frac{(\omega_2^2 - \omega_1^2)^2}{\left[ \sqrt{(\omega_2^2 - \omega_{01}^2)(\omega_{21}^2 - \omega_2^2)} + \sqrt{(\omega_1^2 - \omega_{01}^2)(\omega_{21}^2 - \omega_1^2)} \right]^2}, \end{aligned}$$

then, from Eq. 2.4.19 it can be seen that this expression is equal to  $K$ . Thus,



$$\frac{1 + \sqrt{(1 + K_1)(1 + K_2)}}{\sqrt{1 + K_1} + \sqrt{1 + K_2}} = \sqrt{1 + K}$$

and finally

$$H = \frac{(s^2 + \omega_0^2)}{\sqrt{1 + K} \left[ \sqrt{(s^2 + \omega_1^2)(s^2 + \omega_2^2)} \right]} .$$

This last expression is exactly the expression of the H-function of the E.S.Z section. Therefore the equivalence of the networks in Fig. 2.5.3 and 2.5.5 is established.

The last part of the above discussion can be simplified by the theorem given in the following.

#### THEOREM:

The H-function of a lossless 2-port network will not change if the network is augmented by an ideal transformer connected to one (or both) of its ports.

#### PROOF:

The proof is trivial since by definition

$$H = \sqrt{\frac{Z_{sc}}{Z_{oc}}}$$

and the open and short circuit impedances  $Z_{oc}$  and  $Z_{sc}$  at one of the terminal pairs of this 2-port are either unaltered or both multiplied by the same turns ratio when ideal transformer is added.

Note: The impedance constants on both ports can be multiplied by a constant factor without changing the  $K$ 's of the section as can be seen from the relation

$$R_{\pi} = \frac{K}{1+K} R_T .$$

This means that only the element values of the section are changed.

## 2.7 . Further equivalence characteristics.

The  $H$ -function of the E.S.Z section has the following form

$$H = \frac{1}{\sqrt{1+K}} \frac{(s^2 + \omega_0^2)}{\sqrt{(s^2 + \omega_1^2)(s^2 + \omega_2^2)}} .$$

Note that if  $K$ , as well as the critical frequencies, is not changed the  $H$ -function remains unaltered.

Now consider a network consisting of cascade connected sections of Fig. 2.5.3. Let each of these elementary sections be replaced by its equivalent network, given in Fig. 2.5.5. The resulting network is shown in Fig. 2.7.1. The structure to the left of  $s_1$  is an E.S.Z, the structure between  $s_1$  and  $s_2$ , also that between  $s_2$  and  $s_3$ , can be replaced by E.S.Z's according to the above theorem thereby eliminating the

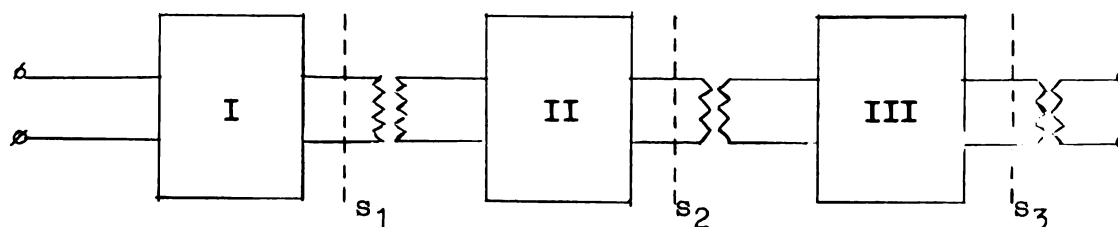


FIG. 2.7.1

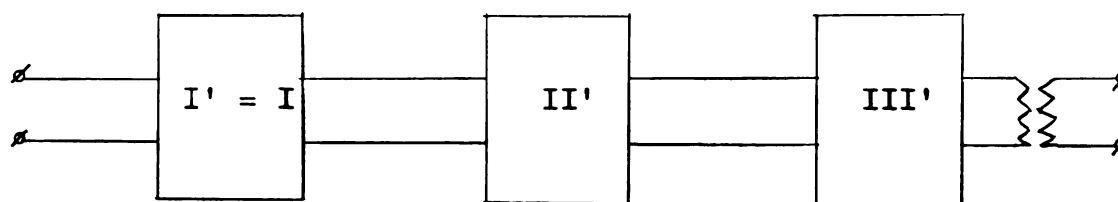


FIG. 2.7.2

transformers. The resulting network will be in the form as in Fig. 2.7.2, having an ideal transformer. This transformer has a different transformer ratio as compared to that last transformer in Fig. 2.7.1, but the H-functions of these networks are identical.

Thus, it can be concluded that any filter consisting of cascade connected pairs of E.S.1 and E.S.2 can be replaced by a filter consisting of E.S.Z sections terminated on an ideal transformer at one of its terminal pairs. Since the H-function will be the same, the calculation of image attenuation and the image phase functions

2.

3.

4.

5.

6.

7.

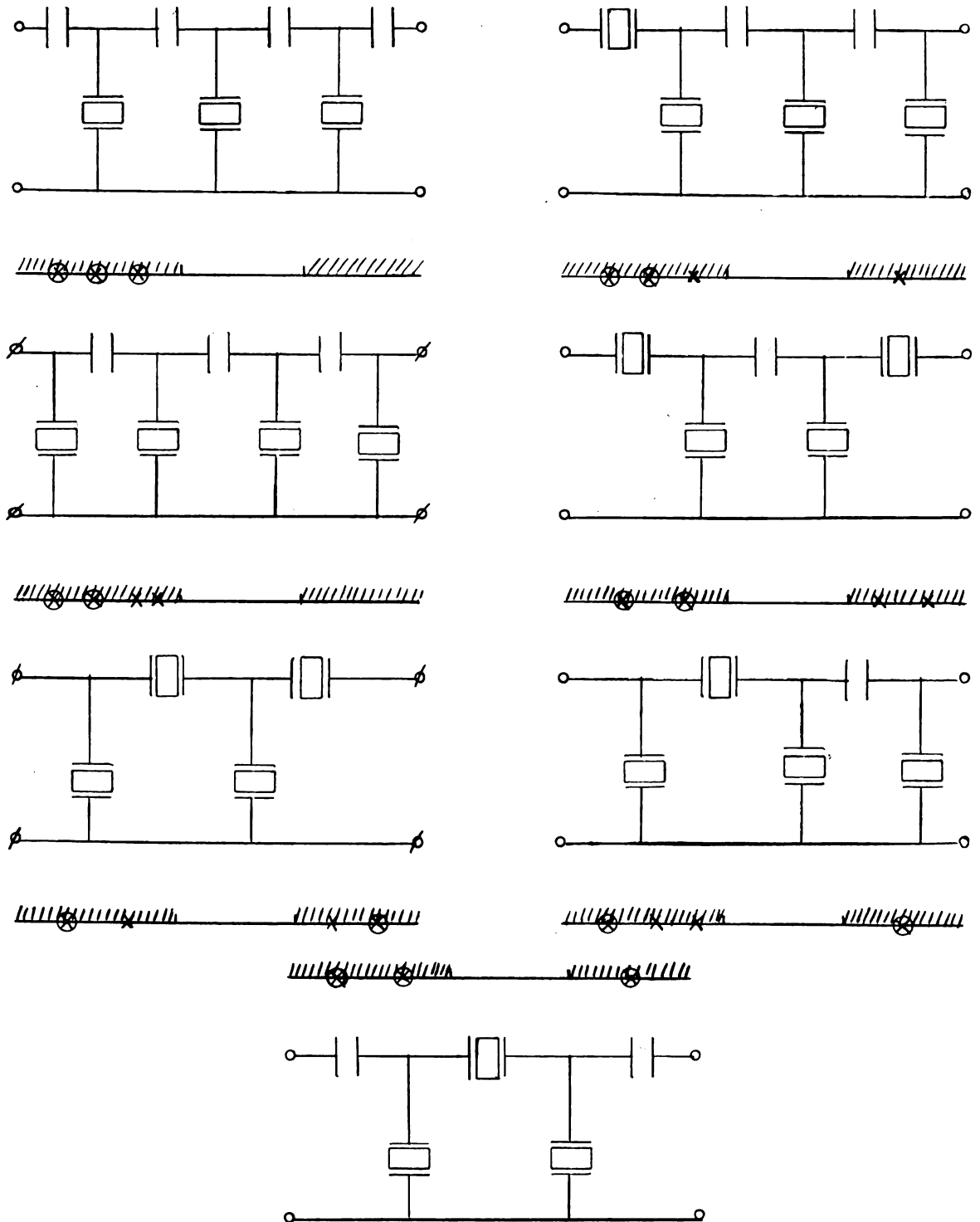
of the complete filter might be easier from one of these networks as compared to the other.

## 2.8 . Pole distributions and structure configurations.

In this section possible locations of the attenuation poles of a band-pass filter containing E.S.1, E.S.2 or E.S.Z are considered. The following rules may be observed:

1. The network consisting only of E.S.1, E.S.2 and E.S.Z will be obtained if there are at most two half poles and the rest of the poles are full poles.
2. Network consisting only of E.S.1 will be obtained if besides the condition 1, all poles are on the lower stop band.
3. Network consisting only of E.S.2 will be obtained if besides the condition 1, all the poles are on the upper stop band.
4. Network consisting only of E.S.Z will be obtained if besides the condition 1, there are equal numbers of poles in the upper as well as the lower stop band. Full poles are counted as two.

Figure 2.8.1 is an example of the application of these rules with six poles.



× half pole

FIG. 2.8.1

⊗ full pole

Possibilities of network configurations  
with 6 attenuation poles

## 2.9 . The impedances.

The filters composed only of elementary sections that have been discussed in detail previously, i.e., E.S.1, E.S.2 and E.S.Z have terminal image impedances of the following forms

$$Z_{\pi}(\omega) = \frac{R_{\pi}}{\omega} \frac{(\omega^2 - \omega_{01}^2)}{\sqrt{(\omega^2 - \omega_1^2)(\omega_2^2 - \omega^2)}}$$

and

$$Z_T(\omega) = \frac{R_T}{\omega} \frac{\sqrt{(\omega^2 - \omega_1^2)(\omega_2^2 - \omega^2)}}{(\omega_{21}^2 - \omega^2)}$$

where

$$s = j\omega$$

$\omega_1, \omega_2$  : angular cut-off frequencies

$R_T$  and  $R_{\pi}$  : constants

$\omega_{21}, \omega_{01}$  : critical frequencies that correspond to the attenuation poles.

Using the frequency transformation discussed in Chapter III, section 3.5, they will have the following form

$$Z_{\pi}(\bar{\omega}) = \frac{R_{\pi}}{\omega_m} \frac{\sqrt{(\alpha^2 - 1)}}{\alpha - \bar{\omega}_{01}} \sqrt{\frac{\alpha - \bar{\omega}}{\alpha + \bar{\omega}}} \frac{(\bar{\omega} - \bar{\omega}_{01})}{\sqrt{1 - \bar{\omega}^2}} \quad (2.9.1)$$

$$Z_T(\bar{\omega}) = \frac{R_T}{\omega_m} \frac{\alpha - \bar{\omega}_{21}}{\sqrt{\alpha^2 - 1}} \sqrt{\frac{\alpha - \bar{\omega}}{\alpha + \bar{\omega}}} \frac{\sqrt{1 - \bar{\omega}^2}}{\bar{\omega} - \bar{\omega}_{21}}$$

$\omega_m = \sqrt{\omega_1 \omega_2}$ ,  $\bar{\omega}$  is the transformed frequency .

The plot in Fig. 2.9.1 represents these impedances.

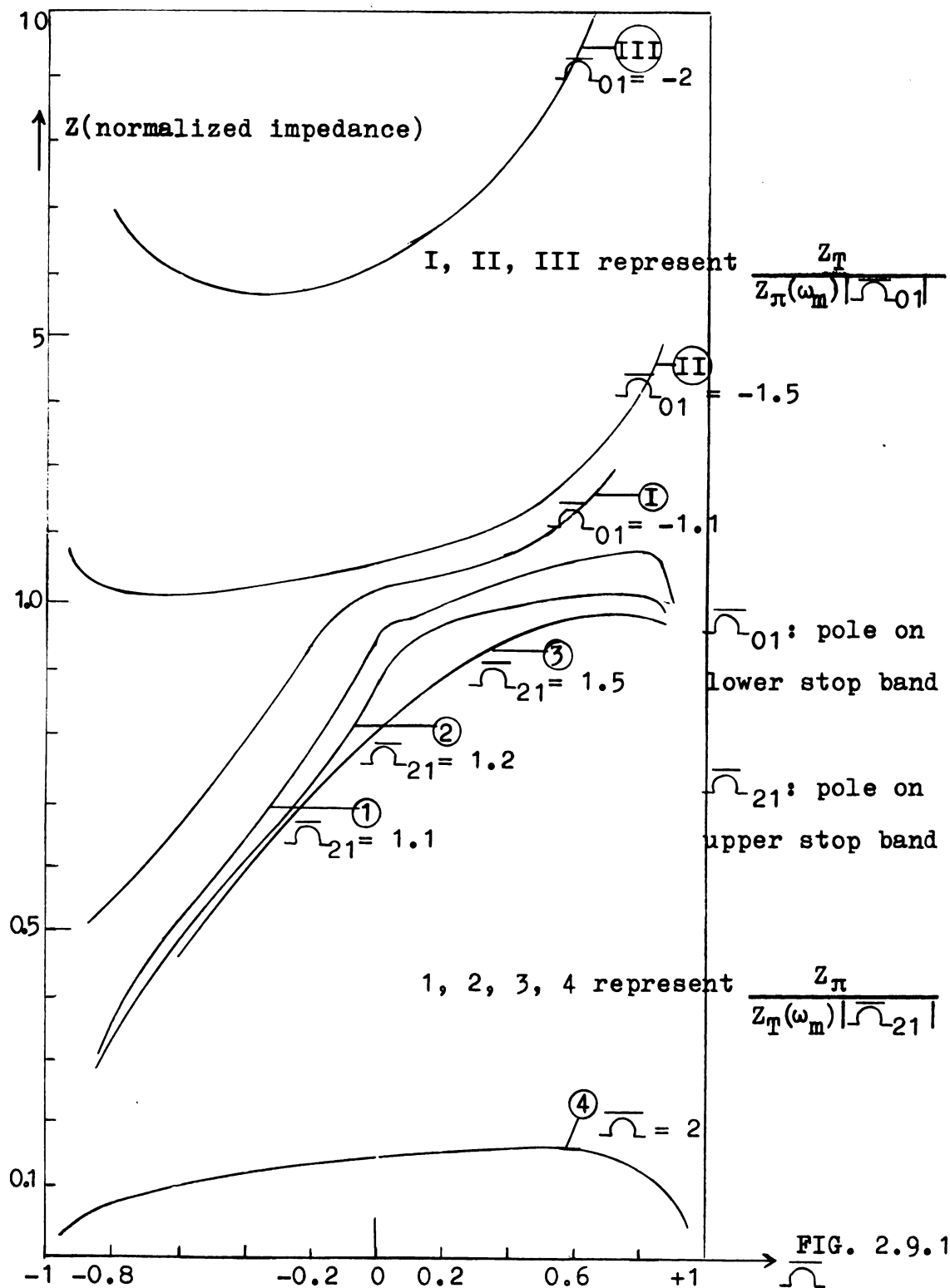
They are normalized with respect to the factors

$$\frac{R_{\pi}}{\omega_m} \frac{\sqrt{\bar{\alpha}^2 - 1}}{\bar{\alpha} - \overline{\mathcal{N}}_{01}} \quad \text{for } Z_{\pi} \quad \text{and} \quad (2.9.2)$$

$$\frac{R_T}{\omega_m} \frac{\bar{\alpha} - \overline{\mathcal{N}}_{21}}{\sqrt{\bar{\alpha}^2 - 1}} \quad \text{for } Z_T.$$

These two factors still leave  $R_T$  and  $R_{\pi}$  free to be selected. In the design of a filter with E.S.1, E.S.2 and E.S.3 as elementary sections,  $R_T$  or  $R_{\pi}$  is one of the numbers that should be given before the design is carried out. It determines the values of the elements. From the plot of the impedance curves in Fig. 2.9.1 it is seen that there is only a narrow effective pass band range, i.e., the range where the impedances are relatively less fluctuating is a small portion of the entire pass band. Thus if a wider effective pass band is needed, a terminating section (T.S.) with higher order image impedance will be necessary. Note that the extremum points of these curves are close to one of the cut-off frequencies. This is mainly due to the fact that the form of these curves is controlled by either  $\overline{\mathcal{N}}_{01}$  or  $\overline{\mathcal{N}}_{21}$  and the extremum points in the pass band are closer to these frequencies which are in the block band. The investigation of these curves then suggests that if the image impedance is a function of at least two control





frequencies and one of them lies in the lower block band and the other in the upper block band, then the extremum point can be pulled towards the center of the pass band or perhaps the impedance curves will now contain two maximums or minimums which are located close to the cut-off frequencies. Indeed, if this is the case then it is possible to improve the matching requirements by arranging the location of the controlling frequencies so that the impedance is relatively less fluctuating in the pass range, i.e., so that there is a wider effective pass band. Two types of sections having image impedances with control frequencies in the upper stop band and lower stop band, i.e., of higher order, can be readily obtained from the E.S.Z. These are sections obtained by series and shunt m-derivations of E.S.Z. They will be used as the terminating sections. These sections will be studied in detail in the rest of this section. In order to simplify the investigation of their image impedances some frequency transformation will be used.

#### 2.9.1. T.S. made of shunt m-derived E.S.Z.

The structure and the image parameters of this section are shown in Fig. 2.9.2. In detail the m-derived impedance is

$$Z_{T_m} = \frac{1}{C_a} \frac{\sqrt{1+K}}{(1-m^2)+K} \frac{1}{\omega} \frac{(\omega^2 - \omega_{01}^2) \sqrt{(\omega^2 - \omega_1^2)(\omega_2^2 - \omega^2)}}{(\omega^2 - \omega_{0p1}^2)(\omega_{2p1}^2 - \omega^2)} \quad (2.9.3)$$

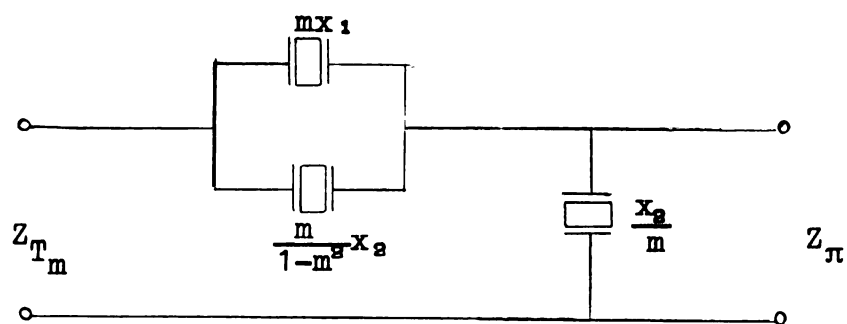


FIG. 2.9.2

Shunt  $m$ -derived - E.S.Z section

$$Z_{\pi} = \frac{R_{\pi}}{s} \frac{(s^2 + \omega_{01}^2)}{\sqrt{(s^2 + \omega_{0p}^2)(s^2 + \omega_{2p}^2)}}$$

$$Z_{T_m} = \frac{R_{T_m}}{s} \frac{(s^2 + \omega_{01}^2) \sqrt{(s^2 + \omega_1^2)(s^2 + \omega_2^2)}}{(s^2 + \omega_{0p}^2)(s^2 + \omega_{2p}^2)}$$

$$s = j\omega$$

$$-1 < m < 1$$

 $\omega_{0p}, \omega_{2p}$  attenuation poles

$$H = \mu \frac{(s^2 + \omega_0^2)}{\sqrt{(s^2 + \omega_1^2)(s^2 + \omega_2^2)}}$$

 $\mu$  : constant

and the H-function ( $H = \tanh P_I$ ) is

$$H = \frac{m}{\sqrt{1+K}} \frac{(\omega_0^2 - \omega^2)}{\sqrt{(\omega_1^2 - \omega^2)(\omega_2^2 - \omega^2)}}. \quad (2.9.4)$$

At the frequencies  $\omega_{0p1}$  and  $\omega_{2p1}$ ,  $H^2(\omega) = 1$ .

Therefore from the expression for H it follows that

$$\frac{\omega_0^2 - \omega_{0p1}^2}{\omega_0^2 - \omega_{2p1}^2} = - \sqrt{\frac{(-\omega_{0p1}^2 + \omega_1^2)(\omega_2^2 - \omega_{0p1}^2)}{(\omega_{2p1}^2 - \omega_1^2)(\omega_{2p1}^2 - \omega_2^2)}}$$

or

$$\omega_0^2 = \frac{\omega_{0p1}^2 + \omega_{2p1}^2 + \sqrt{\frac{(-\omega_{0p1}^2 + \omega_1^2)(\omega_2^2 - \omega_{0p1}^2)}{(\omega_{2p1}^2 - \omega_1^2)(\omega_{2p1}^2 - \omega_2^2)}}}{1 + \sqrt{\frac{(\omega_1^2 - \omega_{0p1}^2)(\omega_2^2 - \omega_{0p1}^2)}{(\omega_{2p1}^2 - \omega_1^2)(\omega_{2p1}^2 - \omega_2^2)}}}. \quad (2.9.5)$$

On the other hand, at the cut-off frequencies  $\omega_1$  and  $\omega_2$ ,  $H(\omega)$  is infinite. Then by a similar discussion to that in section 2.4.3 we have

$$\frac{c_a}{c_b} = \frac{(\omega_0^2 - \omega_1^2)^2}{(\omega_1^2 - \omega_{01}^2)(\omega_{21}^2 - \omega_1^2)} \quad (2.9.6)$$

$$\frac{c_a}{c_b} = \frac{(\omega_2^2 - \omega_0^2)^2}{(\omega_2^2 - \omega_{01}^2)(\omega_{21}^2 - \omega_2^2)}$$

(where  $\frac{c_a}{c_b} = K$ ) .

Equating these last two equations the following is obtained.

$$\omega_{21}^2 = \frac{\omega_2^2 - \omega_1^2 \left[ \frac{(\omega_0^2 - \omega_2^2)(\omega_1^2 - \omega_{01}^2)}{(\omega_0^2 - \omega_1^2)(\omega_2^2 - \omega_{01}^2)} \right]}{1 - \left[ \frac{(\omega_0^2 - \omega_2^2)(\omega_1^2 - \omega_{01}^2)}{(\omega_0^2 - \omega_1^2)(\omega_2^2 - \omega_{01}^2)} \right]} \quad (2.9.7)$$

We also have

$$R_{T_m} = \frac{1}{C_a} \frac{\sqrt{1 + K}}{(1 - m^2) + K} = \frac{R_T}{(1 - m^2) + K} \quad (2.9.8)$$

$$\text{where } R_T = \frac{1}{C_a} \sqrt{1 + K}.$$

2.9.2. T.S. constructed of series  $m$ -derived E.S.Z.

All the formulas from Eq. 2.9.4 to Eq. 2.9.7 above by replacing  $\omega_{01}$  by  $\omega_{21}$ ,  $\omega_{0p1}$  by  $\omega_{0p2}$ ,  $\omega_{2p1}$  by  $\omega_{2p2}$  apply also for this T.S. elementary section. The structure and the image parameters are shown in Fig. 2.9.3. The image impedance in detail has the form

$$Z_{\pi_m} = \frac{R_{\pi_m}}{\omega} \frac{(\omega^2 - \omega_{0p2}^2)(\omega_{2p2}^2 - \omega^2)}{(\omega_{21}^2 - \omega^2) \sqrt{(\omega^2 - \omega_1^2)(\omega_2^2 - \omega^2)}} \quad (2.9.9)$$

$$\text{where } R_{\pi_m} = \frac{R_{\pi} [(1 - m^2) + K]}{1} \quad \text{and} \quad (2.9.10)$$

$$R_{\pi} = \frac{1}{C_b} \frac{1}{\sqrt{1 + K}}.$$

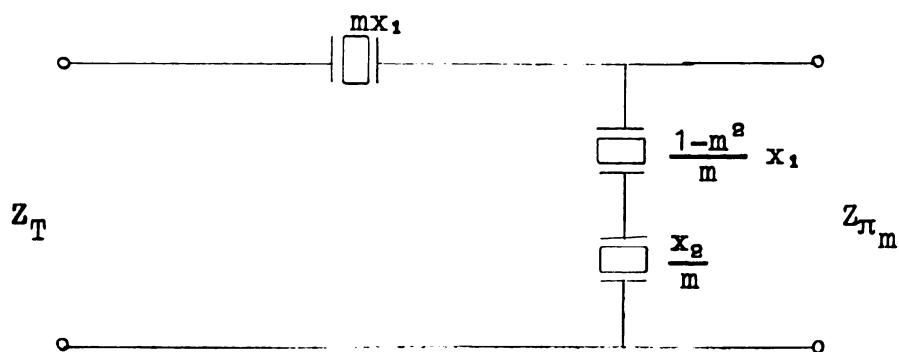


FIG. 2.9.3

Series m-derived E.S.Z section

$$Z_T = \frac{R_T}{s} \frac{\sqrt{(s^2 + \omega_1^2)(s^2 + \omega_2^2)}}{(s^2 + \omega_{21}^2)}$$

$$Z_{\pi_m} = \frac{R_{\pi_m}}{s} \frac{(s^2 + \omega_{0p}^2)(s^2 + \omega_{2p}^2)}{(s^2 + \omega_{21}^2) \sqrt{(s^2 + \omega_1^2)(s^2 + \omega_2^2)}}$$

$$H = \mu \frac{(s^2 + \omega_0^2)}{\sqrt{(s^2 + \omega_1^2)(s^2 + \omega_2^2)}}$$

Note that for series and shunt m-derived cases

$$\omega_{0p} > \omega_{01} \quad \text{and}$$

$$\omega_{2p} < \omega_{21} \quad .$$

### 2.9.3. The frequency transformation.

For the investigation of the impedance curves of  $Z_{T_m}$  and  $Z_{\pi_m}$ , it is convenient to use a frequency transformation. First, let the expressions for the impedances be rewritten for ready reference.

$$Z_{T_m} = R_{T_m} \frac{1}{\omega} \frac{(\omega^2 - \omega_{01}^2)}{(\omega^2 - \omega_{0p1}^2)(\omega_{2p1}^2 - \omega^2)} \sqrt{(\omega^2 - \omega_1^2)(\omega_2^2 - \omega^2)}$$

$$Z_{\pi_m} = R_{\pi_m} \frac{1}{\omega} \frac{(\omega_{2p2}^2 - \omega^2)(\omega^2 - \omega_{0p2}^2)}{(\omega_{21}^2 - \omega^2) \sqrt{(\omega^2 - \omega_1^2)(\omega_2^2 - \omega^2)}}$$

$$\omega_{01} < \omega_{0p} < \omega_1$$

$$\omega_2 < \omega_{2p} < \omega_{21}$$

In these expressions the angular frequencies  $\omega_{01}$  and  $\omega_{21}$  do not correspond to the attenuation poles for the corresponding sections. The frequency transformation used here for  $Z_{T_m}$  will transform  $\omega_{01}$  to  $-\infty$ , and  $\omega_{21}$  to  $+\infty$  for  $Z_{\pi_m}$ . Therefore it will have the form with the following conditions:

$$\omega = \frac{(\omega - \omega_1)(\omega_2 - \delta) + (\omega - \omega_2)(\omega_1 - \delta)}{(\omega_2 - \omega_1)(\omega - \delta)} \quad (2.9.11)$$

where  $\delta$  is  $\omega_{01}$  or  $\omega_{21}$  depending whether  $Z_{T_m}$  or  $Z_{\pi_m}$  is being investigated.

For  $\omega = \omega_1$  we have  $\Omega = -1$   
 $\omega = \omega_2$  we have  $\Omega = +1$   
 $\omega = 0$  we have  $\Omega = \Omega(0) = \frac{2\omega_1\omega_2 - \gamma(\omega_1 + \omega_2)}{\gamma(\omega_2 - \omega_1)}$   
 $\omega = \infty$  we have  $\Omega = \Omega(\infty) = \frac{(\omega_1 + \omega_2) - 2\gamma}{(\omega_2 - \omega_1)}$ .

If  $\delta = \omega_{01}$  (case  $Z_{T_m}$ ),

$$\Omega(0) > \Omega(\infty) \text{ with } \Omega(\infty) > 1.$$

If  $\delta = \omega_{21}$ ,  $\Omega(\infty) < \Omega(0)$  with  $\Omega(0) < -1$ .

Since the frequency transformation is a bilinear transformation, so is the inverse transformation

$$\omega = \delta \frac{\Omega + \left[ \frac{\omega_1 + \omega_2 - \frac{2\omega_1\omega_2}{\delta}}{\omega_2 - \omega_1} \right]}{\Omega - \left[ \frac{\omega_1 + \omega_2 - 2\delta}{\omega_2 - \omega_1} \right]} \quad (2.9.13)$$

Fig. 2.9.4 shows the transformation from the  $\omega$ -axis to the  $\Omega$ -axis. Figs. 2.9.5 and 2.9.6 are the plots of the  $Z_{T_m}$  and  $Z_{\pi_m}$  normalized to  $R_{T_m}$  and  $R_{\pi_m}$  respectively.

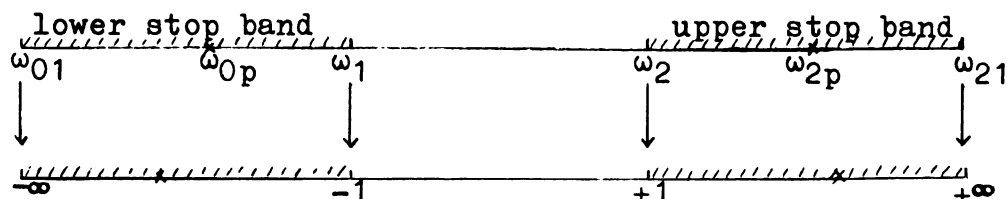
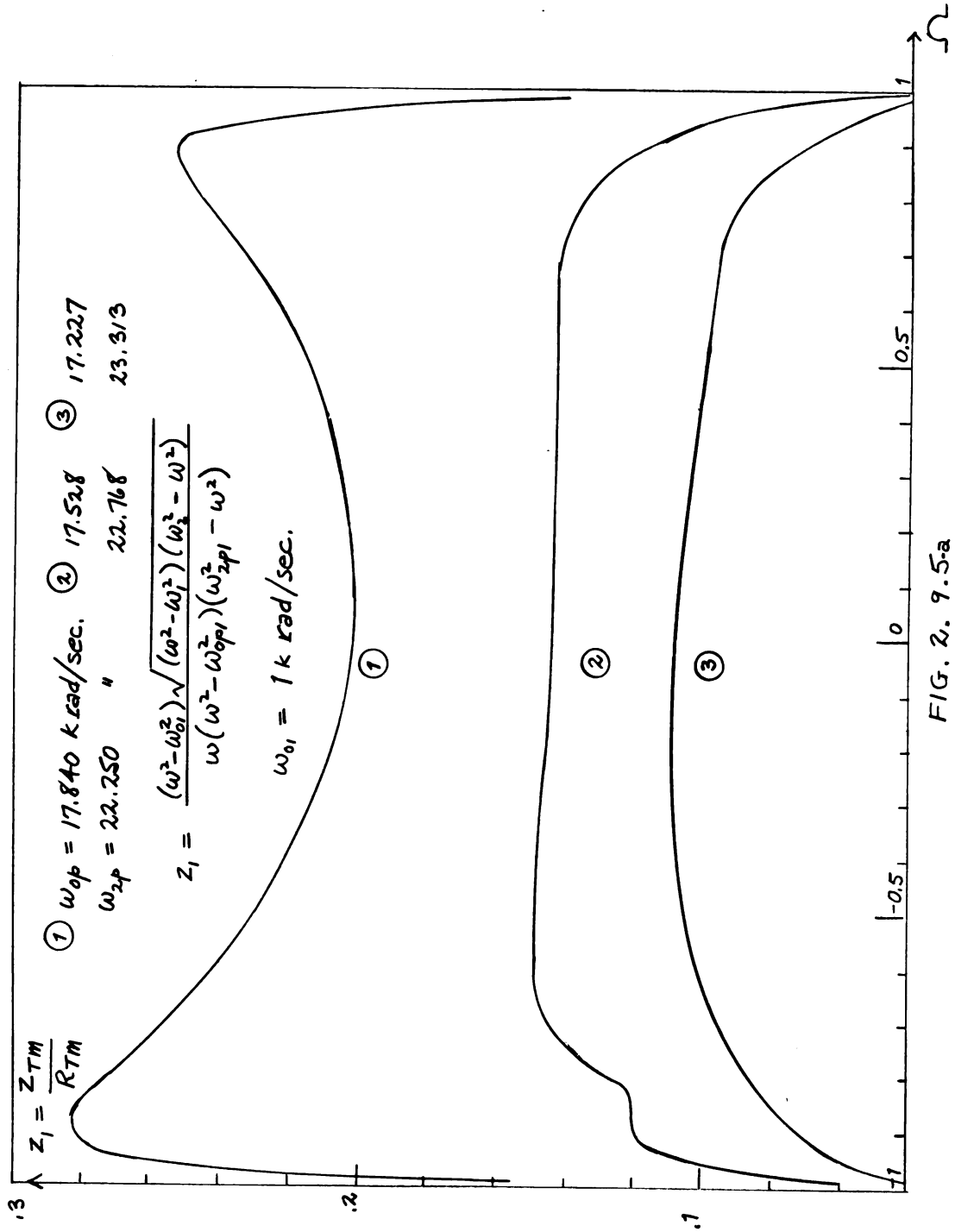


FIG. 2.9.4

Frequency transformation





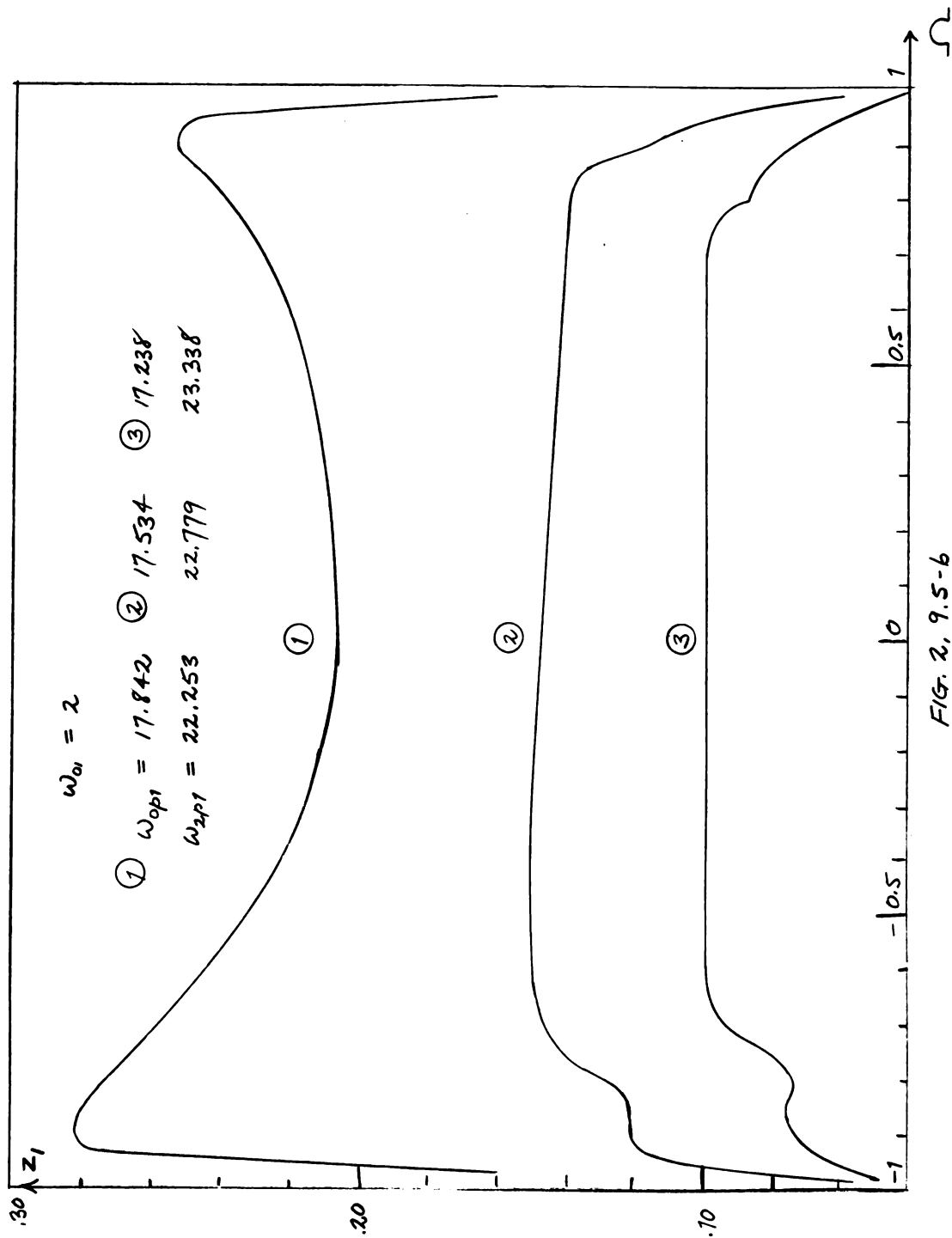


FIG. 2, 9.5-6

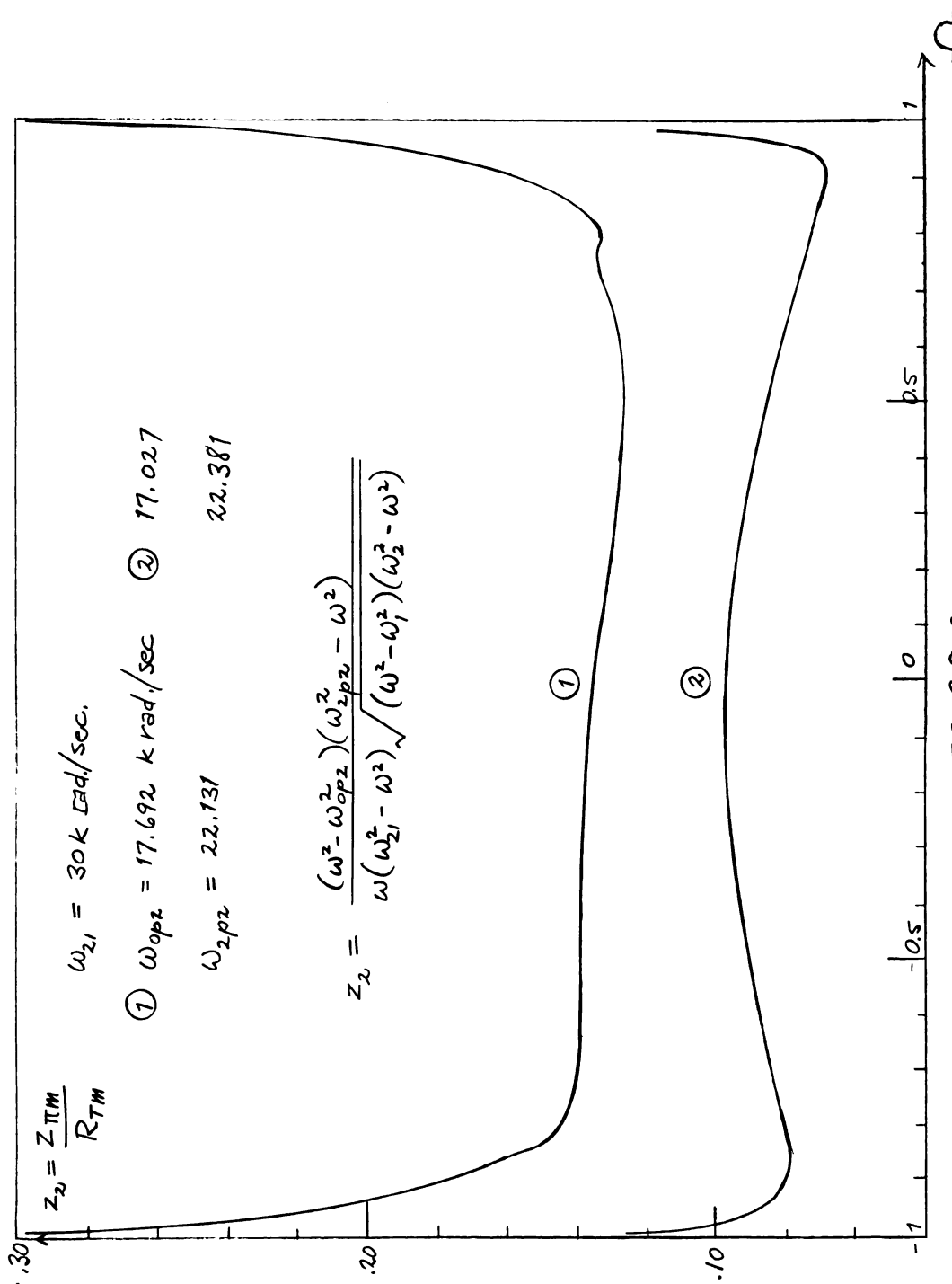


FIG. 2.9.6

The curves in Figs. 2.9.5 and 2.9.6 represent the variation of  $Z_{\pi_m}$  and  $Z_{T_m}$  in the pass-band, respectively. From these figures one can observe that the curves are either flat or have almost a Chebyshev character over a wider range of the pass band. The latter type is preferable. Note that these characteristics are considerably improved as compared to those of elementary sections. Among these impedance curves one should select the "best" curve. Since the best image impedance is the one which causes smallest insertion loss in a given effective pass-band, then this, of course, implies that the image impedance must have Chebyshev behavior in this effective pass-band [CA 1]. In order to obtain best image impedance one has to locate the critical frequencies of this image impedance in the block bands properly. To study the effect of the location of the critical frequencies on the form of the image impedance curves which are already indicated in Figs. 2.9.5 and 2.9.6, a new frequency scale,  $\Omega$ , is used. On this  $\Omega$ -axis, either  $\omega_{01}$  or  $\omega_{21}$  is transformed to infinity. The cut-off angular frequencies  $\omega_1$  and  $\omega_2$  correspond to  $\pm 1$ . On the other hand, the critical frequencies  $\Omega_{0p}$  and  $\Omega_{2p}$  are chosen so that they satisfy the relation

$$\Omega_{0p} + \Omega_{2p} = 0.$$

This relation will provide almost a symmetrical character for the image impedance in the pass band. On the  $\omega$ -axis,

$\angle = 0$  corresponds to an angular frequency which is located in the vicinity of  $\omega_a = \frac{1}{2}(\omega_1 + \omega_2)$ , the arithmetic means angular frequency. Thus, on the  $\omega$ -axis these impedance curves are also relatively symmetrical with respect to  $\omega_a$ . It can be observed that the form of these curves is almost independent of the location of  $\omega_{01}$  or  $\omega_{21}$ , which is the critical frequency of the impedance. Based on these observations one can locate  $\omega_{0p}$  and  $\omega_{2p}$ , perhaps by cut and try method on the computer, to obtain the desired image impedance characteristics.

## Chapter III

### THE FREQUENCY TRANSFORMATION AND THE TEMPLATE METHOD

#### 3.1 . Introduction.

In the design of ideal filters by the image parameter theory, as well as by the insertion loss theory, one of the problems is the determination of the number and the locations of the attenuation poles. One method useful in practical filter design involves use of the template. This method was developed by several authors, [RU 1, LA 1, SA 2, FO 1], each differing slightly from the others. The one discussed and used here is the one set forth by Rumpelt [RU 1], which can be applied to the low-pass, band-pass or high-pass filters.

In this chapter some techniques of frequency transformations are considered. The following sections are devoted to the development of these transformation formulas and their usage.

#### 3.2 . Template for the low-pass filters.

For this type of filters the normalized frequency

with respect to  $\omega_1$  is

$$\omega = \frac{\omega}{\omega_1}$$

where  $\omega_1$  is the cut-off angular frequency of the low-pass filter. The frequency transformation used is

$$\gamma = \frac{1}{2} \ln \left( \frac{\omega^2}{\omega^2 - 1} \right) \quad (3.2.1)$$

$$\omega > 1$$

Since the H-function of the prototype section of the low-pass filters is given as

$$H(j\omega) = \frac{\omega}{\sqrt{\omega^2 - \omega_1^2}} \quad (3.2.2)$$

then

$$H(\omega) = \frac{\omega}{\sqrt{\omega^2 - 1}}, \quad \omega > 1. \quad (3.2.3)$$

From Eqs. 3.2.1 and 3.2.3 the following relation is obtained

$$H(\gamma) = e^\gamma. \quad (3.2.4)$$

The image attenuation function is given as

$$A_I = \ln \left| \frac{1 + H}{1 - H} \right|.$$

Therefore, substituting Eq. 3.2.4 into this equation the following results

$$A_I = \ln \left| \frac{1 + e^\gamma}{1 - e^\gamma} \right| = \ln \coth \left| \frac{\gamma}{2} \right|. \quad (3.2.5)$$

On the other hand a simple  $m$ -derived section of the prototype has an  $H$ -function of the form

$$H(j\omega) = \frac{m\omega}{\sqrt{\omega^2 - \omega_1^2}} \quad (3.2.6)$$

At the attenuation pole  $\omega_{21}$  this  $H$ -function has the value of unity. Therefore we obtain

$$m = \frac{\sqrt{\omega_{21}^2 - \omega_1^2}}{\omega_{21}} \quad (3.2.7)$$

or, letting  $\Omega_{21} = \frac{\omega_{21}}{\omega_1}$ ,

$$\begin{aligned} m &= \frac{\sqrt{\Omega_{21}^2 - 1}}{\Omega_{21}} \\ &= e^{-\gamma_{21}} \end{aligned} \quad (3.2.8)$$

Thus, in general, for an  $m$ -derived section

$$H(\gamma) = e^{\gamma - \gamma_{21}}$$

and

$$A_I(\gamma - \gamma_{21}) = \ln \coth \left| \frac{\gamma - \gamma_{21}}{2} \right| \quad (3.2.9)$$

The total attenuation of a low-pass filter is

$$A_{I_t} = \sum_i A_I(\gamma - \gamma_i) \quad (3.2.10)$$

where  $\gamma_i$  is the attenuation pole.

Thus, the total attenuation curves can be obtained by plotting the curves represented by Eq. 3.2.9 along



the  $\gamma$ -axis such that the peaks of these curves occur at the locations of the attenuation poles on the  $\gamma$ -axis. The value of the attenuation at any frequency can be obtained by adding the ordinates of these curves at that frequency. Repeating this sum for every frequency will then yield the attenuation curve concerned. In Figs. 3.2.1 and 3.2.2 the template and the total attenuation curves are shown respectively.

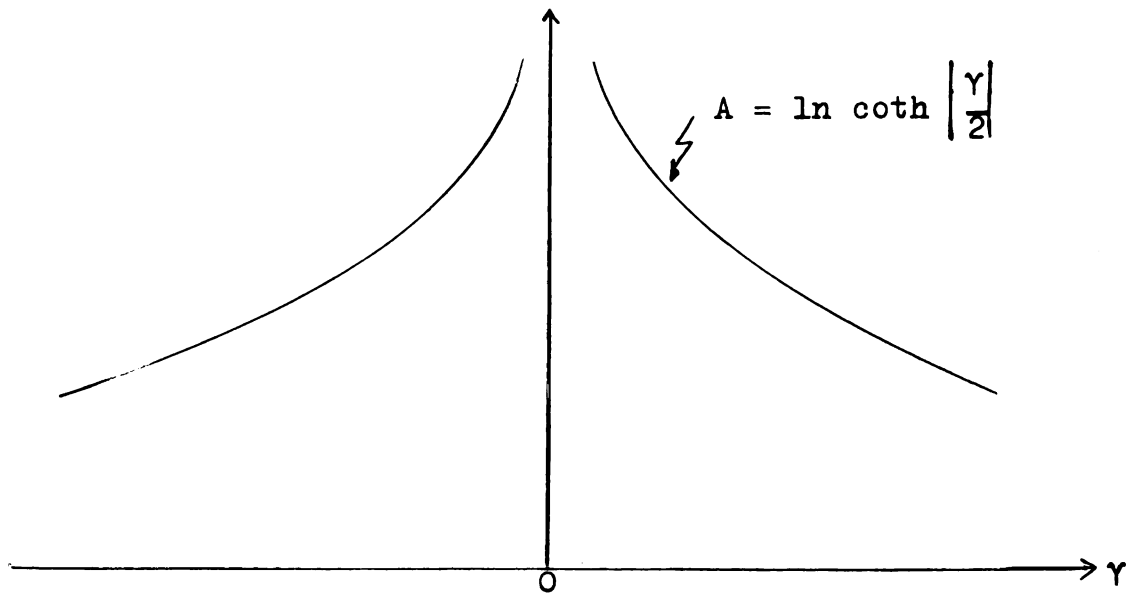


FIG. 3.2.1

Template curve

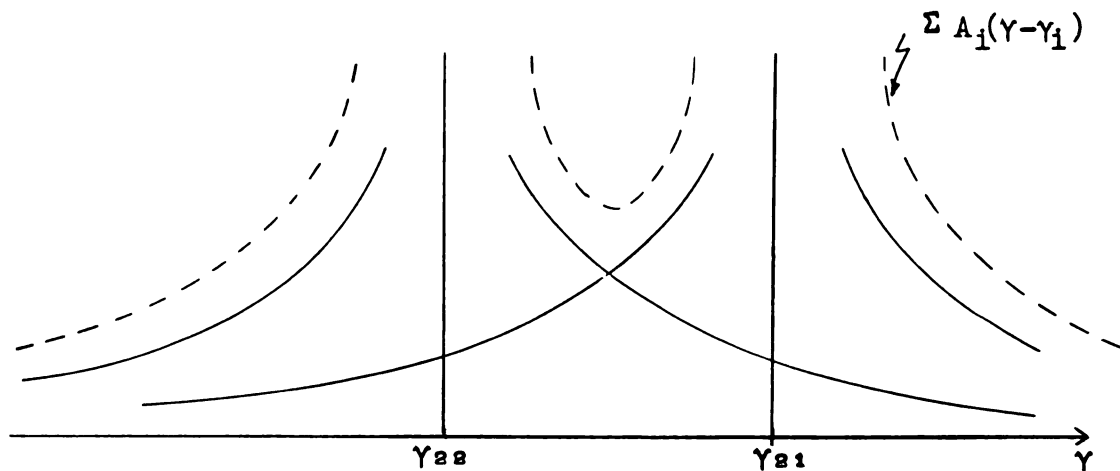


FIG. 3.2.2

Total attenuation

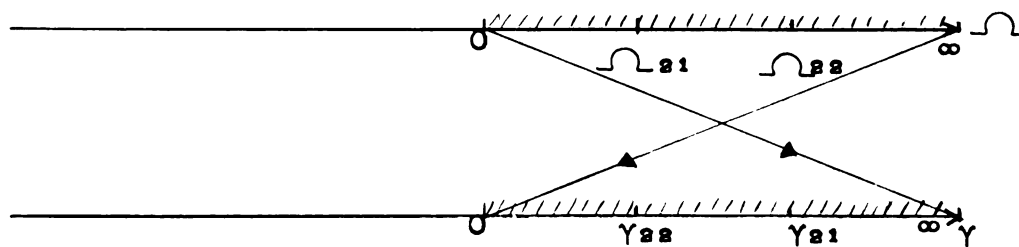


FIG. 3.2.3

Frequency transformation

### 3.3 . Template for the band-pass filters.

There are two types of band-pass attenuation

curves. The first is the frequency symmetrical attenuation curve and the second one is that of the frequency unsymmetrical attenuation curve. For the first type of attenuation curves the development and the use of the template method can be reduced to that of the low-pass filter method. The development of the second type which is more general, will be discussed separately.

### 3.3.1. Frequency symmetrical band-pass filter.

Let  $\omega_1, \omega_2$  be the cut-off frequencies of the band-pass filter and  $\omega_m = \sqrt{\omega_1 \omega_2}$  the geometric mean of these frequencies. The frequency transformation used for the frequency symmetric band pass filter is

$$\Omega = \frac{\omega^2 - \omega_m^2}{\omega(\omega_2 - \omega_1)} \quad (3.2.11)$$

Fig. 3.3.1 shows how the  $\omega$ -axis is transformed into the  $\Omega$ -axis by this transformation. It can be observed from this figure that the  $\Omega$ -scale is symmetrical with respect to  $\Omega = 0$ , which corresponds to  $\omega_m$  in the  $\omega$ -scale. Since the curve of the attenuation is also symmetrical with respect to a vertical axis passing through the zero value of the  $\Omega$ -axis, if there exists an attenuation at  $\omega_\alpha$  in the upper stop band, an identical attenuation will be obtained on the lower stop band corresponding to the mirror image of  $\omega_\alpha$ . Therefore the design of the band-pass filter is reduced to the design of a low-pass filter. Once this low-pass design is obtained,

the desired band-pass filter is then obtained by substituting Eq. 3.2.11 into the element values formulas.

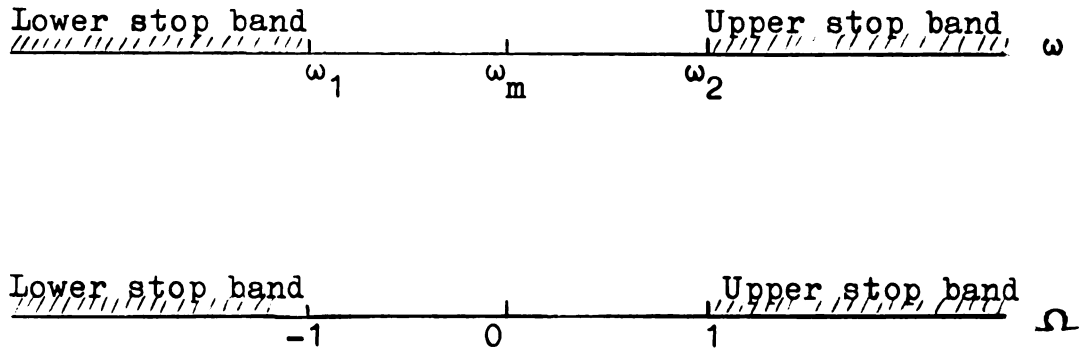


FIG. 3.3.1

### Frequency transformation

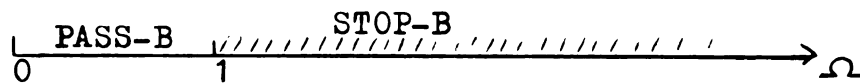


FIG. 3.3.2

The range which is considered  
as low-pass range on the  $\Omega$  scale

### 3.3.2. Frequency unsymmetric band-pass filters.

The several methods of frequency transformations considered here for the frequency unsymmetric filters

differ slightly from that of symmetrical case. The reason it is necessary to have various modifications is that one can then make a choice as to which form is more appropriate to apply to a certain problem in order to treat it in a less complicated manner. These transformations are not only useful in treating the attenuation characteristic but also useful for treating the image impedances. In the pass-band, the consideration of the impedances is particularly essential.

In the following discussions it is necessary to consider the H-functions of the band-pass filters. They are of the following forms

$$H = K_1 \sqrt{\frac{(s^2 + \omega_1^2)}{(s^2 + \omega_2^2)}} \quad (3.2.12-a)$$

or

$$H = K'_1 \sqrt{\frac{(s^2 + \omega_2^2)}{(s^2 + \omega_1^2)}} \quad (3.2.12-b)$$

Only these two forms are considered since for all other forms of the H-functions the treatment can be reduced to the treatment of the above form of the H-functions. Note that the frequency dependence part of these H-functions is similar to that of the H-functions of the basic sections. Three types of frequency transformations are considered here. The last two types are frequently used in the current publications. The H-functions are in Eqs.

3.2.12-a and -b and the composition of these two, i.e.,

$$H = \frac{1}{\sqrt{1 + K''}} \frac{(s^2 + \omega_0^2)}{\sqrt{(s^2 + \omega_1^2)(s^2 + \omega_2^2)}} \quad (3.2.13)$$

where  $s = j\omega$ ,

$\omega_0^2$  : confluent frequency ,

$\omega_1, \omega_2$  : cut-off frequencies ,

$K''$  : a constant.

In the next three sections the various frequency transformations that can be used to study the frequency unsymmetrical filter characteristics are developed.

3.3.2.1. The first method of transformation.

In this method one directly transforms the frequency by not going first through the normalization. This transformation is only useful for the attenuation function. The transformation used is

$$\gamma = \frac{1}{2} \ln \left( \frac{(\omega^2 - \omega_1^2)}{(\omega^2 - \omega_2^2)} \right) \quad (3.2.14)$$

$$\gamma_\infty = \ln \frac{\omega_2}{\omega_1} \quad (3.2.15)$$

$$\begin{array}{ll} \omega_1 & \longrightarrow -\infty \\ \omega_2 & \longrightarrow +\infty \\ 0 & \longrightarrow -\gamma_\infty \\ \infty & \longrightarrow 0 \end{array}$$

Thus here one does not utilize the  $\omega$ -scale but goes straight from the  $\omega$ -scale to the  $\gamma$ -scale.

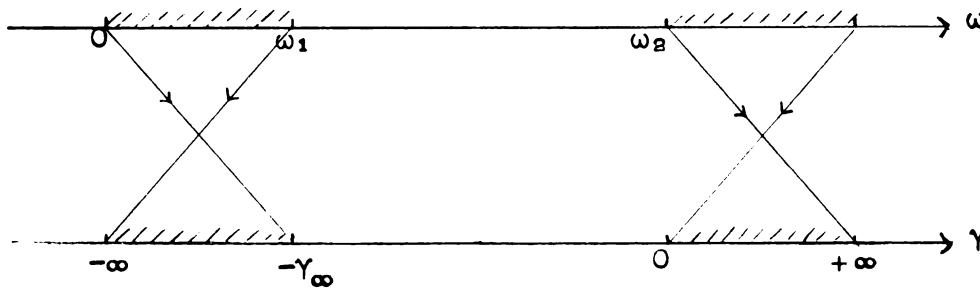


FIG. 3.3.3

#### Frequency axis transformation

The basic section\* has poles either at infinity or at the zero frequency. The H-functions of the sections for the frequency unsymmetric filters have the same forms as those in Eqs. 3.2.12-a and -b. The first one has a pole at infinity and the second one has a pole at the origin. Since the elementary sections of the filters to be discussed in this thesis have the same H-functions except for a constant factor, the basis for the template method here will be the H-functions mentioned above. Thus for the basic sections, the constant of the

---

\* The basic section is discussed in Chapter II, section 2.5.

H-functions are

$$K = 1 \quad \text{and}$$

$$K' = \frac{\omega_1}{\omega_2} \quad . \quad (3.2.16)$$

Therefore from Eqs. 3.2.14, 3.2.15, 3.2.12-a and -b we have

$$H = e^{+\gamma} \quad \text{or} \quad (3.2.17)$$

$$H = e^{-\gamma_\infty} e^{-\gamma} = e^{-(\gamma + \gamma_\infty)} .$$

The attenuation is given by

$$A_I = \ln \coth \left| \frac{\gamma}{2} \right| \quad \text{or} \quad (3.2.18)$$

$$A_I = \ln \coth \left| \frac{\gamma + \gamma_\infty}{2} \right| .$$

### 3.3.2.2. The second method of transformation.

This method [BE 2, TE 1] is also developed without first making a normalization. Thus it is also only useful for the attenuation consideration. It differs from the first method in that the transformed frequency is symmetric with respect to its origin. The transformation used is

$$\gamma = \frac{1}{2} \ln \frac{\omega^2 - \omega_1^2}{\omega^2 - \omega_2^2} \quad (3.2.19)$$

$$\gamma_\infty = \frac{1}{2} \ln \frac{\omega_2}{\omega_1}$$



and

$$\omega_m = \sqrt{\omega_1 \omega_2}$$

$$\begin{array}{ll} 0 & \longrightarrow -\gamma_\infty \\ +\infty & \longrightarrow +\gamma_\infty \\ \omega_1 & \longrightarrow -\infty \\ \omega_2 & \longrightarrow +\infty \\ \pm j\omega_m & \longrightarrow 0 \end{array} .$$

Thus for the basic section we have

$$\begin{aligned} H &= e^{\gamma - \gamma_\infty} & \text{or} \\ H &= e^{-(\gamma + \gamma_\infty)} \end{aligned} \quad (3.2.20)$$

Therefore the attenuation function is

$$\begin{aligned} A_I &= \ln \coth \left| \frac{\gamma - \gamma_\infty}{2} \right| \\ \text{or} \\ A_I &= \ln \coth \left| \frac{\gamma + \gamma_\infty}{2} \right| \end{aligned} \quad (3.2.21)$$

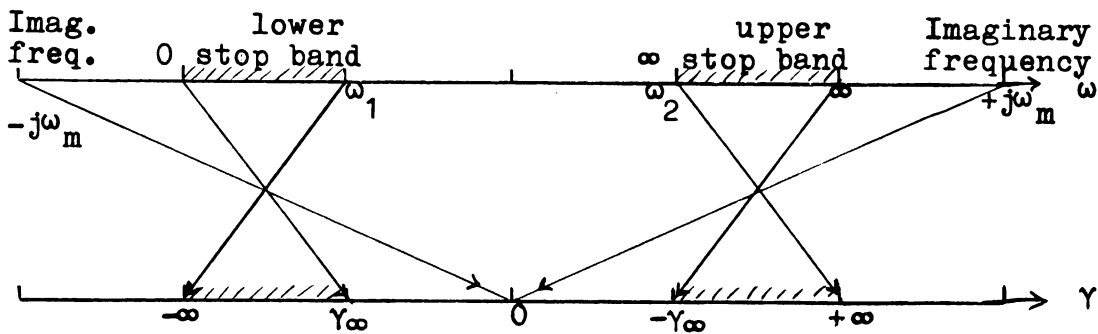


FIG. 3.3.4

Frequency transformation  
γ - axis

The above formula can be extended to the cases when the sections have finite poles. Indeed, suppose there are attenuation poles at  $\gamma_i$  or  $-\gamma_i$ , then the attenuation function becomes

$$A_I = \ln \coth \left| \frac{\gamma - \gamma_i}{2} \right| \quad \text{or} \quad (3.2.22)$$

$$A_I = \ln \coth \left| \frac{\gamma + \gamma_i}{2} \right| .$$

It is important to note that the template to be used for this case will depend on the band width.

### 3.3.2.3. The third method.

In this method, normalization of the frequency variable is performed first and then the transformation follows. The frequency normalization considered here is also useful in treating the image impedances. The normalization is sometimes called the Coth-transformation. This transformation has been used by many authors, particularly by Cauer [CA 1].

#### a. The normalization (First step transformation)

$$\eta = \frac{\omega}{\omega_m} , \quad \omega_m = \sqrt{\omega_1 \omega_2}$$

$$\omega = \alpha \frac{\eta^2 + 1}{\eta^2 - 1} = \frac{\omega_2 - \omega_1}{\omega_2 + \omega_1} \frac{\omega^2 + \omega_m^2}{\omega^2 - \omega_m^2}$$

$$\eta^2 = \frac{\omega + \alpha}{\omega - \alpha} , \quad \omega^2 = \omega_m^2 \frac{\eta^2 + \alpha}{\eta^2 - \alpha}$$

$$\alpha = \frac{\omega_2 - \omega_1}{\omega_2 + \omega_1}$$

Sometimes an inverted  $\overline{\omega}$ -scale is used, i.e.,  $\overline{\omega}$  and this provides some simplicities. Thus we will use this  $\overline{\omega}$ -scale in a greater part of the application of this method.

b. The transformation (second step transformation)

$$\overline{\omega} = \frac{1}{\omega}$$

$$\gamma = \frac{1}{2} \ln \frac{\overline{\omega} + 1}{\overline{\omega} - 1} \quad (3.2.23)$$

$$\frac{1}{\alpha} = \overline{\alpha} \longrightarrow \frac{1}{2} \ln \frac{\omega_2}{\omega_1} = \gamma_{\infty}$$

$$-\frac{1}{\alpha} = -\overline{\alpha} \longrightarrow \frac{1}{2} \ln \frac{\omega_1}{\omega_2} = -\gamma_{\infty}$$

$$1 \longrightarrow \infty$$

$$-1 \longrightarrow -\infty$$

Thus for the basic sections one has

$$H = \sqrt{\frac{\overline{\alpha} + 1}{\overline{\alpha} - 1}} \sqrt{\frac{\overline{\omega} + 1}{\overline{\omega} - 1}} \quad \text{or} \quad (3.2.24)$$

$$H = \sqrt{\frac{\overline{\alpha} + 1}{\overline{\alpha} - 1}} \sqrt{\frac{\overline{\omega} - 1}{\overline{\omega} + 1}}$$

Then, substituting Eqs. 3.2.23 into Eqs. 3.2.24

results in (3.2.25)

$$H = e^{\gamma - \gamma_{\infty}} \quad \text{or} \quad H = e^{-(\gamma + \gamma_{\infty})}$$

Hence,

$$A_I = \ln \coth \left| \frac{\gamma - \gamma_\infty}{2} \right|$$

or

$$A_I = \ln \coth \left| \frac{\gamma + \gamma_\infty}{2} \right| .$$

When the sections with finite poles exist then an analogous method can be used. For example, if there are poles at  $\gamma_1$  and  $-\gamma_1$ , then

$$A = \ln \coth \left| \frac{\gamma \pm \gamma_1}{2} \right| . \quad (3.2.27)$$

As has been mentioned earlier, the normalization can also be applied to the image impedances. The following section is devoted to this matter. The impedances concerned are those which appeared in the development of the filters in an earlier discussion in Chapter II.

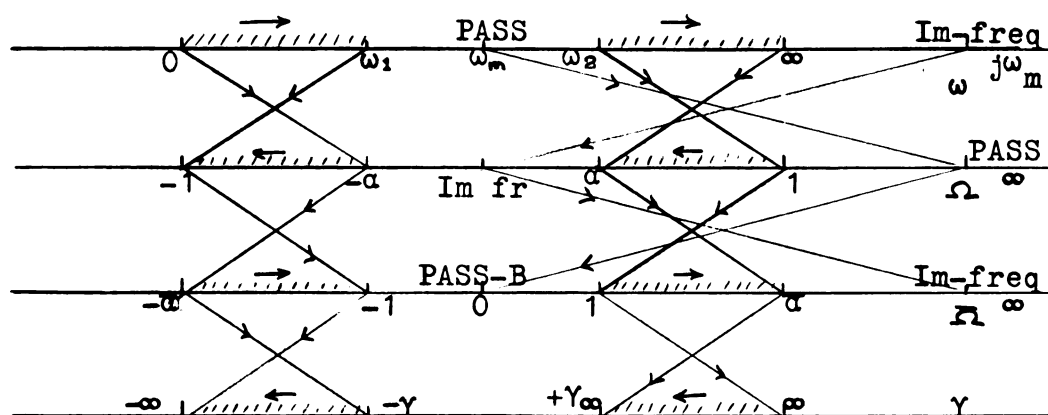


FIG. 3.3.5

First step and second step transformation

### 3.4 . Impedance with normalized frequency.

The image impedances are of the following form

$$Z_{\pi} = \frac{R_{01}}{\omega} \frac{(\omega^2 - \omega_{01}^2)}{\sqrt{(\omega^2 - \omega_1^2)(\omega^2 - \omega_2^2)}} \quad (3.4.1)$$

$$Z_T = \frac{R_{21}}{\omega} \frac{\sqrt{(\omega^2 - \omega_1^2)(\omega^2 - \omega_2^2)}}{(\omega_{21}^2 - \omega^2)}$$

where  $R_{01}$  and  $R_{21}$  are constants.

The following derivations are given to show how the  $\omega$  variables are replaced by the  $\Omega$  variables. Fig. 3.4.1 shows the scales of  $\omega$ ,  $\Omega$  and  $\bar{\Omega}$ . Also it shows the locations of the critical frequencies of these impedances. Notice the locations of the points  $\Omega_{01}$  and  $\Omega_{21}$  in  $-1 < \Omega < 1$ . These points are the reciprocals of the attenuation poles  $\bar{\Omega}_{01}$  and  $\bar{\Omega}_{21}$ . It turns out that  $\Omega_{01}$  and  $\Omega_{21}$  are in the vicinity of the extremum locations of image impedances  $Z_{\pi}$  and  $Z_T$ .

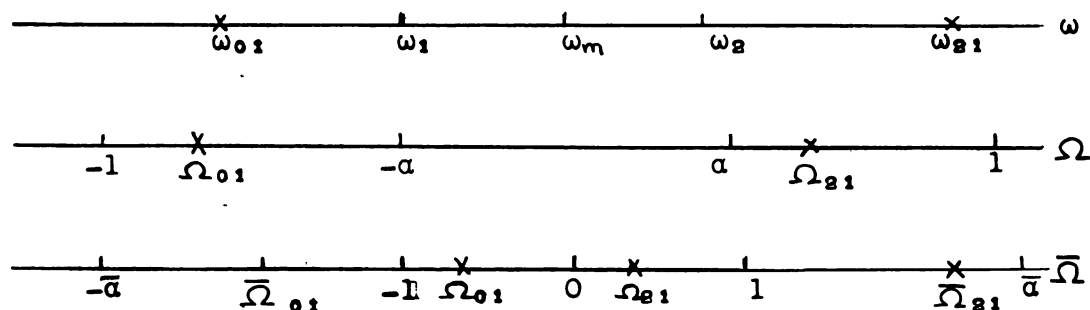


FIG. 3.4.1

The derivation of the changing of variables from  $\omega$  variables to the  $\bar{\omega}$  variables is

$$\omega^2 - \omega_1^2 = \omega_m^2 \left[ \frac{\bar{\omega} + \alpha}{\bar{\omega} - \alpha} - \frac{1 - \alpha}{1 + \alpha} \right] = \omega_m^2 \frac{2\alpha (\bar{\omega} + 1)}{(\bar{\omega} - \alpha)(1 + \alpha)}$$

$$\omega_2^2 - \omega^2 = \omega_m^2 \left[ \frac{1 + \alpha}{1 - \alpha} - \frac{\bar{\omega} + \alpha}{\bar{\omega} - \alpha} \right] = \omega_m^2 \frac{2\alpha (\bar{\omega} - 1)}{(\bar{\omega} - \alpha)(1 - \alpha)} .$$

On the  $\bar{\omega}$ -scale:

$$Z_{\pi} = \frac{R_{01}}{\omega_m} \frac{\sqrt{1 - \alpha^2}}{\bar{\omega}_{01} - \alpha} \frac{\sqrt{\bar{\omega} - \alpha}}{\sqrt{\bar{\omega} + \alpha}} \frac{(\bar{\omega}_{01} - \bar{\omega})}{\sqrt{\bar{\omega}^2 - 1}}$$

$$Z_T = \frac{R_{21}}{\omega_m} \frac{\bar{\omega}_{21} - \alpha}{\sqrt{1 - \alpha^2}} \sqrt{\frac{\bar{\omega} - \alpha}{\bar{\omega} + \alpha}} \frac{\sqrt{\bar{\omega}^2 - 1}}{(\bar{\omega} - \bar{\omega}_{21})} .$$

(3.4.2)

On the  $\bar{\omega}$ -scale:

$$Z_{\pi} = \frac{R_{01}}{\omega_m} \frac{\sqrt{\alpha^2 - 1}}{\bar{\alpha} - \bar{\omega}_{01}} \sqrt{\frac{\bar{\alpha} - \bar{\omega}}{\bar{\alpha} + \bar{\omega}}} \frac{(\bar{\omega} - \bar{\omega}_{01})}{\sqrt{1 - \bar{\omega}^2}}$$

$$Z_T = \frac{R_{21}}{\omega_m} \left( \frac{\sqrt{\alpha^2 - 1}}{\bar{\alpha} - \bar{\omega}_{21}} \right)^{-1} \sqrt{\frac{\bar{\alpha} - \bar{\omega}}{\bar{\alpha} + \bar{\omega}}} \frac{\sqrt{1 - \bar{\omega}^2}}{(\bar{\omega}_{21} - \bar{\omega})} .$$

(3.4.3)

From inspection of the curves of these impedances it is seen that these are not satisfactorily suited for terminating impedances. Note also, on the  $\bar{\omega}$ -scale the two points  $\bar{\omega}_{01}$  and  $\bar{\omega}_{01}$  and also  $\bar{\omega}_{21}$  and  $\bar{\omega}_{21}$  are reciprocals of each other. This fact also

shows clearly on Fig. 2.10.1 when  $\omega_{21}$  or  $\omega_{01}$  approaches the cut-off frequencies then the minimum or maximum points of the image impedance curves in the pass-band also approach the cut-off frequencies. This suggests that these extremum points are in the vicinity of  $\omega_{01}$  or  $\omega_{21}$  in the pass-band on the  $\omega$ -scale.

## Chapter IV

### TERMINATING SECTIONS

#### 4.1 . Introduction.

The image impedances of an image parameter filter are functions of frequencies, whereas the filter is usually terminated in load impedances at both ends which are purely resistive. Thus to minimize the loss at least in the pass band, it is necessary to provide a high order image impedance at the terminal pairs of the filter, so that the mismatch at the terminal pairs is somewhat corrected. This can be done by use of so-called terminating sections [RE 1]. The whole filter then can be considered as being composed of the intermediate sections and the terminating sections. The intermediate section consists of cascade connected elementary sections, which are prototype sections corresponding to the type of the filter, i.e., low-pass, band-pass or high-pass filters. The terminating sections, on the other hand, are also elementary sections or a composition of elementary sections with a higher ordered impedance at one of its ports. One method by which terminating sections can be generated is by the procedures of repeated  $m$ -derivations as



described by Zobel [20 1]. This kind of terminating section, although possessing the desired higher ordered image impedance, is in general rather cumbersome in structure, i.e., it contains an unnecessarily high number of elements and hence is not practical. However, as it will be shown in this thesis, this does not constitute a major objection since by using a network transformation, cascaded Zobel sections can be transformed into the known economical terminating sections. This approach has the advantage over the other methods [T0 1] that it can easily be extended to the general case. These terminating sections suffer from the fact that the poles of their attenuation function are coincident with the control frequencies of their image impedances. These sections then are called "associated sections". It seems that their use limits the design procedure. The other types of filters, the so-called "disassociate sections" will be considered next.

#### 4.2 . The disassociate filter.

The main feature of this filter section is that the attenuation poles do not coincide with the critical frequencies of the image impedances. Therefore they cannot be considered as a collection of matched elementary sections. However they can be considered as the filters

between image parameter filters and insertion loss filters. The notion of this kind of filters has been investigated rather thoroughly in recent years by several authors [CO 1, BE 1, RO 1]. The basic idea involved in these filters comes from the fact that for the lattice sections or symmetric ladder sections, the image impedance critical frequencies do not necessarily coincide with the attenuation poles.

Collins [CO 1], in his research directed at generating new kinds of structures, comes out with dissociate filters produced by using the following procedures:

1. Prescribe the image transmission factor  $\theta$  of the filter to be designed defined by

$$\text{Tanh } \theta = \sqrt{\frac{Z_{sc}}{Z_{oc}}} .$$

2. Prescribe the image impedance of the filter, the critical frequencies, none of which coincide with that of the attenuation poles. The image impedance is:

$$Z_I = \sqrt{Z_{oc} Z_{sc}} .$$

3. The frequencies of the unity value of  $\text{Tanh } \theta$  depend on the parameters  $\underline{m}$  of Zobel. The critical frequencies of the image impedance  $Z_I$  depend on the parameters  $\underline{n}$  which are

not equal to the parameter  $m$ . These parameters are related to the critical frequencies of  $Z_I$  and the relation is identical in form to that relation between the parameters  $m$  and the attenuation poles.

$$4. \quad Z_{oc} = \frac{Z_I}{\tanh \theta}$$

$$Z_{sc} = Z_I \tanh \theta$$

5. Synthesize  $Z_{oc}$  and  $Z_{sc}$  by the zero shifting technique. The resulting filter is the desired filter. It must have the above open and short circuit impedances,  $Z_{oc}$  and  $Z_{sc}$ .

Thus both the image parameter formulations and insertion loss synthesis are involved in this procedure.

Rowland also developed sections of disassociate filters [RO 1,2]. However his section has image impedances of  $m$ -derived type but the critical frequencies of the image impedance do not coincide with the attenuation poles. Later he has shown how his method can be generalized [RO 3].

Belevitch [BE 3] tabulated some of the disassociate filters in which some sections developed earlier are included. Some extensions for higher order image impedances are also given. In the treatment of the disassociate filters the above authors have been dealing

only with the case of low-pass and high-pass filters. However as Collins [CO 1] mentioned, his procedure is also applicable to the band-pass filters. There has not been any explicit discussion on the problem of frequency unsymmetric band-pass disassociate filters.

It appears that, although the disassociate filters provide some savings on the number of elements, they still require relatively complicated calculations as compared to the associated sections. Thus the use of the image parameter theory for the design of filters is still a simple one. A close comparison will easily show that, the disassociated filters will hardly contribute to the attenuation of the stop band, because they do not possess as many attenuation poles as the image parameter T.S. with the same order of image impedance. As a result, we might be able to reduce the number of intermediate sections in the image parameter filters, thereby reducing the number of elements.

The rest of the sections in this chapter are devoted to discussions on the derivation of the terminating sections, i.e., associated sections. The discussion is kept in general and it is applicable to low-pass, high-pass and band-pass filters terminating sections.

The resulting sections when applied to the low-pass filter case agree with the result obtained by Tokad [TO 1] developed by a different approach.

Some network equivalences, which are very important for the further development of our sections, will also be considered in the next following section.

#### 4.3 . The image parameter ladder terminating sections.

The terminating section to be considered is a general one. Some network transformations and the network equivalences are needed for the derivation of these terminating sections.

##### 4.3.1. The transformation and the equivalent network.

This transformation was also used by Tokad in his development of the low-pass terminating sections [TO 1]. It can be best shown by means of diagrams (Figs. 4.1, 4.2, 4.3). Figure 4.1 shows the original general half section. Figures 4.2 and 4.3 are the resulting network on performing the transformation on the original network of Fig. 4.1.

The real parameter  $s$  has values in the interval  $0 < s < 1$ . It is obvious from these figures that the resulting networks, i.e., the networks in Figs. 4.2 and 4.3 are equivalent networks. The network of Fig. 4.2 will be designated as  $T_{\pi}$  network and that of Fig. 4.3 as  $T_T$  network.

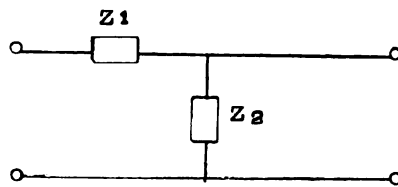


FIG. 4.1

Original section

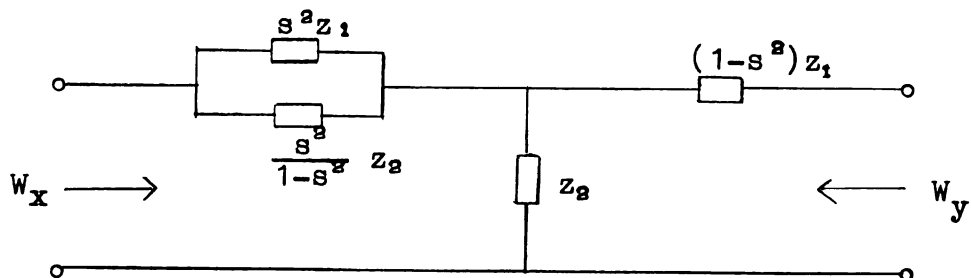


FIG. 4.2

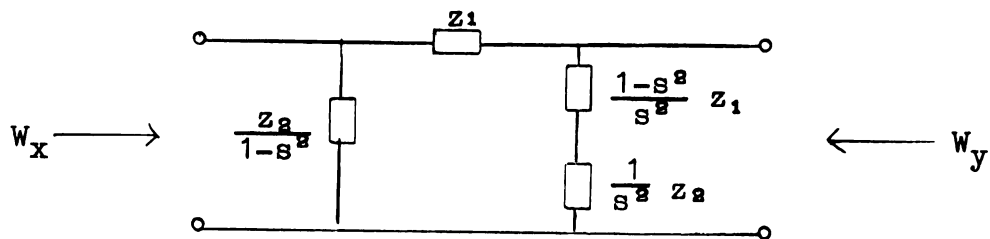
The  $T_T$  sections

FIG. 4.3

The  $T_\pi$  section

$$W_x = \frac{z_2 \sqrt{1 + \frac{z_2}{z_1}}}{(1-s^2) + \frac{z_2}{z_1}} \dots (4.1.1), \quad W_y = \frac{z_1 \left[ (1-s^2) + \frac{z_2}{z_1} \right]}{\sqrt{1 + \frac{z_2}{z_1}}} \dots (4.1.2)$$

#### 4.3.2. The derivation of the terminating sections (TS).

For this purpose we use  $m$ -derived sections. The higher the order of the image impedance which is desired, the more repeated  $m$ -derived section has to be utilized. Terminating sections, having third and fourth order image impedances, will be derived. Higher ordered image impedance possessing terminating sections can be obtained by using more repeated  $m$ -derived sections by the same method. For convenience the  $m$ -derived sections to be used for this purpose are shown in the following diagrams, i.e., Fig. 4.4 and Fig. 4.5. They are the shunt  $m$ -derived and the shunt-series  $m m'$ -derived sections. The procedure for obtaining the terminating section having a third order image impedance is as follows:

1. Cascade the sections in Fig. 4.4 and Fig. 4.5 such that there is an image impedance matching at their interconnected terminal pairs. The resulting network is the network of Fig. 4.6.
2. Make the rearrangement as in Fig. 4.7. The parameter  $s$  is so chosen that the section parallel to  $Z_Y$  is the  $T_\pi$  section.
3. The result of replacing  $T_\pi$  by  $T_T$  in item 2, is given in Fig. 4.8. This is the desired ladder terminating section.

It should be noted that a minimum number of ladder arms

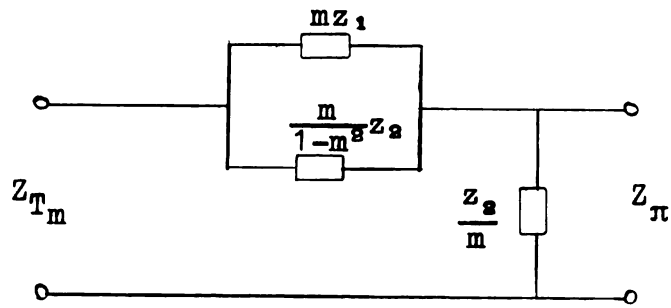


FIG. 4.4

Shunt derived section

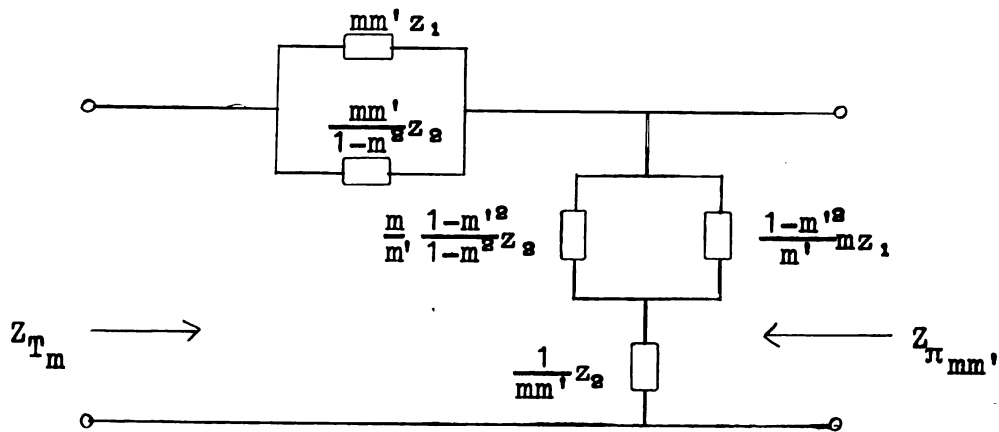


FIG. 4.5

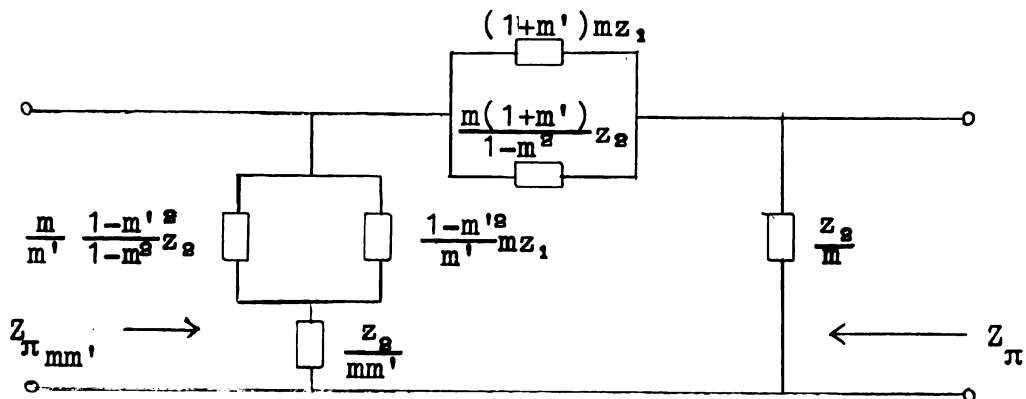
Shunt-series  $mm'$  derived

FIG. 4.6



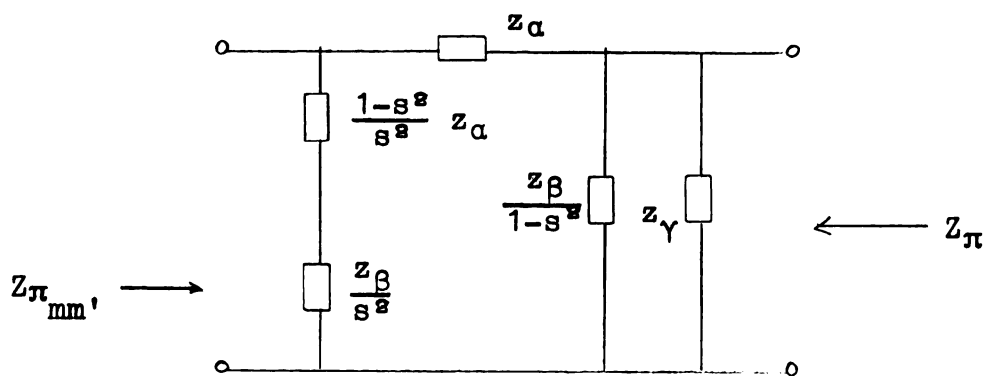


FIG. 4.7

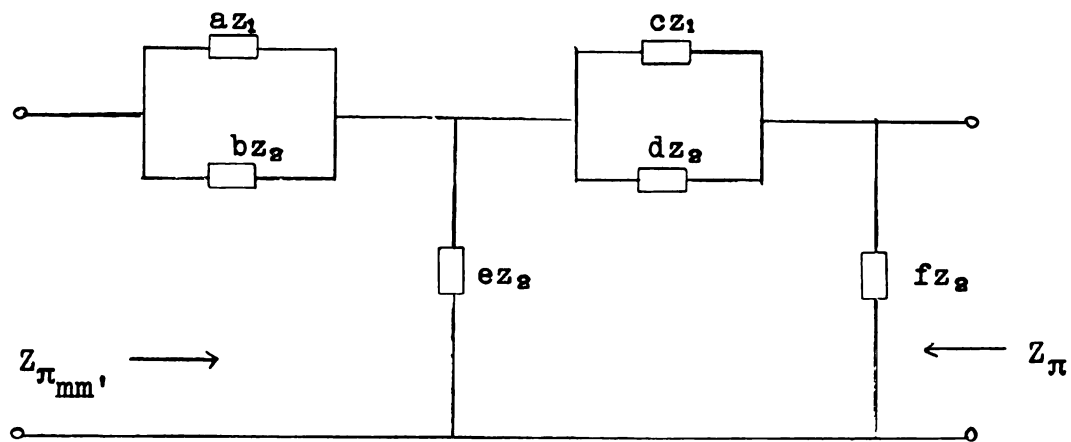


FIG. 4.8

Terminating section

$$a = (1 - m'^2)m$$

$$b = m \frac{1 - m'^2}{1 - m^2}$$

$$c = mm'(1 + m')$$

$$d = \frac{mm'(1 + m')}{1 - m^2 m'^2}$$

$$e = \frac{1}{m}$$

$$f = \frac{1}{mm'}$$

will be obtained if the rearrangement by equivalences, as shown in Fig. 4.7, is always started from the side of the network with the higher ordered image impedance.

If a higher ordered image impedance is required at one of the terminal pairs, higher order derived sections will be used. Thus, for example, if an  $mm'm''$ -derived section is utilized the terminating section of fourth order image impedance will be obtained as shown in Fig. 4.9.

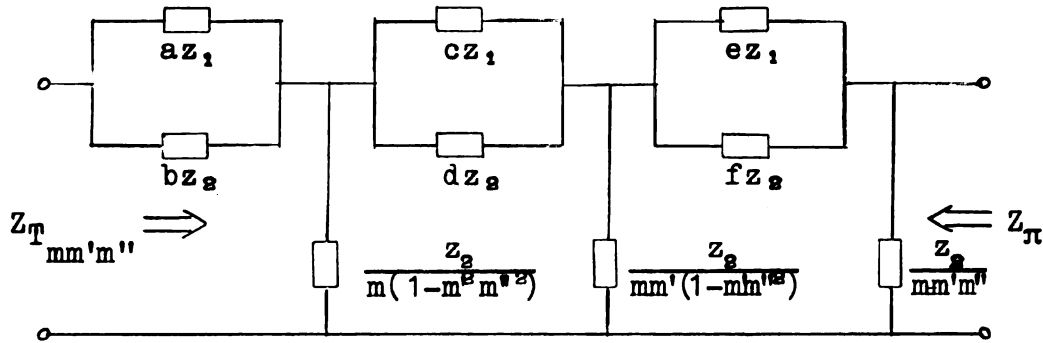


FIG. 4.9

$$a = \frac{m(1-m'^2)}{1-m'^2 m''^2}$$

$$b = \frac{m(1-m'^2)}{(1-m'^2 m''^2)(1-m'^2)}$$

$$c = \frac{mm'(1+m')}{(1-m'^2 m''^2)(1+m' m''^2)}$$

$$d = \frac{mm'(1+m')}{(1+m' m''^2)(1-m'^2 m''^2)(1-m'^2)}$$

$$e = \frac{(1+m' m'')(1+m')}{(1+m' m''^2)} mm' m''$$

$$f = \frac{(1+m' m'')(1+m')}{(1+m' m''^2)} \frac{mm' m''}{[1+m(m' m'' + m'^2 m'' - m)]}$$

The other type of terminating sections can also be derived in a similar manner using the transformed network in Fig. 4.3. These terminating sections are given in Figs. 4.10 and 4.11. It can be shown that these are the dual to those in Figs. 4.4, 4.8 and 4.9.

Since our purpose is to investigate frequency unsymmetric band-pass filters, the T.S. derived from the basic sections and E.S.Z will be as shown in Figs. 4.12, 4.13, and 4.14, respectively.

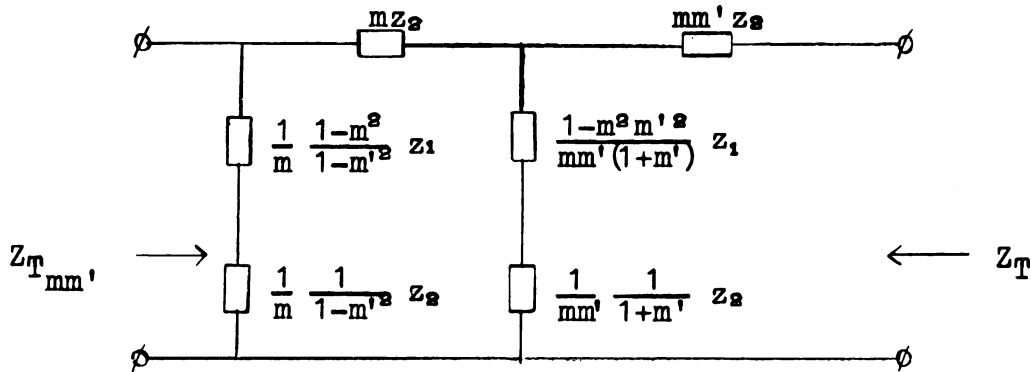


FIG. 4.10

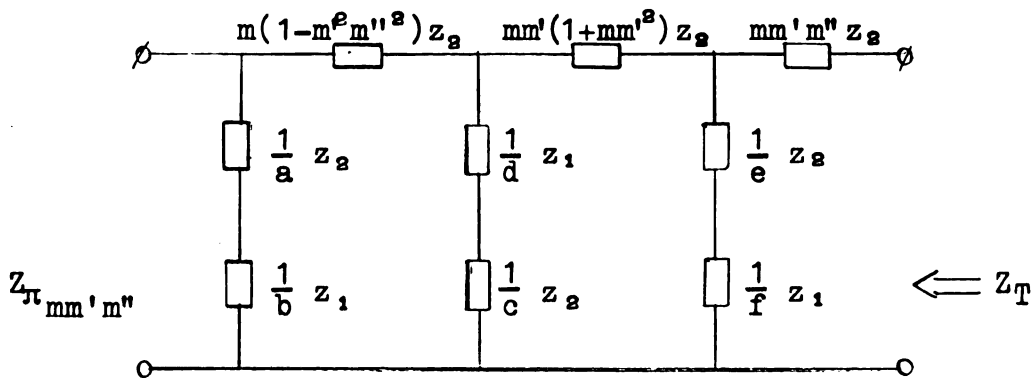


FIG. 4.11

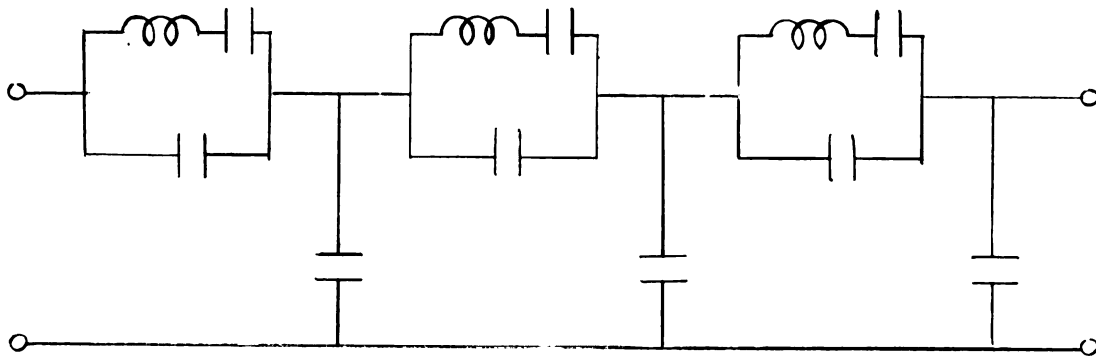


FIG. 4.12

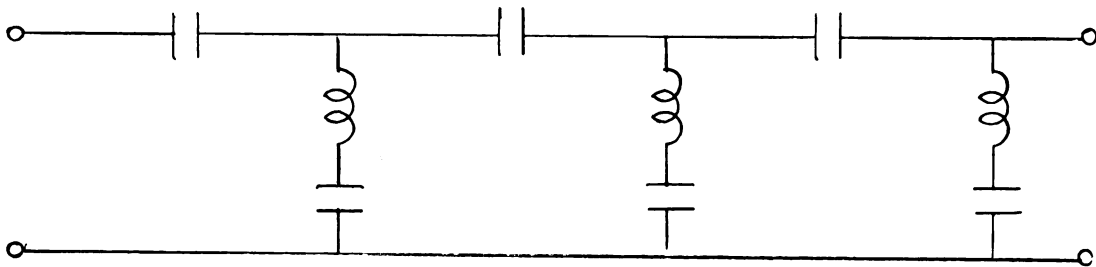


FIG. 4.13

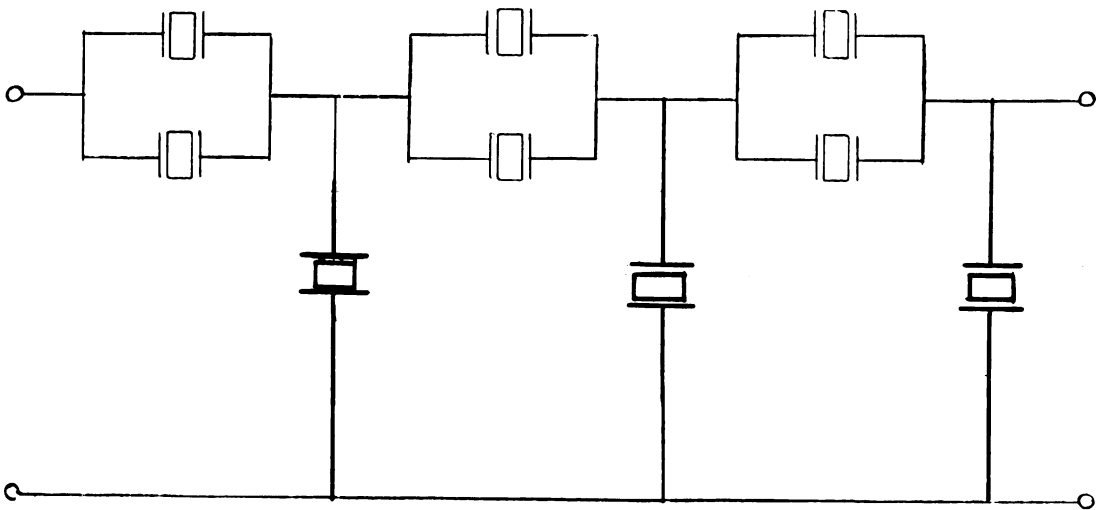


FIG. 4.14

## Chapter V

### FILTER DESIGN I DERIVATION OF FORMULAS

#### 5.1 . Introduction.

For the general design of electrical filters, two different procedures are available. One of them which was established earlier is the image parameter method [ZO 1]. The other is the insertion loss method [DA 1, CA 1]. The image parameter method utilizes the image parameters of the filters, i.e., the image impedance ( $Z_I$ ) and the image transmission factor ( $P_I$ ). On the other hand, in the insertion loss method these parameters are in general, the insertion transmission factor ( $P_g$ ) and the driving point impedance ( $Z_d$ ). For this latter method, some authors prefer to use the reflection factor  $|\rho|$  and the characteristic function  $\Phi$ .

Under certain conditions, the two parameters  $P_g$  and  $P_I$  become identical. This condition is obtained if image impedance matching at all terminals of the filter is provided. This can be clearly seen from the formula derived by Zobel for the insertion loss in terms of the image parameters [TO 1]. Both of the above methods

have their own advantages and disadvantages. In the image parameter method, due to the fact that simpler calculations are required, realization can be achieved in a shorter time. However the resulting filter might contain more elements than is actually needed. The insertion loss method on the other hand generally contains a smaller number of elements. However, a more complicated method of calculation is required which implies the use of electronic calculators in this design. Using the image parameter method for filter design we can immediately obtain the elementary sections completely which are the building block of the filter.

There often arise occasions in which the filters which are designed by the insertion loss method will have the same number of elements as those designed by the image parameter method. The only difference between these two filters is that there is an improvement in the electrical properties of the filters designed by the insertion loss method, which are not really required. In such cases, indeed due to its simplicity, the image parameter method is preferable.

Another design technique which has been established is the reference filter design method. In this design technique both the image parameter and the insertion loss parameters are involved. The synthesis is mainly carried out by the insertion loss method, and the image parameter

is used for finding the locations of the attenuation poles and also to determine the characteristic function. This can be seen from the following formula of the characteristic function for the filter

$$\varphi = \mathcal{D} \sinh (P_I)$$

where  $\mathcal{D}$  is a constant,  $\varphi$  is the characteristic function,  $P_I$  is the transmission factor of an image parameter filter (reference filter) which has nothing to do with the actual filter, except that it has identical attenuation pole locations with this filter. The advantage of the reference filter method over the image parameter method is that it provides a flat loss in the pass band, i.e., the Chebyshev type of attenuation characteristics. However, the calculation of the filter elements is by no means as easy as that of the filter designed by the image parameter method.

It is then desirable at this point to establish some formula which will furnish the relationship between the insertion loss properties of the filters and its image parameters. When such a relationship is established, then from the given insertion loss requirements, the image parameters of the filter can be obtained so that the filter can be designed by means of the image parameter method. Based on these parameters, some exact design procedures for low-pass filters exist and can be found elsewhere [TO 1]. Fisher [FIS 1] has used an approximation

formula and carried out an insertion loss design for symmetrical and antimetrical band-pass filters utilizing the image parameter. However the design was completed by insertion loss synthesis. Some fundamental discussions on the attenuation and phase functions, especially for symmetric and antimetric filters, are given by Belevitch [BE 1,2].

The present work is the extension of the method presented by Tokad [TO 1] to the design of frequency unsymmetric band-pass filters, especially those having dissymmetrical characteristics. In the following sections of this chapter the important features of the insertion loss and image parameter methods as well as the topics pertinent to the development of the desired formulas are presented.

## 5.2 . The characterizing function of the image parameter filters.

The salient features of the image parameters, i.e., the image impedances and the transmission factor ( $Z_{I_1}$ ,  $Z_{I_2}$  and  $P_I$ ) are considered first.

### 5.2.1. Input and output image impedances, $Z_{I_1}$ and $Z_{I_2}$ .

For convenience, normalized values of image impedances are used. The normalization being with respect to the terminating resistors. The normalized impedances



are indicated by the symbols  $z_1$  and  $z_2$  and their properties are as follows:

- (i) in the pass band they are real and a function of the angular frequency  $\omega$ .
- (ii) in the stop band they are purely imaginary and a function of  $\omega$ .
- (iii) for symmetrical filters,  $z_1 = z_2$ .
- (iv) for antimetrical filters,  $z_1 z_2 = \text{constant}$ , usually taken as unity.

5.2.2. The transmission factor,  $P_I$ .

$$P_I = A_I + jB_I$$

where  $A_I$  is the image attenuation or loss function.

$A_I$  is identically zero in the pass band and non-negative in the stop band for all types of lossless filters, i.e., all elements are lossless.  $B_I$  is the image phase function. It has distinct features for different types of filters. The following are the properties of  $B_I$  and  $A_I$  in detail.

5.2.2.1. In the pass band.

$A_I$  is zero.  $B_I$  is monotonic increasing as a function of frequency. The properties are

- (i) For frequency unsymmetric band-pass filters.

- 1. Symmetrical types

$$-m\pi \leq B_I \leq n\pi \quad (5.2.1)$$

- 2. Antimetrical filter types

$$-(m\pi + \pi/2) \leq B_I \leq (n\pi + \pi/2) \quad (5.2.2)$$

where  $m$  and  $n$  are the number of the attenuation pole locations in the lower and upper stop bands respectively.

(ii) For low-pass filters.

1. Symmetrical types

$$0 \leq B_I \leq n \quad (5.2.3)$$

2. Antimetrical types

$$0 \leq B_I \leq (n\pi + \pi/2) \quad (5.2.4)$$

where  $n$  is the number of the locations of the attenuation poles. The properties of the frequency symmetrical band-pass filters are implicitly covered by the low-pass filters.

(iii) For dissymmetrical filters we have the possibilities of either one of the cases in (ii) and (i).

5.2.2.2. In the stop band.

$A_I > 0$ . ( $A_I = 0$  at cut-off frequencies.)  $B_I$  is a constant except at the pole locations where it jumps down by  $\pi$  or  $\pi/2$  depending whether there is a full pole or a half pole. The properties are

(i) For frequency unsymmetric band-pass filters.

1. Symmetrical types

I. In the lower stop band

$$B_I = -(m-\mu)\pi, \dots, -(m-2)\pi, \dots, \\ -(m-1)\pi, -m\pi \quad (5.2.5)$$

II. In the upper stop band

$$B_I = n\pi, (n-1)\pi, \dots, (n-v)\pi \quad (5.2.6)$$

2. Antimetrical types

I. In the lower stop band

$$B_I = 0, -[(m-p)\pi + \pi/2], \dots, \\ -[(m-1)\pi + \pi/2], -[m\pi + \pi/2] \quad (5.2.7)$$

II. In the upper stop band

$$B_I = n\pi + \pi/2, (n-1)\pi + \pi/2, \dots, \\ (n-v)\pi + \pi/2, 0 \quad (5.2.8)$$

3. For dissymmetrical filters  $B_I$  could be given as in 1 or 2.

(ii) For low-pass filters.

1. Symmetrical types

$$B_I = n\pi, (n-1)\pi, \dots, (n-v)\pi \quad 5.2.9)$$

2. Antimetrical types

$$B_I = n\pi + \pi/2, (n-1)\pi + \pi/2, \dots, \\ (n-v)\pi + \pi/2, 0 \quad (5.2.10)$$

3. For dissymmetrical types  $B_I$  could be given as in 1 or 2.

where:  $p = 0, \dots, m$

$v = 0, \dots, n$ .

### 5.3 . The chain matrix.

In order to obtain a formula for the insertion loss function in terms of the image parameters, the chain matrix of the 2-port filter network is utilized. It relates the terminal currents and voltages of the filter. From the diagram in Fig. 5.3.1, we have the following relationships

$$\begin{aligned} V_1 &= AV_2 + BI_2 = AV_2 + BV_2/R_2 \\ I_1 &= CV_2 + DI_2 = CR_2 I_2 + DI_2 \end{aligned} \quad (5.3.1)$$

where A, B, C, D are the elements of the chain matrix.

If  $R_1 = Z_{I_1}$  and  $R_2 = Z_{I_2}$ , i.e., matching at the terminations, then  $V_1/I_1 = Z_{I_1}$  and  $V_2/I_2 = Z_{I_2}$  and from Eq. 5.3.1 we have

$$\begin{aligned} Z_{I_1} &= \frac{AZ_{I_2} + B}{CZ_{I_2} + D} \\ Z_{I_2} &= \frac{DZ_{I_1} + B}{CZ_{I_1} + D} \end{aligned} \quad (5.3.2)$$

From these equations we obtain

$$\begin{aligned} Z_{I_1} Z_{I_2} &= B/C \\ Z_{I_1}/Z_{I_2} &= A/D \end{aligned} \quad (5.3.3)$$

Hence

$$\begin{aligned} Z_{I_1} &= \sqrt{\frac{BA}{CD}} \\ Z_{I_2} &= \sqrt{\frac{BD}{CA}} \end{aligned} \quad (5.3.4)$$

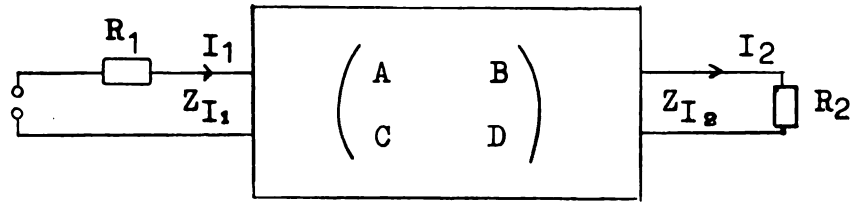


FIG. 5.3.1

4 T.N. Reactance network

5.4 . Current and voltage transmission factors (M and N).

These functions are used by Cauer [CA 1] in treating the insertion loss filter design technique. From Eq.

5.3.1 we have

$$V_1 = AV_2 + BI_2 = AV_2 + BV_2/R_2$$

$$I_1 = CI_2R_2 + DI_2$$

Therefore

$$I_1/I_2 = CR_2 + D = M \quad (5.4.1)$$

$$V_1/V_2 = (1/R_2)(AR_2 + B) = N.$$

The driving point impedance is

$$Z = V_1/I_1 = R_2 (N/M). \quad (5.4.2)$$

5.5 . Entries of chain matrix in terms of the image parameters.

From Eq. 5.4.2, we have

$$Z_{oc} = A/C \quad (R_2 = \infty)$$

$$Z_{sc} = B/D \quad (R = 0) . \quad (5.5.1)$$

Then the H-function is given by

$$H = \sqrt{\frac{Z_{oc}}{Z_{sc}}} = \sqrt{\frac{BC}{AD}} . \quad (5.5.2)$$

From this equation, since  $H = \tanh P_I$ , we have

$$e^{P_I} = \frac{(1 + H)}{(1 - H)} = \frac{(\sqrt{BC} + \sqrt{AD})}{(\sqrt{AD} - \sqrt{BC})}$$

$$e^{P_I} = \frac{(\cosh P_I + \sinh P_I)}{(\cosh P_I - \sinh P_I)} .$$

Therefore

$$\begin{aligned} \sqrt{AD} &= \cosh P_I \\ \sqrt{BC} &= \sinh P_I \end{aligned} \quad (5.5.3)$$

Since

$$AD - BC = -\sinh^2 P_I + \cosh^2 P_I = 1,$$

passivity of the network is implied.

From Eqs. 5.5.3 and 5.3.3, the following expressions are immediate:

$$\begin{aligned} A &= \sqrt{\frac{Z_{I_1}}{Z_{I_2}}} = \cosh P_I \\ B &= \sqrt{Z_{I_1} Z_{I_2}} \sinh P_I \\ C &= \frac{1}{\sqrt{Z_{I_1} Z_{I_2}}} \sinh P_I \\ D &= \sqrt{\frac{Z_{I_2}}{Z_{I_1}}} \cosh P_I . \end{aligned} \quad (5.5.4)$$

## 5.6 . Insertion loss parameters.

Figures 5.6.1 and 5.6.2 are to be used as an aid in deriving an expression for the insertion function. It is assumed that the reactance 2-port network is terminated in two resistances,  $R_1$  and  $R_2$ , and driven by the voltage driver  $E$ .

### 5.6.1. The insertion transmission function.

In Fig. 5.6.1, the power delivered to the load through the 2-ports is given by

$$|N_1| = |I_2^2 R_2| = \left| \frac{V_2^2}{R_2} \right|. \quad (5.6.1)$$

The power delivered directly to the load as can be seen from Fig. 5.6.2, is

$$|N_d| = |I_2'^2 R_2| = \left| \frac{V_2'^2}{R_2} \right|. \quad (5.6.2)$$

The insertion transmission factor is defined as

$$P_s = \frac{1}{2} \ln \frac{N_d}{N_1} \quad (5.6.3-a)$$

$$= \frac{1}{2} \ln \left| \frac{N_d}{N_1} \right| + j \arg \left( \frac{N_d}{N_1} \right)$$

$$P_s = A_s + jB_s .$$

Thus

$$A_s = \frac{1}{2} \ln \left| \frac{N_d}{N_1} \right| = \ln \left| \frac{I_2'}{I_2} \right| = \ln \left| \frac{V_2'}{V_2} \right|$$

$$B_s = \arg \frac{I_2}{I_1} = \arg \frac{V_2}{V_1} , \quad (5.6.3-b)$$

where

$A_s$  = attenuation function

$B_s$  = phase function .

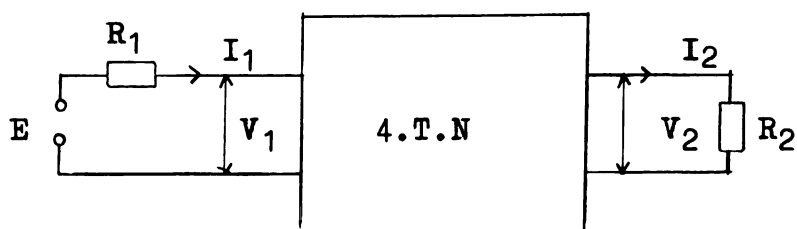


FIG. 5.6.1

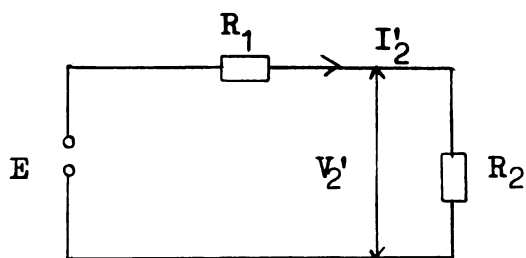


FIG. 5.6.2

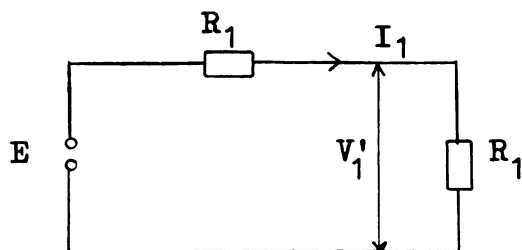


FIG. 5.6.3



### 5.6.2. The echo-loss (return-loss).

This loss function is related to the power reflected back to the driver. Thus, it is the power delivered directly to the load minus that delivered through the 2-port, i.e.,

$$|N_e| = |N_d| - |N_l|. \quad (5.6.4)$$

The echo transmission factor is defined as

$$\begin{aligned} P_e &= \frac{1}{2} \ln \frac{N_d}{N_e} = \frac{1}{2} \ln \left| \frac{N_d}{N_e} \right| + j \arg \left[ \frac{N_d}{N_e} \right] \\ &= A_e + jB_e. \end{aligned}$$

Thus, the echo-loss is given by

$$A_e = \ln \left| \frac{N_d}{N_e} \right|. \quad (5.6.5)$$

### 5.6.3. The characteristic function.

From the relation in Eq. 5.6.4 we have

$$\begin{aligned} |N_d| &= |N_l| + |N_e| \\ 1 &= \left| \frac{N_l}{N_d} \right| + \left| \frac{N_e}{N_d} \right| \\ 1 &= e^{-2A_s} + e^{-2A_e}. \end{aligned}$$

Therefore

$$e^{2A_s} = 1 + \frac{e^{-2A_e}}{e^{-2A_s}}.$$

The characteristic function is defined as

$$|\varphi|^2 = \left| \frac{e^{-2A_e}}{e^{-2A_s}} \right|. \quad (5.6.6)$$

Thus

$$A_s = \frac{1}{2} \ln [1 + |\varphi|^2].$$

### 5.7 . The effective (operating) loss.

The definition of insertion transmission factor given in Eq. 5.6.3-a can be modified if Fig. 5.6.2 is replaced by Fig. 5.6.3. This will yield a new transmission factor,  $P_o$ , which is called the effective or operating transmission function.  $P_s$  and  $P_o$  will be identical if the terminating resistances are identical. The advantage of using  $P_o$  in the design is that it will avoid the occurrence of negative losses in the pass band. The possibility that negative loss occurs is evident from the definition of  $P_s$  in Eq. 5.6.3. When an ideal transformer at one port is used, as will be apparent later, the form of the formula is also simplified.

#### 5.7.1. Effective transmission factor.

Using the diagram in Fig. 5.6.3, the maximum available power is

$$|N_m| = |I_1^2 R_1|. \quad (5.7.1)$$

The power delivered to the load, from Fig. 5.6.1, is

$$|N_1| = |I_2^2 R_2|. \quad (5.7.2)$$

The transmission factor is defined as

$$P_o = \frac{1}{2} \ln \frac{N_m}{N_1} = \frac{1}{2} \ln \frac{R_1}{R_2} + \frac{1}{2} \ln \frac{I_1^2}{I_2^2} \quad (5.7.3)$$

$$P_o = A_o + jB_o .$$

Thus the attenuation is:

$$A_0 = \frac{1}{2} \ln \frac{R_1}{R_2} + \ln \frac{I_1}{I_2}$$

and the phase is:

$$B_0 = \arg\left(\frac{I_1}{I_2}\right) . \quad (5.7.4)$$

The characteristic function is also defined here as before

$$|\varphi|^2 = \frac{e^{-2A_e}}{e^{-2A_0}} , \quad (5.7.5)$$

where  $A_e$  is the effective return loss (echo loss).

#### 5.7.2. The echo loss.

The echo power here is defined as the total maximum available power minus the power delivered to the load. Thus, in the definition of the characteristic function above, we have the situation that a fraction  $e^{-2A_0}$  of the total power is delivered to the load and another fraction,  $e^{-2A_e}$ , is reflected, hence

$$1 = e^{-2A_0} + e^{-2A_e}$$

(a relation due to Feldtkeller).

To study the relationship between  $A_e$  and the terminating impedances  $R_1$  and  $Z$  (or  $Z_I$ ), consider Figs. 5.7.1, 5.7.2 and 5.7.3. In general, it is sufficient to consider only Fig. 5.7.2 and Fig. 5.7.3. In Fig. 5.7.2,  $Z$  represents the load impedance. The circuit in Fig. 5.7.3 contains the same driver  $E$ , but instead of  $Z$  there is a driver  $V_e$ , representing the

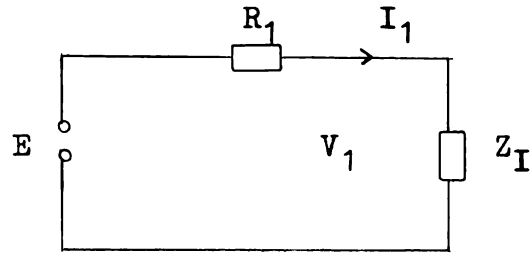


FIG. 5.7.1

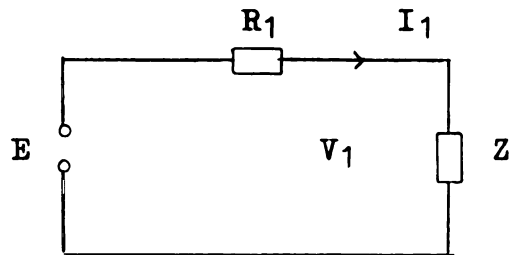


FIG. 5.7.2

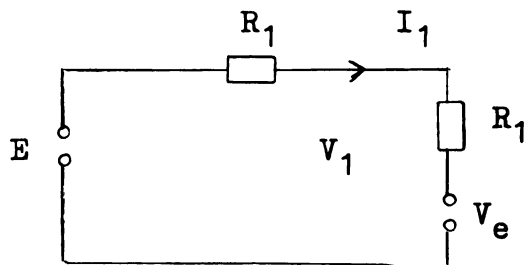


FIG. 5.7.3

echo, and resistor  $R_1$ .  $V_e$  is selected in such a way that the current  $I_1$  and the voltage  $V_1$  in Fig. 5.7.3 are identical to those in Fig. 5.7.2. Then the following

relationship can be written

$$\frac{E}{R_1 + Z} = \frac{E - V_e}{2R_1}$$

or

$$V_e = \frac{Z - R}{Z + R} E \quad .$$

Hence

$$\begin{aligned} |N_m| &= \left| \frac{E^2}{2R_1} \right| \\ |N_e| &= \left| \frac{V_e^2}{2R_1} \right| = \left| \frac{Z - R}{Z + R} E \right|^2 / 4R_1^2 \quad . \end{aligned}$$

Thus

$$A_e = \frac{1}{2} \ln \left| \frac{N_m}{N_e} \right| = \ln \left| \frac{Z + R_1}{Z - R_1} \right| \quad . \quad (5.7.6)$$

Let

$$\left| \frac{Z + R_1}{Z - R_1} \right| = \frac{1}{|\rho|}$$

where  $|\rho|$  is referred to as the reflection factor.

The echo loss is important for the filter design by the insertion loss method in the pass band. In the remaining parts of this section, discussion is devoted to the study of the echo loss, in the pass band, for dissymmetrical filters. Substituting Eq. 5.4.2 into Eq. 5.7.6 we obtain

$$\begin{aligned} A_e &= \ln \left| \frac{M + N}{M - N} \right| \\ &= \ln \left| \frac{CR_2 + B/R_2 + D + A}{CR_2 - B/R_2 + D - A} \right| \end{aligned}$$

$$A_e = \frac{1}{2} \ln \left[ \frac{(az_1 + [1/a]z_2)^2 \cos^2 B_I + (1/a + az_1 z_2) \sin^2 B_I}{(az_1 - [1/a]z_2)^2 \cos^2 B_I + (1/a - az_1 z_2) \sin^2 B_I} \right]$$

where  $a = \sqrt{\frac{R_1}{R_2}}$

$$A_e = \frac{1}{2} \ln \left[ \frac{(a^2 z_1 + z_2^2)^2 + (1 - z_2^2)(1 - a^4 z_1^2) \sin^2 B_I}{(a^2 z_1 - z_2^2)^2 + (1 - z_2^2)(1 - a^4 z_1^2) \sin^2 B_I} \right] \quad (5.7.7)$$

In order to determine a bound on  $A_e$  function let  
Eq. 5.7.7 be written as

$$A_e = \frac{1}{2} \ln \left[ \frac{(a^2 z_1 + z_2)^2 + \{(1 + a^2 z_1 z_2)^2 - (a^2 z_1 + z_2)^2\} \sin^2 B_I}{(a^2 z_1 - z_2)^2 + \{(1 - a^2 z_1 z_2)^2 - (a^2 z_1 - z_2)^2\} \sin^2 B_I} \right]. \quad (5.7.8)$$

From Eq. 5.7.8 it can be seen that if

$$(a^2 z_1 + z_2)^2 > (1 + a^2 z_1 z_2)^2$$

then also

$$(a^2 z_1 - z_2)^2 > (1 - a^2 z_1 z_2)^2.$$

Since, in the pass band,  $z_1$ ,  $z_2$ , and  $a$  are positive,  
then

$$(a^2 z_1 + z_2)^2 > (a^2 z_1 - z_2)^2$$

$$(1 + a^2 z_1 z_2)^2 > (1 - a^2 z_1 z_2)^2.$$

The value of the numerator expression in Eq. 5.7.8 is  
always between  $(a^2 z_1 + z_2)^2$  and  $(1 + a^2 z_1 z_2)^2$  and the

value of the denominator is between  $(a^2 z_1 - z_2)^2$  and  $(1 - a^2 z_1 z_2)^2$ . The curve corresponding to the denominator will always be below that corresponding to the numerator. In Fig. 5.7.4 the curves are sketched.

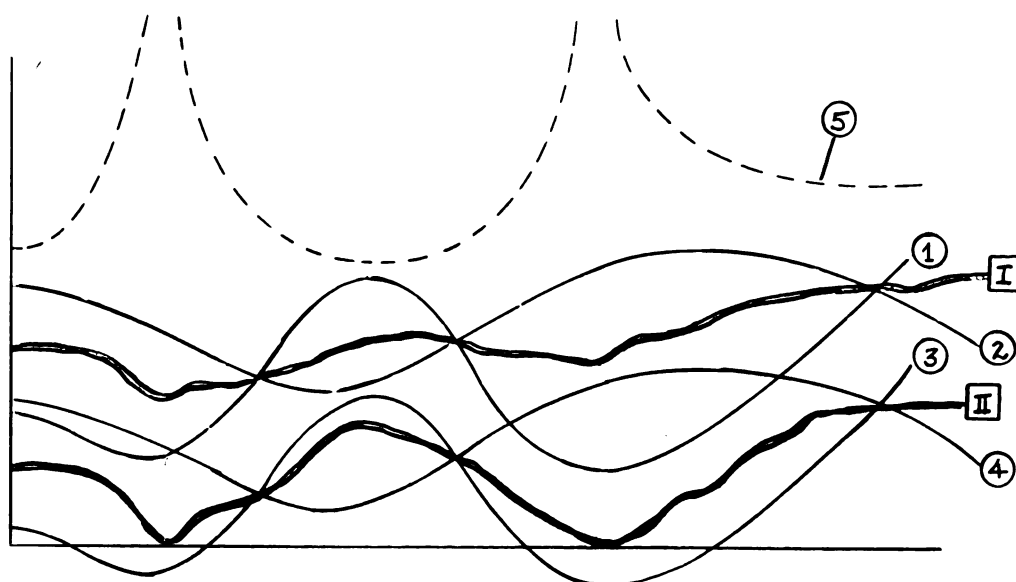


FIG. 5.7.4

Curves 1 and 2 correspond to the numerator of Eq.

5.7.8 when  $\sin^2 B_I$  is 0 and 1, respectively.

Curves 3 and 4 correspond to the denominator of Eq.

5.7.8 when  $\sin^2 B_I$  is 0 and 1, respectively.

Curve 5 is the echo-loss,  $A_e$ .

Curve I corresponds to the numerator of Eq. 5.7.8.

Curve II corresponds to the denominator of Eq. 5.7.8.

5.8 . Derivation of insertion loss parameters in terms of image parameters.

Referring to Figs. 5.6.1 and 5.6.2, consider Eq. 5.6.3:

$$P_s = \ln \left( \frac{I_2'}{I_2} \right) .$$

This relation can be put into the following form

$$P_s = \ln \left( \frac{I_2'}{I_2} \frac{I_1}{I_1} \right) = \ln \left( \frac{I_2'}{I_2} \right) + \ln \left( \frac{I_1}{I_2} \right) . \quad (5.8.1)$$

From Figs. 5.6.1 and 5.6.2 we also have

$$\begin{aligned} I_2' &= \frac{E}{R_1 + R_2} \\ I_1 &= \frac{E}{R_1 + Z} . \end{aligned}$$

Equation 5.4.1 gives

$$\frac{I_1}{I_2} = CR_2 + D = M .$$

Substituting these expressions into Eq. 5.8.1 we obtain

$$P_s = \ln \frac{R_1 + Z}{R_1 + R_2} + \ln M . \quad (5.8.2)$$

When Eq. 5.4.2 for Z is substituted into Eq. 5.8.2, it gives

$$P_s = \ln \frac{R_1 + R_2(N/M)}{R_1 + R_2} M = \ln \left( \frac{MR_1 + NR_2}{(R_1 + R_2)} \right) .$$

Using the expressions for N and M we have



$$P_s = \ln \frac{\sqrt{R_1 R_2}}{R_1 + R_2} + \ln \left[ \sqrt{R_1 R_2} C + \sqrt{\frac{R_1}{R_2}} D + \sqrt{\frac{R_2}{R_1}} A + \frac{B}{\sqrt{R_1 R_2}} \right].$$

Substituting Eq. 5.5.4 into this equation and making the following normalizations,

$$\begin{aligned} z_1 &= \frac{Z_{I_1}}{R_1} \\ z_2 &= \frac{Z_{I_2}}{R_2}, \end{aligned} \quad (5.8.3)$$

the desired result is obtained as

$$P_s = \ln \frac{2\sqrt{R_1 R_2}}{R_1 + R_2} + \ln \left[ \frac{1 + z_1 z_2}{2\sqrt{z_1 z_2}} \sinh P_I + \frac{z_1 + z_2}{2\sqrt{z_1 z_2}} \cosh P_I \right]. \quad (5.8.4)$$

Since  $P_s = A_s + jB_s$  the derivations of the attenuation function  $A_s$  and the phase function  $B_s$  for special types of structures, i.e., symmetrical, antisymmetrical or dissymmetrical filters are considered next.

#### 5.8.1. Symmetrical filters.

For this filter since, by definition,

$$z_1 = z_2 = z,$$

then

$$P_s = \ln \frac{\sqrt{R_1 R_2}}{R_1 + R_2} + \ln 2 \left[ \cosh P_I + \frac{1 + z^2}{2z} \sinh P_I \right].$$

a) In the pass band

$$A_I = 0$$

$$P_I = jB_I$$

$z_1, z_2$  are real, thus  $z$  is real.

Then

$$\begin{aligned}
 P_S &= \ln \frac{2 \sqrt{R_1 R_2}}{R_1 + R_2} + \ln \left[ \cos B_I + j \frac{1 + z^2}{2z} \sin B_I \right] \\
 &= \ln \frac{2 \sqrt{R_1 R_2}}{R_1 + R_2} + \frac{1}{2} \ln \left[ \cos^2 B_I + \frac{(1 + z^2)^2}{4z^2} \sin^2 B_I \right] \\
 &\quad + j \arctan \left[ \frac{1 + z^2}{2z} \tan B_I \right] \\
 &= A_S + j B_S .
 \end{aligned}$$

Therefore, we have:

$$\begin{aligned}
 A_S &= \ln \frac{2 \sqrt{R_1 R_2}}{R_1 + R_2} + \frac{1}{2} \ln \left[ \cos^2 B_I + \frac{(1 + z^2)^2}{4z^2} \sin^2 B_I \right] \\
 &\quad (5.8.5) \\
 B_S &= \arctan \left[ \frac{1 + z^2}{2z} \tan B_I \right] .
 \end{aligned}$$

b) In the stop band

$z$  is purely imaginary

$$z = jx$$

$$P_I = A_I + jk\pi, \quad (k = 0, \pm 1, \dots)$$

and

$$\cosh P_I = \pm \cosh A_I$$

$$\sinh P_I = \pm \sinh A_I$$

where the upper or lower signs must be used simultaneously.

Therefore

$$\begin{aligned}
 P_S &= \ln \frac{2 \sqrt{R_1 R_2}}{R_1 + R_2} + \frac{1}{2} \ln \left[ \cosh^2 A_I + \left( \frac{1 - x^2}{2x} \right)^2 \sinh^2 A_I \right] \\
 &\quad + j \arctan \left[ - \frac{1 - x^2}{2x} \tanh A_I \right]
 \end{aligned}$$

$$A_S = \ln \frac{2 \sqrt{R_1 R_2}}{R_1 + R_2} + \frac{1}{2} \ln \left[ \cosh^2 A_I + \left( \frac{1 - x^2}{2x} \right)^2 \sinh^2 A_I \right]$$

$$B_S = \arctan \left[ - \frac{1 - x^2}{2x} \tanh A_I \right] \quad . \quad (5.8.6)$$

### 5.8.2. Antimetric filters.

For this filter  $Z_{I_1} Z_{I_2} = R_1 R_2$ . Thus, using the same normalization as in Eq. 5.8.3 we have

$$z_2 z_1 = 1$$

$$z_1 = 1/z_2 = z \quad .$$

The transmission factor is then

$$P_S = \ln \frac{2 \sqrt{R_1 R_2}}{R_1 + R_2} + \ln \left[ \sinh P_I + \frac{1 + z^2}{2z} \cosh P_I \right]$$

a) In the pass band

$$A_I = 0$$

$$P_I = jB_I$$

and

$$\sinh P_I = \sinh jB_I = j \sin B_I$$

$$\cosh P_I = \cosh jB_I = \cos B_I \quad .$$

Then

$$P_S = \ln \frac{2 \sqrt{R_1 R_2}}{R_1 + R_2} + \ln \left[ j \sin B_I + \frac{1 + z^2}{2z} \cos B_I \right]$$

$$= \ln \frac{2 \sqrt{R_1 R_2}}{R_1 + R_2} + \frac{1}{2} \ln \left[ \sin^2 B_I + \left( \frac{1 + z^2}{2z} \right)^2 \cos^2 B_I \right]$$

$$+ j \arctan \left[ \frac{2z}{1 + z^2} \tan B_I \right] \quad .$$

Therefore,

$$A_S = \frac{1}{2} \ln \left[ \sin^2 B_I + \frac{(1+z^2)^2}{4z^2} \cos^2 B_I \right] + \ln \frac{2\sqrt{R_1 R_2}}{R_1 + R_2}$$

$$B_S = \arctan \left[ \frac{2z}{1+z^2} \tan B_I \right] . \quad (5.8.7)$$

b) In the block band

$$z = jx$$

$$P_I = A_I + (k\pi + \pi/2), \quad k = 0, \pm 1, \dots$$

$$\sinh P_I = \pm \sinh (A_I + j \pi/2) = \pm j \cosh A_I$$

$$\cosh P_I = \pm \cosh (A_I + j \pi/2) = \pm j \sinh A_I .$$

Then:

$$P_S = \ln \frac{2\sqrt{R_1 R_2}}{R_1 + R_2} + \ln \left[ j \cosh A_I + \left( \frac{1-x^2}{2x} \right) \sinh A_I \right]$$

$$= \ln \frac{2\sqrt{R_1 R_2}}{R_1 + R_2} + \frac{1}{2} \ln \left[ \cosh^2 A_I + \left( \frac{1-x^2}{2x} \right)^2 \sinh^2 A_I \right]$$

$$+ j \arctan \left[ \frac{2x}{1-x^2} \coth A_I \right]$$

and

$$A_S = \ln \frac{2\sqrt{R_1 R_2}}{R_1 + R_2} + \frac{1}{2} \ln \left[ \cosh^2 A_I + \left( \frac{1-x^2}{2x} \right)^2 \sinh^2 A_I \right]$$

$$B_S = \arctan \left[ \frac{2x}{1-x^2} \coth A_I \right] . \quad (5.8.8)$$

#### 4.8.3. Dissymmetrical filters.

The transmission factor is

$$P_s = \ln \frac{2 \sqrt{R_1 R_2}}{R_1 + R_2} + \ln \left[ \frac{1 + z_1 z_2}{2 \sqrt{z_1 z_2}} \sinh P_I + \frac{z_1 + z_2}{2 \sqrt{z_1 z_2}} \cosh P_I \right].$$

a) In the pass band

$z_1, z_2$  are real

$$A_I = 0$$

$$P_I = jB_I :$$

Therefore,

$$P_s = \ln \frac{2 \sqrt{R_1 R_2}}{R_1 + R_2} + \ln \left[ \frac{z_1 + z_2}{2 \sqrt{z_1 z_2}} \cos B_I + j \frac{1 + z_1 z_2}{2 \sqrt{z_1 z_2}} \sin B_I \right]$$

and thus

$$A_s = \ln \frac{2 \sqrt{R_1 R_2}}{R_1 + R_2} + \frac{1}{2} \ln \left[ \frac{(1 + z_1 z_2)^2}{4 z_1 z_2} \sin^2 B_I + \frac{(z_1 + z_2)^2}{4 z_1 z_2} \cos^2 B_I \right]$$

$$B_s = \arctan \left[ \frac{1 + z_1 z_2}{z_1 + z_2} \tan B_I \right]. \quad (5.8.9)$$

b) In the stop band

$$z_1 = jx_1$$

$$z_2 = jx_2$$

$$P_I = A_I + jk\pi \quad \text{or}$$

$$P_I = A_I + j(k\pi + \pi/2), \quad k = 0, \pm 1, \dots$$

$$(i) \quad P_I = A_I + jk\pi, \quad k = 0, \pm 1, \pm 2, \dots$$

$$P_s = \ln \frac{2 \sqrt{R_1 R_2}}{R_1 + R_2} + \ln \left[ \frac{1 - x_1 x_2}{2j \sqrt{x_1 x_2}} \sinh A_I + \frac{x_1 + x_2}{2 \sqrt{x_1 x_2}} \cosh A_I \right]$$

$$\begin{aligned}
A_S &= \ln \frac{2 \sqrt{R_1 R_2}}{R_1 + R_2} \\
&\quad + \frac{1}{2} \ln \left[ \frac{(1-x_1 x_2)^2}{4x_1 x_2} \sinh^2 A_I + \frac{(x_1 + x_2)^2}{4x_1 x_2} \cosh^2 A_I \right] \\
B_S &= \arctan \left[ - \frac{1 - x_1 x_2}{x_1 + x_2} \tanh A_I \right] .
\end{aligned}$$

$$(ii) P_I = A_I + j(k\pi + \pi/2)$$

$$\begin{aligned}
P_S &= \ln \frac{2 \sqrt{R_1 R_2}}{R_1 + R_2} \\
&\quad + \ln \left[ \frac{1 - x_1 x_2}{2 \sqrt{x_1 x_2}} \cosh A_I - j \frac{x_1 + x_2}{2 \sqrt{x_1 x_2}} \sinh A_I \right] \\
A_S &= \ln \frac{2 \sqrt{R_1 R_2}}{R_1 + R_2} \\
&\quad + \frac{1}{2} \ln \left[ \frac{(1-x_1 x_2)^2}{4x_1 x_2} \cosh^2 A_I + \frac{(x_1 + x_2)^2}{4x_1 x_2} \sinh^2 A_I \right] \\
B_S &= \arctan \left[ - \frac{x_1 + x_2}{1 - x_1 x_2} \tanh A_I \right]
\end{aligned} \tag{5.8.10}$$

As was mentioned earlier the operating loss will be the same as the insertion loss if the terminating resistors at both terminal pairs are identical. Thus, in the operating loss, we have the same formula as in the case of insertion loss, except that the term containing  $R_1$ ,  $R_2$  disappears. Thus, we have a more convenient set of formulas if operating loss formulas are used. This is what will be done in the following sections and if insertion

loss is required then the term

$$\ln \frac{2\sqrt{R_1 R_2}}{R_1 + R_2}$$

will be added to the formula. In the next section the formulas for the operating loss will be presented.

### 5.9 . Formulas for the operating loss design technique.

The operating transmission factor is

$$P_0 = \ln \left[ \frac{1 + z_1 z_2}{2 \sqrt{z_1 z_2}} \sinh P_I + \frac{z_1 + z_2}{2 \sqrt{z_1 z_2}} \cosh P_I \right] \quad (5.9.1)$$

#### 5.9.1. For symmetrical filters.

a) In the pass band

$$A_0 = \frac{1}{2} \ln \left[ \cosh^2 B_I + \frac{(1 + z^2)^2}{4z^2} \sinh^2 B_I \right] \quad (5.9.2)$$

$$B_0 = \arctan \left[ \frac{1 + z^2}{2z} \tan B_I \right].$$

b) In the stop band

$$A_0 = \frac{1}{2} \ln \left[ \cosh^2 A_I + \frac{(1 - x^2)^2}{4x^2} \sinh^2 A_I \right] \quad (5.9.3)$$

$$B_0 = \arctan \left[ - \frac{1 - x^2}{2x} \tanh A_I \right].$$

#### 5.9.2. Antimetric filters.

a) In the pass band

$$A_0 = \frac{1}{2} \ln \left[ \sin^2 B_I + \frac{(1+z^2)^2}{4z^2} \cos^2 B_I \right] \quad (5.9.4)$$

$$B_0 = \arctan \left[ \frac{2z}{1+z^2} \tan B_I \right] .$$

b) In the block band

$$A_0 = \frac{1}{2} \ln \left[ \cosh^2 A_I + \frac{(1-x^2)^2}{4x^2} \sinh^2 A_I \right] \quad (5.9.5)$$

$$B_0 = \arctan \left[ \frac{2x}{1-x^2} \coth A_I \right] .$$

### 5.9.3. Dissymmetrical filters.

a) In the pass band

$$A_0 = \frac{1}{2} \ln \left[ \frac{(1+z_1 z_2)^2}{4z_1 z_2} \sin^2 B_I + \frac{(z_1 + z_2)^2}{4z_1 z_2} \cos^2 B_I \right] \quad (5.9.6)$$

$$B_0 = \arctan \left[ \frac{1 + z_1 z_2}{z_1 + z_2} \tan B_I \right] .$$

b) In the block band

$$(i) \quad A_0 = \frac{1}{2} \ln \left[ \frac{(1-x_1 x_2)^2}{4x_1 x_2} \sinh^2 A_I + \frac{(x_1 + x_2)^2}{4x_1 x_2} \cosh^2 A_I \right] \quad (5.9.7-a)$$

$$B_0 = \arctan \left[ - \frac{1 - x_1 x_2}{x_1 + x_2} \tanh A_I \right] ,$$

or

$$(ii) \quad A_0 = \frac{1}{2} \ln \left[ \frac{(1-x_1 x_2)^2}{4x_1 x_2} \cosh^2 A_I + \frac{(x_1 + x_2)^2}{4x_1 x_2} \sinh^2 A_I \right] \quad (5.9.7-b)$$

$$B_0 = \arctan \left[ - \frac{x_1 + x_2}{1 - x_1 x_2} \tanh A_I \right] .$$



## Chapter VI

### FILTER DESIGN II

#### APPROXIMATION AND DESIGN PROCEDURE

##### 6.1 . Introduction.

The filter design procedure considered in this chapter is based on the image parameter method. It is assumed that the insertion (effective loss) requirements of the filter are specified. The synthesis of the filter network is carried out using the image parameter method. Some exact design procedures for the filter utilizing the image parameter method and approximate techniques for symmetrical and antimetrical filters with the insertion loss method are already developed [TO 1, FIS 1]. In this thesis the work is mainly devoted to the design of frequency unsymmetric band-pass filters, especially those having dissymmetric configurations. The realization procedure is carried out by the image parameter method. The elementary sections used in this type of filter cannot be obtained as those of frequency symmetrical filters by the frequency transformation from a low-pass filter. The technique developed by Laurent, to generate elementary sections for general filters, can be utilized. However

these generated sections must be used as is without referring to how they are generated [LA 1]. There are other techniques available to generate a set of elementary sections [BR 1, SH 1, MA 1, NO 1, BO 1, CO 1, SA 1]. These elementary sections should be used as is. Since each elementary section is considered as independent, its properties must be investigated separately. The necessary information required for the design can be obtained from analytical investigations.

One method which seems to be less complicated than others, hence preferable, is to develop the elementary sections from the basic sections by m-derivation [NO 1, BO 1, see also Chapter II, section 2.5]. One other factor to be considered before developing relations for the elementary section is the fact that these sections should contain a minimum number of inductors [SA 1, WA 1]. The elementary sections which are suited to the discussion of this thesis are those E.S.1, E.S.2, and E.S.3 which are presented in Chapter II.

The approximation of the loss functions for symmetric and antisymmetric filters are given by the formulas

$$A_s \geq A_I - \ln 2 \text{ Nepers} \quad \text{for stop band}$$

$$A_s \leq 2 \ln \frac{(z + 1)^2}{4z} \text{ Nepers} \quad \text{for pass band}$$

where

$A_s$  is the insertion attenuation

$A_I$  is the image attenuation

$z$  is the normalized image impedance .

The approximation has to satisfy the overall requirements, i.e.,

- (1) in the pass band  $A_s \leq A_{s \text{ min}}$
- (2) in the stop band  $A_s \geq A_{s \text{ max}}$  .

An improvement on the approximation in the stop band for symmetrical and antisymmetrical filters [FIS 1] is

$$A_o \approx A_I + \ln \left[ \frac{z^2 + 1}{2z} \right]^2 - \ln 2 \quad \text{Nepers}$$

where

$A_I$  is the effective attenuation

$A_I \geq 3 \quad \text{Nepers} \quad .$

## 6.2 . Approximation for the attenuation function of dissymmetrical filters.

In the pass band Belevitch [BE 1] has made an extensive discussion especially for the low-pass filters, frequency symmetrical and unsymmetrical band-pass filters of symmetrical and antimetrical types. However for the dissymmetrical case he considered only special types of filters. Here formulas for completely dissymmetrical filters will be established. From Eq. 5.9.6-a and -b, in the pass band, we have

$$e^{2A_0} = \left[ \frac{(1+z_1 z_2)^2}{4z_1 z_2} \sin^2 B_I + \frac{(z_1+z_2)^2}{4z_1 z_2} \cos^2 B_I \right]$$

$$e^{2A_0} = \left[ \frac{(1+z_1 z_2)^2}{4z_1 z_2} + \left( \frac{(z_1+z_2)^2}{4z_1 z_2} - \frac{(1+z_1 z_2)^2}{4z_1 z_2} \right) \cos^2 B_I \right].$$

Let

$$\frac{(1 + z_1 z_2)^2}{4z_1 z_2} = B$$

$$\frac{(z_1 + z_2)^2}{4z_1 z_2} = C.$$

Consider now the value of the function  $e^{2A_0}$  at a fixed frequency. If  $C - B < 0$  then, at this frequency,  $e^{2A_0}$  will have a maximum when  $\cos^2 B_I = 0$ . This maximum is  $B$ . The minimum at this frequency will occur when  $\cos^2 B_I = 1$ . This minimum is  $C$ . The converse is true when  $B - C < 0$ . Thus, the curve of  $A_0$  will always lie between the two curves of  $\frac{1}{2} \ln \frac{(1+z_1 z_2)^2}{4z_1 z_2}$  and  $\frac{1}{2} \ln \frac{(z_1+z_2)^2}{4z_1 z_2}$  as is shown in Fig. 6.2.1.

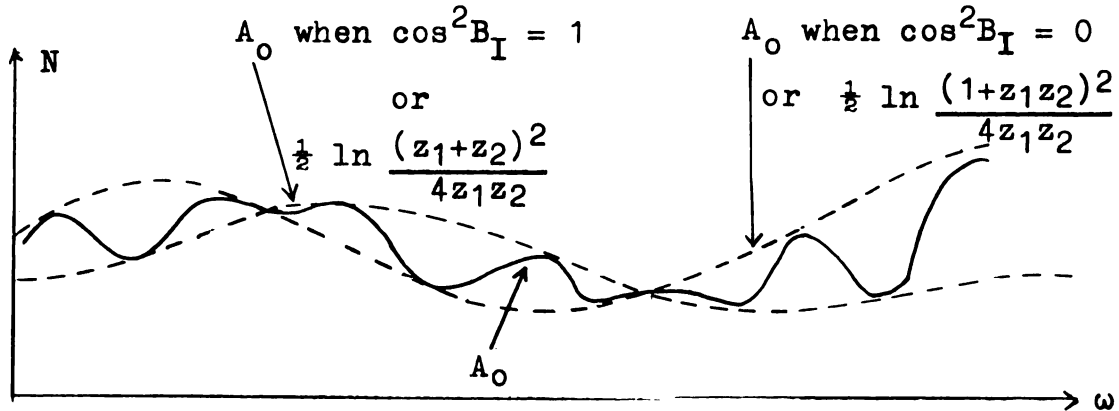


FIG. 6.2.1

In the block band, from Eqs. 5.9.7-a and -b, it is evident that

$$e^{2A_0} = \frac{1}{4} \left[ \frac{(1-x_1x_2)^2}{x_1x_2} \sinh^2 A_I + \frac{(x_1+x_2)^2}{x_1x_2} \cosh^2 A_I \right]$$

or

$$e^{2A_0} = \frac{1}{4} \left[ \frac{(1-x_1x_2)^2}{x_1x_2} \cosh^2 A_I + \frac{(x_1+x_2)^2}{x_1x_2} \sinh^2 A_I \right] .$$

If  $A_I \geq 3$  Neper the following approximations can be made

$$\sinh A_I \approx \cosh A_I \approx e^{A_I/2}$$

$$\sqrt{e^{2A_I} - 1} \approx e^{A_I} .$$

Thus, the above formulas of  $e^{2A_0}$ , using these approximations give

$$e^{2A_0} \approx \frac{1}{4} \left[ \frac{(1-x_1x_2)^2}{x_1x_2} \frac{e^{2A_I}}{4} + \frac{(x_1+x_2)^2}{x_1x_2} \frac{e^{2A_I}}{4} \right]$$

$$A_0 \approx A_I + \frac{1}{2} \ln \frac{(1+x_1^2)(1+x_2^2)}{4x_1x_2} - \ln 2 .$$

Hence,

$$A_I \approx A_0 - \frac{1}{2} \ln \frac{(1+x_1^2)(1+x_2^2)}{4x_1x_2} + \ln 2 . \quad (6.2.1)$$

If  $\frac{1}{2} \ln \frac{(1+x_1^2)(1+x_2^2)}{4x_1x_2}$  is equal to  $\ln 2$  then  $A_0 = A_I$ .

This will occur when  $|z_1| = |z_2| = 1$ , which is the case when an image impedance matching exists. On the other hand if

$$f(x_1, x_2) = \frac{1}{2} \ln \frac{(1+x_1^2)(1+x_2^2)}{4x_1x_2} > \ln 2 ,$$

then  $A_I < A_0$ . Therefore it is necessary to investigate the behavior of the function  $f(x_1, x_2)$  to check if the condition  $\ln 2 < f(x_1, x_2)$  is possible.

Since

$$f(x_1, x_2) = \frac{1}{2} \ln \frac{(1+x_1^2)(1+x_2^2)}{4x_1x_2} ,$$

then

$$\frac{\partial f}{\partial x_1} = \frac{(1+x_2^2)}{2x_2} \frac{(x_1^2-1)}{x_1^2}$$

$$\frac{\partial^2 f}{\partial x_1^2} = \frac{(1+x_2^2)}{x_2} \frac{1}{x_1^3}$$

$$\frac{\partial f}{\partial x_2} = \frac{(1+x_1^2)}{2x_1} \frac{(x_2^2-1)}{x_2^2}$$

$$\frac{\partial^2 f}{\partial x_2^2} = \frac{(1+x_1^2)}{x_1} \frac{1}{x_2^3}$$

$$\frac{\partial^2 f}{\partial x_1 \partial x_2} = \frac{x_1^2-1}{x_1^2} \frac{x_2^2-1}{x_2^2} .$$

If  $\frac{\partial f}{\partial x_1} = 0 \longrightarrow x_1 = 1$

$$\frac{\partial f}{\partial x_2} = 0 \longrightarrow x_2 = 1$$

$$D = f_{x_1 x_1} f_{x_2 x_2} - f_{x_1 x_2}^2 \bigg|_{\substack{x_1=1 \\ x_2=1}} = 4 > 0$$

$$f_{x_1 x_1} \bigg|_{\substack{x_1=1 \\ x_2=1}} = 2 > 0$$

$$f_{x_2 x_2} \bigg|_{\substack{x_1=1 \\ x_2=1}} = 2 > 0 \quad .$$

Thus we will have an extremum at  $(x_1, x_2) = (1, 1)$  because  $D > 0$ . However this extremum is a minimum ( $f_{x_1 x_1} > 0$ ,  $f_{x_2 x_2} > 0$ ). From this discussion it is seen that  $f(x_1, x_2)$  can be made as large as we desire. This, of course, implies that, according to Eq. 6.1.2,  $A_I$  can be made as small as possible, thus a minimum number of elements will be required in the filter. However, this possibility is limited by the available types of impedances,  $z_1$  and  $z_2$ .

### 6.3 . The design procedure.

As the starting points for the design for the insertion loss filters, the following requirements are given:

- I. Effective pass band and the required effective return loss in this range, i.e.,

$$A_e \quad \text{or} \quad |\rho| = e^{-A_e} \quad .$$

- II. Effective stop band and the corresponding attenuation requirements.
- III. The requirements on the input and output impedances in the stop band.

For the image parameter filters we have the following requirements:

- I'. The interval in which the image impedances are real.
- II' and III' as in the II and III above.

Consider the function

$$f(x_1, x_2) = \frac{1}{2} \ln \frac{(1+x_1^2)}{2x_1} + \frac{1}{2} \ln \frac{(1+x_2^2)}{2x_2} \quad .$$

The following curve in Fig. 6.2.2 is the curve of  $\frac{1}{2} \ln \frac{(1+x^2)}{2x}$ , where  $x > 0$ . This curve is to be used as an aid in determining the attenuation curve in the stop band. The curve is symmetric with respect to  $x = 1$ . Thus only the part of this curve for  $x < 1$  is plotted in Fig. 6.2.2.



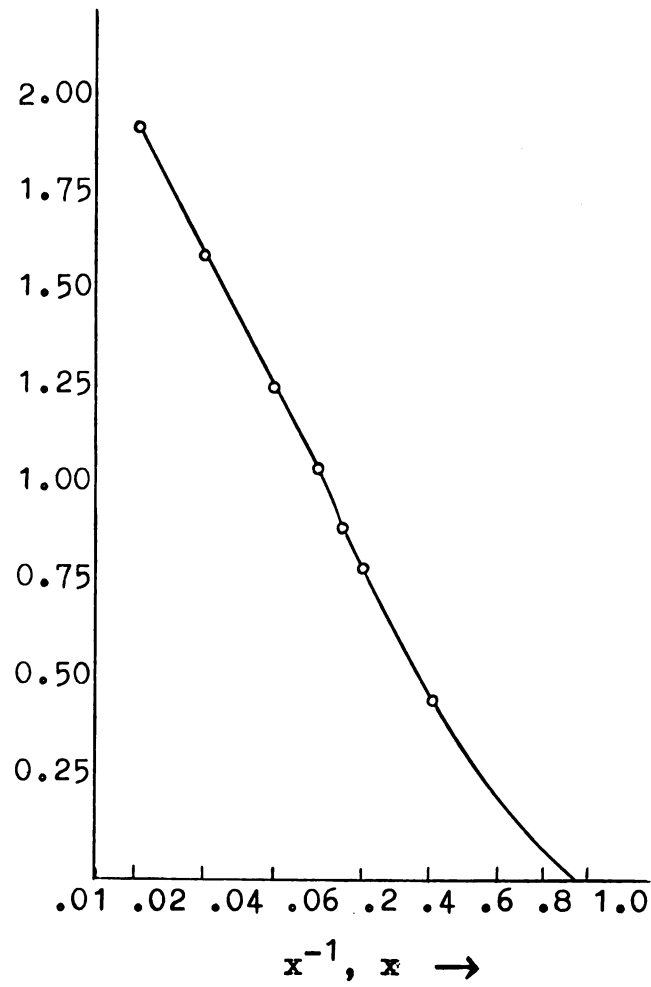


FIG. 6.2.2

$$\frac{1}{2} \ln \frac{(1+x^2)}{2x} \quad \text{Nepers}$$

The design procedure consists of the considerations of the following items: I', II', III'.

- I'. Gives the cut-off frequencies.
- II'. Gives the lower bound on the attenuation or the poles of attenuation.

III'. Gives the types of image impedances.

Additional requirements are: filter is lossless and contains a minimum number of inductors. The procedure is described briefly in the following:

- (i) Plot the  $\gamma$ -scale.
- (ii) Plot the impedances on the  $\gamma$ -scale, then with the aid of Fig. 6.2.2, plot  $\ln f(x_1, x_2)$  on the  $\gamma$ -scale.
- (iii) Subtract the curve in (ii) from the required attenuation curve.
- (iv) The remaining curve is usually, after adding  $\ln 2$  to it, the requirement for the intermediate section.

By using the template we can find the poles of attenuation, as is shown in Fig. 6.2.4. In Fig. 6.2.3 the plots of  $A_0 \min$  and  $\ln f(x_1, x_2)$  are shown. In Fig. 6.2.4 the template curves which will approximate  $A_I$  are illustrated, i.e., the image attenuation of the intermediate section to be designed. Since the terminating image impedances are supposed to be given in advance, this means that the conditions in the pass band are completely satisfied.

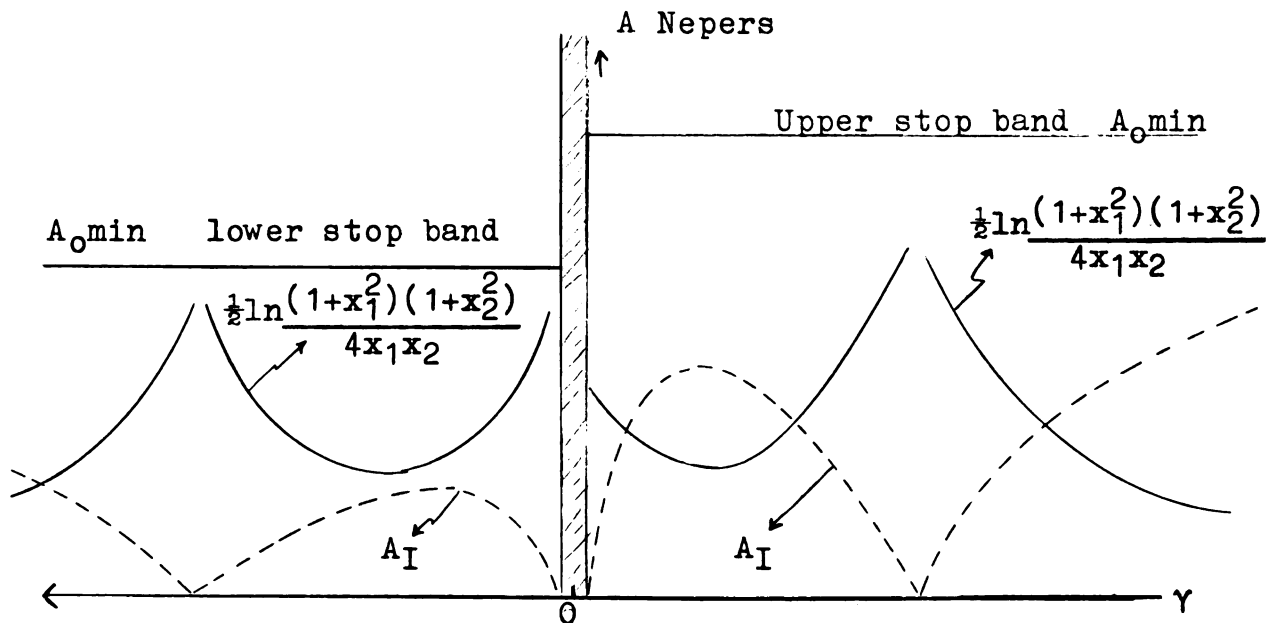


FIG. 6.2.3

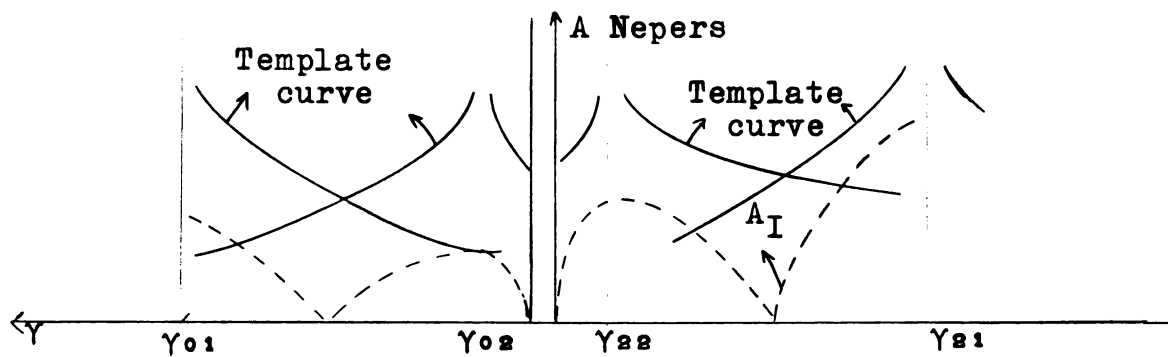


FIG. 6.2.4

#### 6.4 . Some more study of the high order image impedance

$$\underline{Z_{T_m}} \text{ and } \underline{Z_{\pi_m}}.$$

In Chapter II, general discussions of these types of impedances are given. In this section these impedances are studied to obtain some details useful in the filter design.

Figures 6.3.1 and 6.3.2 illustrate the plot of the image impedances  $Z_{T_m}$  and  $Z_{\pi_m}$ , which are normalized with respect to the constants  $R_{T_m}$  and  $R_{\pi_m}$ . Note that the frequency axis is the  $\omega$ -axis described in Chapter II rather than the actual  $\omega$ -axis. These curves are calculated with the aid of digital computer. In these figures, curve (1) represents the image impedance with critical frequencies (attenuation poles),  $\omega_{0p}$  and  $\omega_{2p}$  which are relatively close to the cut-off frequencies. In the image impedance corresponding to curve (2), the critical frequencies are taken far from the cut-off frequencies, and finally curve (3) corresponds to the situation that the critical frequencies are taken still farther from the cut-off frequencies. The effect of the location of the critical frequencies of the image impedance on the impedance curve is evident from these examples. It is to be noted that the shape of these curves depends also on the band width. In filter design, using these types of impedances, one should

plot  $z_1$  or  $z_2$  and choose the best curve fitting the requirements.

The following is a table of the quantities which is useful in the design. All of the quantities are calculated for a fixed band width of  $(22-18) = 4$  k rad/sec and only the best curves are included in the table where:

$\omega_{\min}, \omega_{\max}, \omega_e$  are extremum frequencies

$D_1$  : maximum

$D_2$  : minimum

$\omega_2 - \omega_1$  : effective band width

$A_{\max}$  : expected attenuation in the pass-band .

Table I

$z_1 = Z_{T_m}/R_{T_m}$  (refer to Fig. 6.3.1)

$\omega_{01}$	1	2	5	10	k rad/sec
$\omega_{0p1}$	-1.10	-1.10	-1.10	-1.10	
$\omega_{2p1}$	1.10	1.10	1.10	1.10	
$\omega_{\min}$	0.090	0.050	0.090	0.120	
$\omega_{\max}$	-0.895	-0.890	-0.965	-0.965	
$\omega_e$	0.875	0.990	0.870	0.885	
$\omega_1$	-0.965	-0.970	-0.965	-0.965	
$\omega_2$	0.945	0.945	0.915	0.925	
$D_1$	0.282	0.283	0.269	0.215	
$D_2$	0.208	0.283	0.192	0.152	
$A_{\max}$	0.0275	0.0190	0.0195	0.02	Nepers

Table II  
(refer to Fig. 6.3.2)

$\omega_{21}$	35	49	30	k rad/sec
$\rho_{0p2}$	-1.10	-1.10	-1.10	
$\rho_{2p2}$	1.10	1.10	1.10	
$\rho_{\max}$	-0.110	-0.105	-0.150	
$\rho_{\min}$	0.895	0.990	0.885	
$\rho_e$	-0.875	-0.930	-0.870	
$\rho_1$	-0.925	-0.950	-0.920	
$\rho_2$	0.960	0.975	0.965	
$D_1$	$5.88 \cdot 10^{-3}$	$2.42 \cdot 10^{-3}$	$9.9 \cdot 10^{-3}$	
$D_2$	$4.16 \cdot 10^{-3}$	$1.61 \cdot 10^{-3}$	$6.9 \cdot 10^{-3}$	
$A_{\max}$	0.019	0.02N	0.02N	Nepers

In general the image impedances are normalized with respect to the terminating resistance,  $R_L$ . Thus, the normalized impedance used in the design is

$$\frac{Z_{T_m}}{R_L} = Z_I = \frac{Z_{T_m}}{R_{T_m}} \frac{R_{T_m}}{R_L} = z_1 \frac{R_{T_m}}{R_L}$$

or

$$\frac{Z_{\pi_m}}{R_L} = Z_{II} = \frac{Z_{\pi_m}}{R_m} \frac{R_m}{R_L} = z_2 \frac{R_m}{R_L}.$$

Let

$$Z_{T_m}^{\max} Z_{T_m}^{\min} = R_L^2 \quad (\text{or} \quad Z_{\pi_m}^{\max} Z_{\pi_m}^{\min} = R_L^2).$$

Then  $R_{\pi_m}/R_L$  (or  $R_{T_m}/R_L$ ) is equal to  $1/\sqrt{D_1 D_2}$ .

Thus,  $R_{T_m} = R_L/\sqrt{D_1 D_2}$  ( $R_{\pi_m} = R_L/\sqrt{D_1 D_2}$ ) which can also be used to determine the value of  $R_{T_m}$  or  $R_{\pi_m}$ .

Note that the expected attenuation in the pass band,  $A_{\max}$ , is the only required condition for the determination of the image impedance if the filter is symmetric.





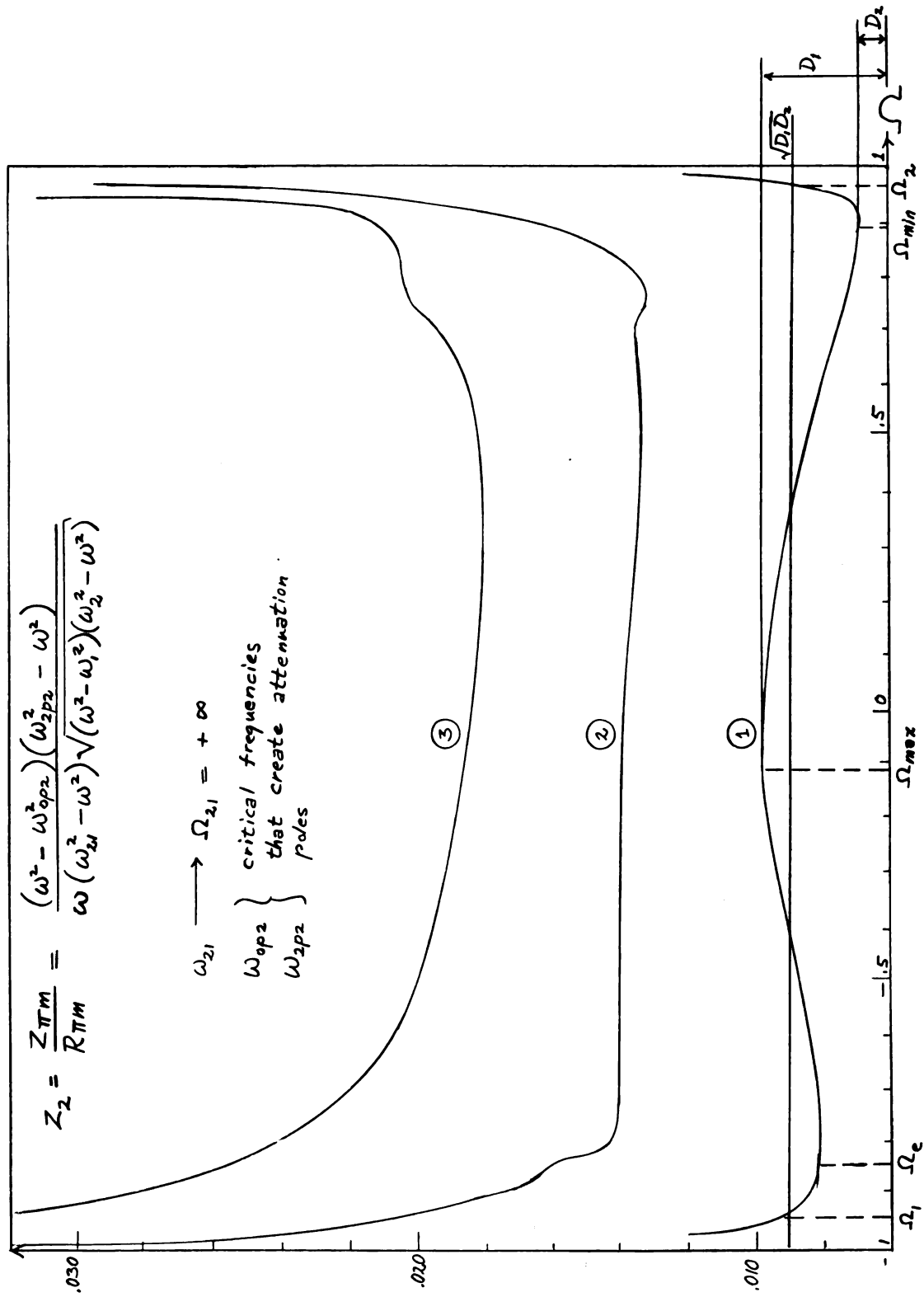


FIG. 6.3.2

## Chapter VII

### CONCLUSIONS AND FURTHER PROBLEMS

Complete characterizations of elementary band-pass filter sections have been developed as well as formulas for the values of the elements of these sections. The elementary sections discussed in this thesis are of special types (see Chapter II). However, the development can also be applied to other types of sections. The reason that only the special type of sections are considered here is that a filter made out of these sections is an economical filter, i.e., it contains a minimum number of elements. A systematic design technique is described using an approximation formula for the attenuation function, which takes into consideration the effect of image impedance. The effects of image impedances are generally omitted in the earlier approximation formulas for the attenuation function.

The study of higher order image impedances by using a frequency transformation technique is discussed and the selection of the location of the critical frequencies of the impedance function is considered. For the determination of the location of these critical frequencies a digital computer program has been employed.

After using a frequency transformation on the image impedance expression, through a trial and error method these frequencies are located to give the "best" image impedance function. However, an analytical approach, perhaps utilizing elliptic functions, could be used. Such an approach is not considered in this thesis, but rather is left as a further problem.

In this thesis only lossless band-pass filters are considered. In the case of incidental losses, as is known for the low-pass case [T0 1], as long as the losses are assumed to be uniformly distributed, a simple computer program can be written to take into account the effect of losses. In this thesis, the program written and used for the calculation of the insertion loss function can easily be extended to the lossy case. However, since the main objective in this thesis for the designing of "zig-zag" type of band-pass filter is to describe an exact design procedure, such an additional program covering the lossy case is not written.

## BIBLIOGRAPHY

- [BE 1,2] : Belevitch, V., "Elements in the design of Conventional filters", Electrical Communications, Vol. 26, March, 1949, pp 84-90 and June 1949, p 180.
- [BE 3] : \_\_\_\_\_, "Recent developments in filter theory", IRE Transaction on Circuit Theory, Vol. CT-5, December, 1954, pp 236-240.
- [BO 1] : Bode, H.W., "A general theory of Electric Wave Filters", J. Math. Phys., Vol. XIII, 1934, pp 275-362.
- [BR 1] : Brandt, R.V., "Ein einheitliches System der Dimensionierung von Bandpässen nach Zobel und Laurent", Frequenz, Band 7, Juni 1953, Nr 6, pp 167-180.
- [CA 1] : Cauer, W., "Theorie der linearen Wechselstromschaltungen" (book), Akademie Verlag Berlin, 1954, 2nd edition.
- [CAM 1] : Campbell, G.A., "Physical Theory of the Electric Wave Filters", B.S.T.J., Vol. 1, pp 1-32, November 1922.
- [CO 1] : Collins, J.E., "Les Filtres dissociés Passe-bas et Passe-haut", Cables et Transmission, 19<sup>e</sup> Année, Janvier 1965, No 1, pp 9-19.

- [DA 1] : Darlington, S., "Synthesis of reactance four poles", J. Math. and Phys., Vol. 28, September 1939, pp 257-353.
- [FIS 1] : Fischer, B.J., "Über elektrischer Wellenfilter mit vorgegebenen Betriebseigenschaften", A.E.Ü., Band 14, Juli 1960, Heft 7.
- [FIS 2] : \_\_\_\_\_, "Ein Beitrag zur Berechnung elektrischer Wellenfilter", A.E.Ü., Band 17, Heft 6, Juni 1963, Heft 7, Juli 1963.
- [FU 1] : Fujisawa, T., "Realizability theorem for Mid-Series or Mid-Shunt Low-Pass Ladders Without Mutual Inductance", IRE. Transc. on Circuit Theory, Vol. CT-2, December 1955, pp 236-252.
- [FR 1] : Fromagoet, A. and LaLande, M.A., "Utilisation d'une methode degabarit pour le calcul pratigue des filters", Ann. Télécomm., Septembre 1950, pp 277-290.
- [FU 2] : \_\_\_\_\_, "Theory and Procedure for optimazation of low-pass attenuation characteristics", IEEE Transact. Of Circuit Theory, Vol. CT-11, No 4, December 1964.
- [LA 1] : Laurent, T., "Vierpoletheorie und Frequenztransformation" (book), Springer-Verlag, Berlin/Göttingen, Heidelberg, 1956.

- [MA 1] : Mason, W.P., "Electromechanical transducers and Wave Filters" (book), D. von Nostrand Company, Inc., New York, Second edition 1958.
- [MO 1] : Mole, J.H., "Filter design data for Communication Engineers" (book), John Wiley & Sons, Inc., New York, 1952.
- [NO 1] : Nonnemacher, W., "Über den Aufbau von Bandpässen aus Stamgliedern", Frequenz, Vol.16, 1957.
- [RE 1] : Reed, M.B., "Electric Network Synthesis" (book), Prentice Hall, Englewood Cliffs, N.J., 1955.
- [RO 1] : Rowlands, R.O., "Composite ladder filters", Wireless Engrs., Vol. 24, January 1952, No 340, pp 50-55.
- [RO 2] : \_\_\_\_\_, "Double derived Terminations", Wireless Engr., Vol. 23, pp 52-56, February 1946 and pp 292-295, November 1946.
- [RO 3] : \_\_\_\_\_, "Impedance transformations in Four element Band-Pass Filters", Proc. Inst. Radio Engrs., Vol. 37, November 1949, pp 1337-1340.
- [RU 1] : Rumpelt, Z., "Schablonverfahren für den Entwurf elektrischer Wellenfilter aus der Grundlage der Wellenparameter", T.F.T., August 1942, Vol. 31, pp 203-210.

- [SA 1] : Saraga, W., "Minimum inductor or capacitor filters", Wireless Engr., Vol. 30, No 5, May 1953.
- [SA 2] : \_\_\_\_\_, and Fosgate, L., "New Graphical methods for analysis and design", Wireless Engr., January, 1952, Vol. 24, pp 50-55.
- [SC 1] : Schoeffler, J., "On the existence of Crystal ladder filters", Proc, First Allerton Conference on Circuit Theory, November 1963.
- [SC 2] : \_\_\_\_\_, "A solution to the approximation and realization problems for Crystal Ladder filters", 1964 IEEE International Convention record Part 1, March 23-26.
- [SH 1] : Shea, T.E., "Transmission Network and Wave filters" (book), Von Nostrand Company, Inc., New York, 1929.
- [SK 1] : Sykes, R.A., "A new approach to the design of high frequency crystal filters", IRE National Conv. Rec., Part 2, March 24-27, 1958.
- [TO 1] : Tokad, Y., "Some improvement of the image parameter methods of the design of L-C filters", Doctoral thesis at Michigan State University, 1959.
- [WA 1] : Watanabe, H., "Synthesis of Band-Pass Ladder Network", IRE Transact. on Circuit Theory, Vol. CT-5, September 1958, No 3.

[Z0 1] : Zobel, O.J., "Theory and design of uniform  
and composite electric Wave Filters", B.S.T.J.  
Vol. 2, No 1, January 1923, pp1- 46



## APPENDIX

### EVALUATION OF ATTENUATION FUNCTION BY DIGITAL COMPUTER

The following is an example of the evaluation of attenuation function using a digital computer. The filter considered in this example is of the form shown in Fig. A-1. The ideal transformer of turn ratio  $1:n$  is used to make both the image impedances of this filter identical.

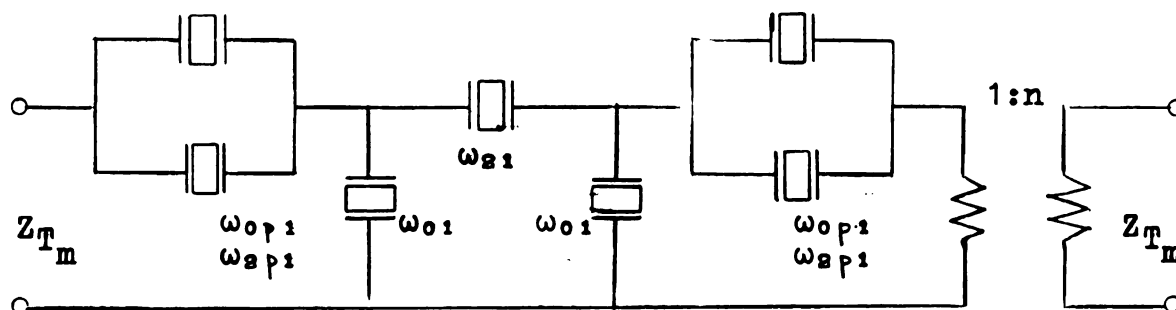


FIG. A-1

The following table gives the explanation of the symbols used in the computer program. The program is also included after the table and it is used for the filter in Fig. A-1 with the following parameter values.

$$\begin{aligned}\omega_{01} &= 10 \text{ kc/sec} \\ \omega_{21} &= 30 \text{ kc/sec}\end{aligned}$$

$$\Omega_{0p1} = \Omega(\omega_{0p1}) = -1.1$$

$$\Omega_{2p1} = \Omega(\omega_{2p1}) = 1.1$$

$A_{\max}$  : max. attenuation in the pass band  
0.02 Nepers

(see also Table I on page 122 for case  $\omega_{01} = 10$ )

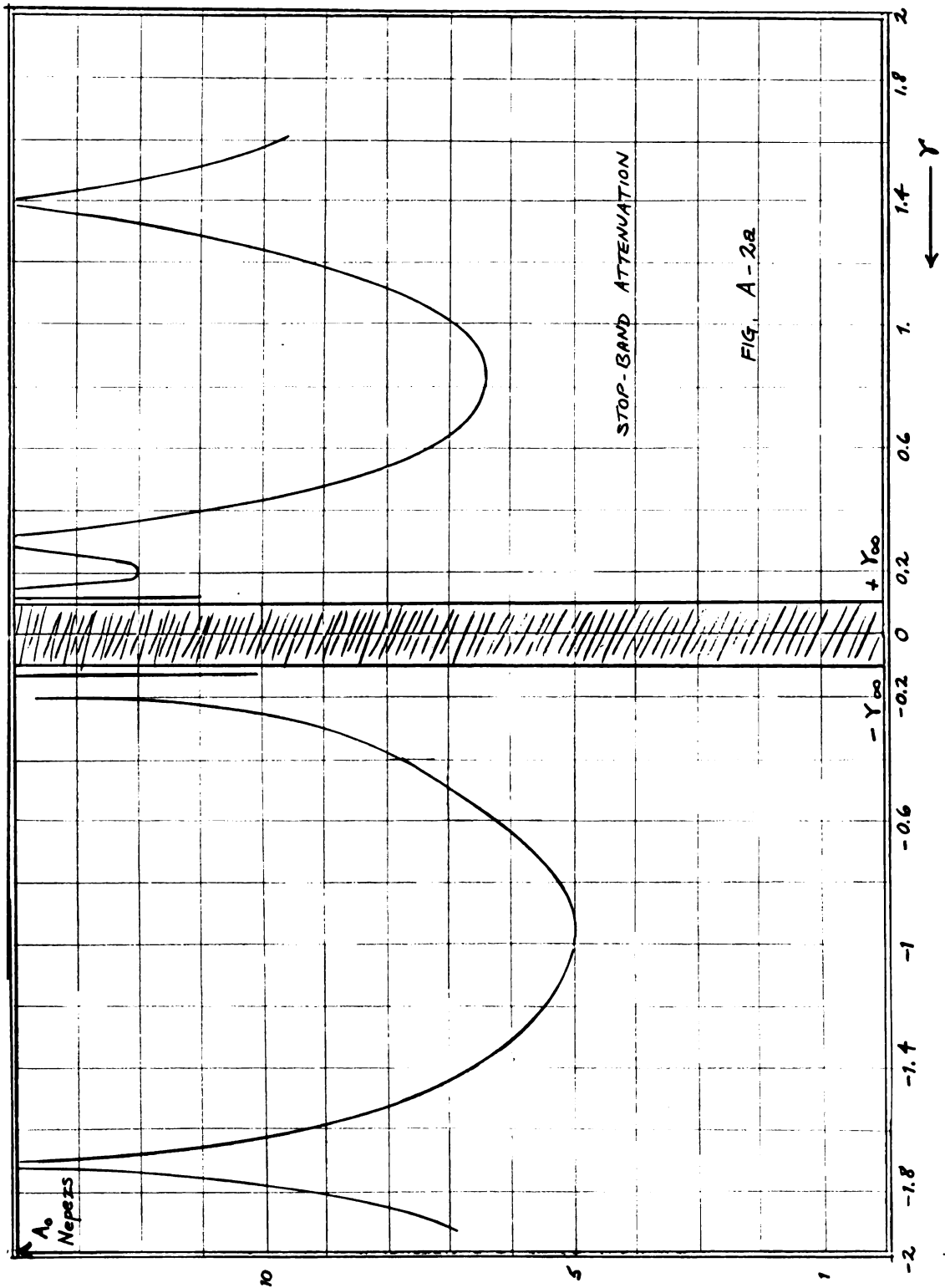
The result is included in the following and the sketch of the attenuation function in both stop bands and pass band are given in Fig. A-2.

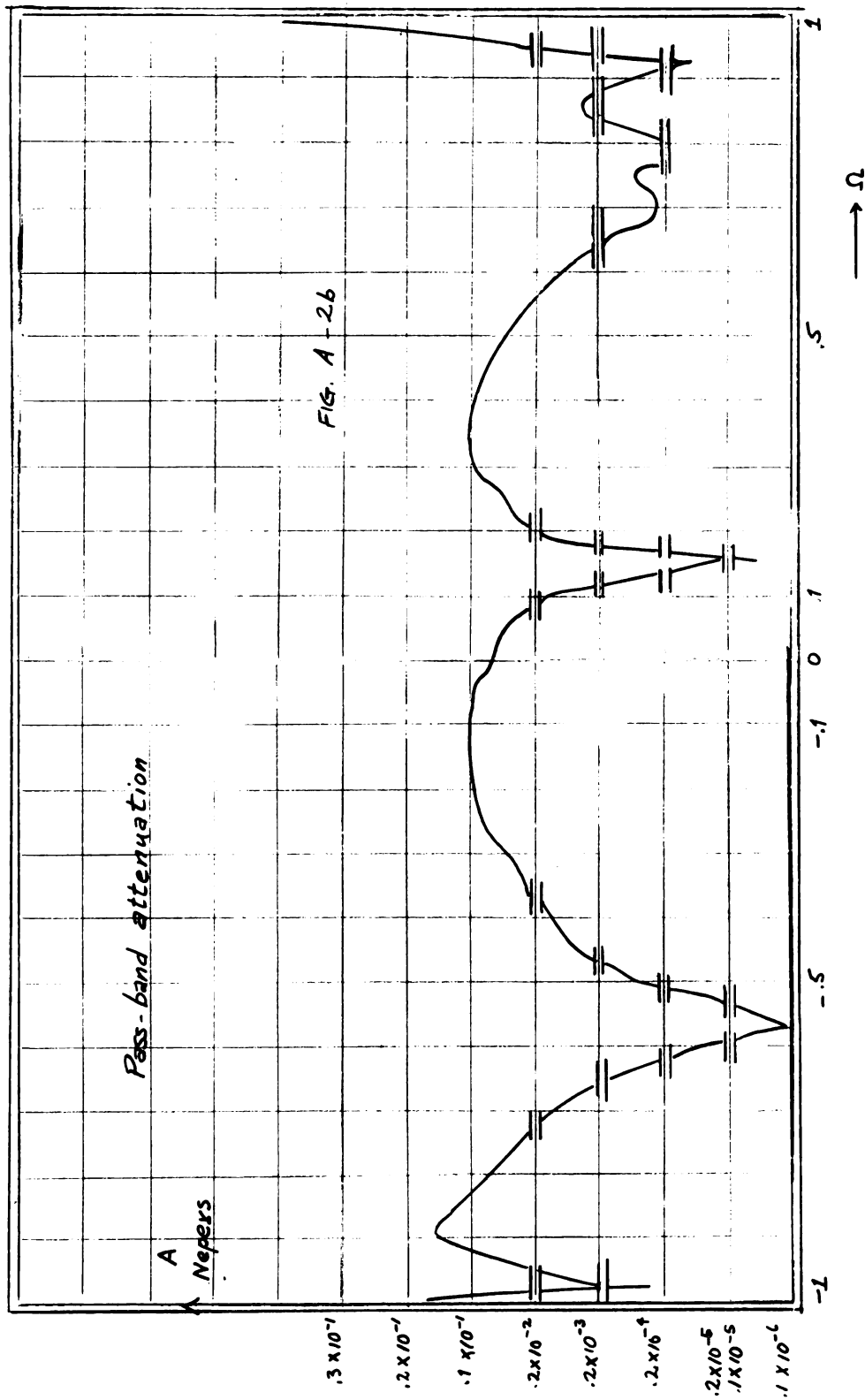
Table III

Symbol used in the program	Meaning	Symbol used in the text
$\left. \begin{array}{l} PO1(I) \\ PO2(I) \end{array} \right\}$	attenuation poles in the upper and the lower stop band ( $I$ = number of E.S.Z. sections or its $m$ derived)	$\omega_{01}$ $\omega_{21}$
$\left. \begin{array}{l} PP1 \\ PP2 \end{array} \right\}$	transformed critical frequencies in impedance investigation ( $PP1 = -PP2$ )	$\Omega_{0p1}$ $\Omega_{2p1}$
$\left. \begin{array}{l} P1(I) \\ P2(I) \end{array} \right\}$	attenuation poles in the $\bar{\Omega}$ -scale	$\bar{\Omega}_{01}$ $\bar{\Omega}_{21}$
$\left. \begin{array}{l} GAP1(I) \\ GAP2(I) \end{array} \right\}$	attenuation poles in the $\gamma$ -scale (logarithmic scale)	$\gamma_{01}$ $\gamma_{21}$
$H(I)$	the $H$ -function of E.S.Z. of its $m$ -derived section	$H_1$
	$H_1^2 = m_1^2 \frac{(\bar{\alpha}^2 - 1)}{(\bar{\alpha} - \bar{\Omega}_0(i))^2} \frac{(\bar{\Omega} - \bar{\Omega}_0(i))^2}{(\bar{\Omega}^2 - 1)}$	
$S(I)$	confluence frequency of each E.S.Z. in the $\bar{\Omega}$ -scale	$\bar{\Omega}_0(i)$
	$\bar{\Omega}_0(i) = \frac{\bar{\Omega}_{2p1} \sqrt{\bar{\Omega}_{0p1}^2 - 1} + \bar{\Omega}_{0p1} \sqrt{\bar{\Omega}_{2p1}^2 - 1}}{\sqrt{\bar{\Omega}_{2p1}^2 - 1} + \sqrt{\bar{\Omega}_{0p1}^2 - 1}}$	
$Z0(I)$	constant of the $H$ -function	$m_1$
	$m_1 = \frac{1}{\sqrt{\bar{\alpha}^2 - 1}} \frac{(\bar{\alpha} - \bar{\Omega}_{2p1}) \sqrt{\bar{\Omega}_{0p1}^2 - 1} + (\bar{\alpha} - \bar{\Omega}_{0p1}) \sqrt{\bar{\Omega}_{2p1}^2 - 1}}{\bar{\Omega}_{2p1} - \bar{\Omega}_{0p1}}$	
$ATI$	total attenuation	$A_{It}$
	$A_{It} = \sum A_I$	

(Table III continued)

Symbol used in the program	Meaning	Symbol used in the text
AI	image attenuation of each section $A_I = \ln \left  \frac{1+H}{1-H} \right $	$A_I$
BIT	total image phase $B_{It} = \Sigma B_I$	$B_{It}$
BI	image phase $B_I = \arctan [2H_1]$	$B_I$
X1	normalized impedance $X1 = Z_{Tm}/R_{Tm}\sqrt{D_1 D_2}$	$Z_{Tm}/R_L$
A01	STOP band attenuation (exact)	$A_{01}$
A03	STOP band attenuation (approx)	$A_{03}$
Z	$0.5 \log f(x_1, x_2)$	
G	logarithmic frequency scale	$\gamma$
DEL	transformed frequency for impedance investigation	$\Omega$
OS } OB }	angular frequency	$\omega$
A0	pass band attenuation	$A_0$
OM	transformed angular frequency	$\bar{\Omega}$





\* 041917 SOEMINTAPOERA

PROGRAM DESIGN

ODIMENSION PO1(2),PO2(2),P1(2),P2(2),GAP1(2),GAP2(2),S(2),  
IZO(2),H(2),HA(2),AG(2),AI(2),BI(2)

PP1=-1.100

PP2=1.100

PO1(2)=10.000

PO1(1)=PPO(PO1(2),PP1)

PO2(1)=PPO(PO1(2),PP2)

PO2(2)=30.000

DO 2 I=1,2

2 P1(I)=POLE(PO1(I))

PRINT 3, (P1(I),I=1,2)

3 FORMAT (1H0,3X,7HPOLE1= ,F8.3,3X,F8.3)

DO 4 I=1,2

4 P2(I)=POLE(PO2(I))

PRINT 5, (P2(I),I=1,2)

5 FORMAT (1H0,3X,7HPOLE2= ,F8.3,3X,F8.3)

DO 6 I=1,2

6 GAP1(I)=0.5\*LOGF((P1(I)+1.)/(P1(I)-1.))

PRINT 7, (GAP1(I),I=1,2)

7 FORMAT (1H0,3X,6HGAP1= ,F8.3,3X,F8.3)

DO 8 I=1,2

8 GAP2(I)=0.5\*LOGF((P2(I)+1.)/(P2(I)-1.))

PRINT 9, (GAP2(I),I=1,2)

9 FORMAT (1H0,3X,6HGAP2= ,F8.3,3X,F8.3)

DO 10 I=1,2

10 S(I)=COL(P1(I),P2(I))

PRINT 11, (S(I),I=1,2)

11 FORMAT (1H0,3X,12HCONFLUENCE= ,3X,E15.8,3X,E15.8)

DO 12 I=1,2

12 ZO(I)=CONS(P1(I),P2(I))

PRINT 13, (ZO(I),I=1,2)

13 FORMAT (1H0,3X,12HM ,3X,F15.8,3X,F15.8)

PRINT 100

100 FORMAT (1H0,3X,25HSTOP BAND ATTEN IN NEPERS)

OM=-9.25

DO 14 K=1,68

IF(K-33) 15,15,16

15 GO TO 17

16 IF (K-34) 15,18,15

18 OM=OM+2.25

GO TO 17

17 IF (K-1) 20,21,20

21 PRINT 22

220FORMAT (1H0,6X,2HOM,10X,3HGAM,16X,3HATI,18X,3HA01,18X,3HA03,  
115X,11HLOGF(X1,X2))

20 CONTINUE

ATI=0

DO 23 I=1,2

H(I)=RATH(ZO(I),S(I),OM)

HA(I)=ABSF(H(I))

IF (HA(I)-1.) 24,25,24

25 GO TO 23

24 AG(I)=ABSF((1.+HA(I))/(1.-HA(I)))

IF (AG(I)) 23,23,38

```

38 IF (AG(I)-10.**8) 39,39,23
39 AI(I)=2.*LOGF(AG(I))
23 ATI=ATI+AI(I)
   ST1=(SINH(ATI))**2
   OB=ABSF(SQRTF((18.*22.)*(10.+OM)/(10.-OM)))
   X1=ZIM(OB,PO1(2),PO1(1),PO2(1))
   IF (X1) 27,28,27
28 GO TO 14
27 C=ABSF(X1)
   IF (C-1.) 29,30,29
   IF (C-10.**6) 29,29,30
30 GO TO 14
29 CONTINUE
   Q=((1.+X1**2)/(2.*X1))**2
   D=ABSF(1.+Q*ST1)
   IF (D) 40,40,41
40 GO TO 14
41 A01==0.5*LOGF(D)
   T=ABSF(SQRTF(Q))
   IF (T) 42,42,43
42 GO TO 14
43 Z=LOGF(T)
   G=0.5*LOGF(ABSF((OM+1.)/(OM-1.)))
   A03=ATI+Z-LOGF(2.)
   PRINT 31, OM,G,ATI,A01,A03,Z
31 FORMAT (3X,F8.2,5(3X,E15.8))
14 OM=OM+0.25
   PRINT 110
110 FORMAT (1H0,3X,21HPASS BAND ATTENUATION)
   PRINT 34
34 FORMAT (1H0,8X,2HX1,18X,2HA0,18X,3HBIT,12X,2HOM,12X,3HDEL)
   DEL=-1.000
   DO 19 L=1,64
   IF (L-10) 49,49,50
49 GO TO 60
50 IF (L-55) 70,70,49
60 DEL=DEL+0.01
   GO TO 80
70 DEL=DEL+0.04
   GO TO 80
80 OS=PPO(PO1(2),DEL)
   OM=POLE(OS)
   BIT=0
   DO 35 I=1,2
   H(I)=RATH(ZO(I),S(I),OM)
   BI(I)=2.*(ATANF(2.*H(I)))
35 BIT=BIT+BI(I)
   ST2=(SINF(BIT))**2
   X1=ZIM(OS,PO1(2),PO1(1),PO2(1))
   Q2=((1.-X1**2)/(2.*X1))**2
   A0=0.5*LOGF(ABSF(1.+Q2*ST2))
   PRINT 36,X1,A0,BIT,OM,DEL
36 FORMAT (3(3X,E15.5),3X,F8.3,3X,F8.3)
19 CONTINUE

```



```

STOP
END
FUNCTION COL(A,B)
DIMENSION A(3),B(3)
P=SQRTF(A*A-1.)
Q=SQRTF(B*B-1.)
COL=(A*Q+B*P)/(Q+P)
RETURN
END
FUNCTION CONS(A,B)
DIMENSION A(3),B(3)
C=10.
P=(C-A)*SQRTF(B*B-1.)
Q=(C-B)*SQRTF(A*A-1.)
R=B-A
S=SQRTF(C*C-1.)
CONS=(Q+P)/(R*S)
RETURN
END
FUNCTION RATH(A,B,C)
DIMENSION A(3),B(3)
D=10.
G=SQRTF(D*D-1.)
T=D-B
P=C-B
Q=SQRTF(ABSF(C*C-1.))
RATH=(A*G*P)/(T*Q)
RETURN
END
FUNCTION ZIM(P,Q,U,S)
TOR1=(1./P)*(P*P-Q*Q)/((P*P-U*U)*(S*S-P*P))
TOR2=SQRTF(ABSF((P*P-18.*18.)*(22.*22.-P*P)))
D1=0.215
D2=0.152
C01=1./SQRTF(D1*D2)
ZIM=TOR1*TOR2*C01
RETURN
END
FUNCTION POLE(Q)
G=SQRTF(18.*22.)
A=0.1
TA=A*(Q*Q+G*G)/(Q*Q-G*G)
POLE=1./TA
RETURN
END
FUNCTION PPO(A,B)
PEN=B+(40.-2.*18.*22./A)/4.
PEM=B-(40.-2.*A)/4.
PPO=A*PEN/PEM
RETURN
END
END

```

## STOP BAND ATTENUATION IN NEPERS

OM	GAM	ATI	A01	A03
-9.25	-.10853225E+00	.12153058E+02	.12032159E+02	.12032159E+02
-9.00	-.11157178E+00	.12239682E+02	.12291305E+02	.12291305E+02
-8.75	-.11478722E+00	.12337574E+02	.12547024E+02	.12547024E+02
-8.50	.11819439E+00	.12449155E+02	.12809294E+02	.12809294E+02
-8.25	-.12181104E+00	.12577634E+02	.13086837E+02	.13086837E+02
-8.00	-.12565721E+00	.12727381E+02	.13388769E+02	.13388769E+02
-7.75	-.12975560E+00	.12904549E+02	.13726091E+02	.13726091E+02
-7.50	-.13413199E+00	.13118161E+02	.14113623E+02	.14113623E+02
-7.25	-.13881587E+00	.13382188E+02	.14573289E+02	.14573289E+02
-7.00	-.14384106E+00	.13719900E+02	.15140750E+02	.15140750E+02
-6.75	-.14924649E+00	.14174373E+02	.15881228E+02	.15881228E+02
-6.50	-.15507746E+00	.14839844E+02	.16936590E+02	.16936590E+02
-6.25	-.16138670E+00	.15998955E+02	.18731231E+02	.18731231E+02
-6.00	-.16823612E+00	.20222259E+02	.25121373E+02	.25121373E+02
-5.75	-.17569894E+00	.16282573E+02	.19266597E+02	.19266597E+02
-5.50	-.18386239E+00	.14626395E+02	.16836987E+02	.16836987E+02
-5.25	-.19283124E+00	.13636026E+02	.15406330E+02	.15406330E+02
-5.00	-.20273255E+00	.12896565E+02	.14352611E+02	.14352611E+02
-4.75	-.21372201E+00	.12286595E+02	.13494065E+02	.13494065E+02
-4.50	-.22599256E+00	.11753083E+02	.12751526E+02	.12751526E+02
-4.25	-.23978654E+00	.11267581E+02	.12082758E+02	.12082758E+02
-4.00	-.25541281E+00	.10812592E+02	.11462015E+02	.11462015E+02
-3.75	-.27327185E+00	.10376121E+02	.10871897E+02	.10871897E+02
-3.50	-.29389333E+00	.99491111E+01	.10299546E+02	.10299546E+02
-3.25	-.31799438E+00	.95240619E+01	.97346209E+01	.97346209E+01
-3.00	-.34657359E+00	.90941730E+01	.91681059E+01	.91681059E+01
-2.75	-.38107003E+00	.86527426E+01	.85915444E+01	.85915444E+01
-2.50	-.42364893E+00	.81926852E+01	.79965588E+01	.79965589E+01
-2.25	-.47775572E+00	.77061754E+01	.73747732E+01	.73747732E+01
-2.00	-.54930614E+00	.71847347E+01	.67189042E+01	.67189041E+01
-1.75	-.64964149E+00	.66215437E+01	.60285976E+01	.60285965E+01
-1.50	-.80471896E+00	.60274069E+01	.53417830E+01	.53417774E+01
-1.25	-.10986123E+01	.55911123E+01	.50112407E+01	.50112324E+01
1.25	.10986123E+01	.72523363E+01	.71047596E+01	.71047598E+01
1.50	.80471896E+00	.71555523E+01	.65006564E+01	.65006555E+02
1.75	.64964149E+00	.77167214E+01	.70268563E+01	.70268561E+01
2.00	.54930614E+00	.83498361E+01	.77054453E+01	.77054453E+01
2.25	.47775572E+00	.89980807E+01	.84210205E+01	.84210205E+01
2.50	.42364893E+00	.96632370E+01	.91593188E+01	.91593188E+01
2.75	.38107003E+00	.10364844E+02	.99344433E+01	.99344433E+01
3.00	.34657359E+00	.11138853E+02	.10780384E+02	.10780348E+02
3.25	.31799438E+00	.12054583E+02	.11765822E+02	.11765822E+02
3.50	.29389333E+00	.13282581E+02	.13061211E+02	.13061211E+02
4.00	.25541281E+00	.16207818E+02	.16114935E+02	.16114935E+02
4.25	.23978654E+00	.14039082E+02	.14007811E+02	.14007811E+02
4.50	.22599256E+00	.13163435E+02	.13192399E+02	.13192399E+02
4.75	.21372201E+00	.12643360E+02	.12731470E+02	.12731470E+02
5.00	.20273255E+00	.12289783E+02	.12436238E+02	.12436238E+02
5.25	.19283124E+00	.12031465E+02	.12235745E+02	.12235745E+02
5.50	.18386239E+00	.11833969E+02	.12095841E+02	.12095841E+02
5.75	.17569894E+00	.11678126E+02	.11997651E+02	.11997651E+02
6.00	.16823612E+00	.11552237E+02	.11929784E+02	.11929784E+02
6.25	.16138670E+00	.11448683E+02	.11884955E+02	.11884955E+02

6.50	.15507746E+00	.11362254E+02	.11858321E+02	.11858321E+02
6.75	.14924649E+00	.11289252E+02	.11846602E+02	.11846602E+02
7.00	.14384104E+00	.11226971E+02	.11847579E+02	.11847579E+02
7.25	.13881587E+00	.11173381E+02	.11859813E+02	.11859813E+02
7.50	.13413199E+00	.11126930E+02	.11882479E+02	.11882479E+02
7.75	.12975560E+00	.11086407E+02	.11915300E+02	.11915300E+02
8.00	.12565721E+00	.11050855E+02	.11958558E+02	.11958558E+02
8.25	.12181104E+00	.11019507E+02	.12013198E+02	.12013198E+02
8.50	.11819439E+00	.10991742E+02	.12081077E+02	.12081077E+02
8.75	.11478722E+00	.10967051E+02	.12165502E+02	.12165502E+02
9.00	.11157178E+00	.10945013E+02	.12272414E+02	.12272414E+02
9.25	.10853225E+00	.10925278E+02	.12413356E+02	.12413356E+02
9.50	.10565455E+00	.10907553E+02	.12614687E+02	.12614687E+02
9.75	.10292603E+00	.10891589E+02	.12961136E+02	.12961136E+02

## PASS BAND ATTENUATION IN NEPERS

X1	A0	BIT	OM	DEL
.67256E+00	.15919E-01	-.58256E+01	-.993	-.990
.87333E+00	.33414E-02	-.56363E+01	-.985	-.980
.98897E+00	.31149E-04	-.54911E+01	-.978	-.970
.10622E+01	.11420E-02	-.53687E+01	-.971	-.960
.11103E+01	.39808E-02	-.52609E+01	-.963	-.950
.11421E+01	.71442E-02	-.51635E+01	-.956	-.940
.11631E+01	.99590E-02	-.50738E+01	-.948	-.930
.11763E+01	.12150E-01	-.49904E+01	-.941	-.920
.11840E+01	.13651E-01	-.49119E+01	-.933	-.910
.11877E+01	.14501E-01	-.48376E+01	-.926	-.900
.11794E+01	.13285E-01	-.45715E+01	-.895	-.860
.11545E+01	.89334E-02	-.43396E+01	-.865	-.820
.11250E+01	.48403E-02	-.41300E+01	-.834	-.780
.10954E+01	.21128E-02	-.39360E+01	-.802	-.740
.10625E+01	.69647E-03	-.37532E+01	-.771	-.700
.10410E+01	.14442E-03	-.35787E+01	-.739	-.660
.10170E+01	.99766E-05	-.34104E+01	-.706	-.620
.99512E+00	.13073E-06	-.32463E+01	-.673	-.580
.97530E+00	.99010E-06	-.30853E+01	-.640	-.540
.95736E+00	.43464E-04	-.29260E+01	-.607	-.500
.94114E+00	.24592E-03	-.27675E+01	-.573	-.460
.92650E+00	.75248E-03	-.26089E+01	-.538	-.420
.91332E+00	.16767E-02	-.24492E+01	-.503	-.380
.90148E+00	.30576E-02	-.22878E+01	-.465	-.340
.89089E+00	.48310E-02	-.21238E+01	-.433	-.300
.88145E+00	.68230E-02	-.19566E+01	-.397	-.260
.87311E+00	.87651E-02	-.17855E+01	-.360	-.220
.86579E+00	.10332E-01	-.16099E+01	-.323	-.180
.85945E+00	.11201E-01	-.14292E+01	-.286	-.140
.85405E+00	.11122E-01	-.12428E+01	-.248	-.100
.84955E+00	.99949E-02	-.10505E+01	-.210	-.060
.84594E+00	.79361E-02	-.85182E+00	-.171	-.020
.84318E+00	.53053E-02	-.64672E+00	-.132	.020
.84128E+00	.26743E-02	-.43524E+00	-.092	.060
.84023E+00	.71311E-03	-.21765E+00	-.052	.100
.84004E+00	.47371E-06	.55562E-02	-.012	.140
.84073E+00	.81422E-03	.23366E+00	.029	.180
.84230E+00	.29902E-02	.46574E+00	.071	.220
.84480E+00	.59341E-02	.70077E+00	.113	.260

.84826E+00	.88024E-02	.93762E+00	.156	.300
.85272E+00	.10782E-01	.11752E+01	.199	.340
.85825E+00	.11352E-01	.14126E+01	.243	.380
.86491E+00	.10431E-01	.16490E+01	.288	.420
.87278E+00	.83613E-02	.18838E+01	.332	.460
.88195E+00	.57581E-02	.21170E+01	.378	.500
.89253E+00	.32843E-02	.23486E+01	.424	.540
.90460E+00	.14317E-02	.25792E+01	.471	.580
.91829E+00	.38675E-03	.28096E+01	.518	.620
.93365E+00	.23730E-04	.30411E+01	.566	.660
.95070E+00	.22847E-04	.32756E+01	.615	.700
.96926E+00	.65044E-04	.35155E+01	.664	.740
.98878E+00	.21663E-04	.37642E+01	.714	.780
.10078E+01	.17872E-04	.40265E+01	.764	.820
.10224E+01	.20803E-03	.43101E+01	.815	.860
.10226E+01	.24743E-03	.46283E+01	.867	.900
.10176E+01	.15267E-03	.47159E+01	.880	.910
.10092E+01	.41875E-04	.48081E+01	.893	.920
.99614E+00	.71882E-05	.49056E+01	.907	.930
.97652E+00	.25796E-03	.50097E+01	.920	.940
.94761E+00	.12176E-02	.51224E+01	.933	.950
.90500E+00	.36901E-02	.52464E+01	.946	.960
.84115E+00	.91383E-02	.53866E+0	.960	.970
.74149E+00	.20132E-01	.55520E+01	.973	.980
.57003E+00	.41003E-01	.57668E+01	.987	.990

MICHIGAN STATE UNIVERSITY LIBRARIES



3 1293 03175 1658